



UNIVERSIDAD NACIONAL AUTÓNOMA DE MEXICO
PROGRAMA DE MAESTRÍA Y DOCTORADO EN CIENCIAS QUÍMICAS

REPOSICIONAMIENTO DE FÁRMACOS QUE REVIERTAN EL FENOTIPO TRONCAL EN CÉLULAS DE
CÁNCER DE MAMA

TESIS

PARA OPTAR POR EL GRADO DE

DOCTOR EN CIENCIAS

PRESENTA

M. en C. LUZ XOCHIQUETZALLI VÁSQUEZ BOCHM

DR. MARCO ANTONIO VELASCO VELAZQUEZ

FACULTAD DE MEDICINA

CIUDAD DE MÉXICO, ENERO 2020



Universidad Nacional
Autónoma de México

Dirección General de Bibliotecas de la UNAM

Biblioteca Central



UNAM – Dirección General de Bibliotecas
Tesis Digitales
Restricciones de uso

DERECHOS RESERVADOS ©
PROHIBIDA SU REPRODUCCIÓN TOTAL O PARCIAL

Todo el material contenido en esta tesis esta protegido por la Ley Federal del Derecho de Autor (LFDA) de los Estados Unidos Mexicanos (México).

El uso de imágenes, fragmentos de videos, y demás material que sea objeto de protección de los derechos de autor, será exclusivamente para fines educativos e informativos y deberá citar la fuente donde la obtuvo mencionando el autor o autores. Cualquier uso distinto como el lucro, reproducción, edición o modificación, será perseguido y sancionado por el respectivo titular de los Derechos de Autor.

UNIVERSIDAD NACIONAL AUTÓNOMA DE MÉXICO

PROGRAMA DE MAESTRÍA Y DOCTORADO EN CIENCIAS
QUÍMICAS

REPOSICIONAMIENTO DE FÁRMACOS QUE REVIERTAN EL FENOTIPO TRONCAL
EN CÉLULAS DE CÁNCER DE MAMA

T E S I S

PARA OPTAR POR EL GRADO DE

DOCTOR EN CIENCIAS

P R E S E N T A

M. en C. LUZ XOCHIQUETZALLI VÁSQUEZ BOCHM

DR. MARCO ANTONIO VELASCO VELAZQUEZ

FACULTAD DE MEDICINA

INDICE

AGRADECIMIENTOS.....	9
RESUMEN	10
ABSTRACT.....	11
1. INTRODUCCIÓN.....	12
1.1. CÁNCER.....	12
1.2. CLASIFICACIÓN DE CÁNCER	13
1.3. EPIDEMIOLOGÍA	14
1.4. CÁNCER DE MAMA.....	15
1.5. DETECCIÓN	17
1.6. TRATAMIENTO CONTRA EL CÁNCER DE MAMA	17
1.7. CÉLULAS TRONCALES TUMORALES	18
1.7.1. Definición y características de las células troncales tumorales.....	18
1.7.2. Teorías del inicio de las células troncales tumorales.....	19
1.7.3. Evidencia de las CTT en tumores	20
1.7.4. Células troncales en cáncer de mama	20
1.7.5. Marcadores de CTT en cáncer de mama	21
1.7.5.1. Factor de transcripción SOX2.....	21
1.7.5.2. Factor de transcripción OCT4.....	23
1.7.5.3. ALDH.....	24
1.7.6. Importancia clínica de las células troncales tumorales en cáncer de mama	25
1.7.7. Desarrollo de terapias contra las CTT	26
1.8. REPOSICIONAMIENTO DE FÁRMACOS.....	27
1.8.1. Definición	27
1.8.2. Estrategias transcriptómicas para el reposicionamiento	28
1.8.3. CMap.....	28
1.9. ESTATINAS.....	31
2. JUSTIFICACIÓN.....	33
3. OBJETIVO.....	33
4. HIPÓTESIS	33
5. MATERIALES Y MÉTODOS.....	34

5.1.	SELECCIÓN DE LA FIRMA DE EXPRESIÓN DEFERENCIAL EN CÉLULAS TRONCALES DE CÁNCER DE MAMA.....	34
5.2.	SELECCIÓN DE FÁRMACOS.....	34
5.3.	RELACIÓN ESTRUCTURA ACTIVIDAD.....	35
5.4.	FÁRMACOS.....	35
5.5.	LÍNEAS CELULARES.....	35
5.6.	ENSAYOS DE VIABILIDAD.....	36
5.7.	ENSAYO DE GEN REPORTERO DEPENDIENTE DE LA TRANSACTIVACIÓN DE LOS PROMOTORES DE SOX2 U OCT4.....	37
5.8.	ENSAYO DE FORMACIÓN DE MAMoesFERAS.....	37
5.9.	ENSAYO DE ACTIVIDAD DE LA ENZIMA ALDEHÍDO DESHIDROGENASA....	38
5.10.	ANÁLISIS DE ENRIQUECIMIENTO DE GENES.....	39
5.11.	WESTERN BLOT.....	39
6.	RESULTADOS.....	41
6.1.	PREDICCIÓN <i>IN SILICO</i> DE FÁRMACOS CONTRA CTTM.....	41
6.2.	EFECTO DE LOS FÁRMACOS EN LA VIABILIDAD.....	43
6.3.	ENSAYO DE GEN REPORTERO PARA DETERMINAR LA TRANSACTIVACIÓN DEL PROMOTOR DE SOX2 U OCT4.....	45
6.4.	ENSAYO DE FORMACIÓN DE MAMoesFERAS.....	48
6.5.	ENSAYO DE ACTIVIDAD DE LA ENZIMA ALDEHÍDO DESHIDROGENASA....	51
6.6.	EVALUACIÓN DE LA EXPRESIÓN DE LA PROTEÍNA SOX2.....	53
6.7.	PARTICIPACIÓN DE LA ENZIMA 3-HIDROXI-3-METIL-GLUTARIL-COA REDUCTASA EN LOS EFECTOS DE LOVASTATINA.....	55
6.8.	VALIDACIÓN <i>IN VIVO</i> DE LOS EFECTOS DE LOVASTATINA.....	61
7.	DISCUSIÓN.....	63
8.	CONCLUSIONES.....	67
9.	BIBLIOGRAFIA.....	68

INDICE DE FIGURAS

Figura 1. Alteraciones esenciales.	12
Figura 2. Estadísticas de incidencia y mortalidad de las principales neoplasias a nivel mundial.	14
Figura 3. Pronóstico según subtipo molecular	16
Figura 4. Heterogeneidad tumoral..	19
Figura 5. Flujo de trabajo en Connectivity Map..	30
Figura 6. Evaluación de la similitud estructural..	42
Figura 7. Evaluación en MANTRA.	43
Figura 8. Curvas-dosis respuestas representativas del porcentaje de viabilidad obtenidas para cada fármaco contra la respuesta observada en el control.....	44
Figura 9. Transactivación del promotor de SOX2.	46
Figura 10. Transactivación del promotor de OCT4.	46
Figura 11. Curva dosis respuesta de la transactivación del promotor de SOX2 a diferentes concentraciones de lovastatina.	47
Figura 12. Curva dosis respuesta de la transactivación del promotor de SOX2 a diferentes concentraciones de fasudil.	47
Figura 13. Eficiencia de formación mamoesferas al tratar células MDA-MB-231 con lovastatina durante 7 días.	48
Figura 14. Eficiencia de formación mamoesferas al tratar células MDA-MB-231 con fasudil durante 7 días.	49
Figura 15. Eficiencia de formación mamoesferas al tratar células MDA-MB-231 con lovastatina durante 24 h.	50
Figura 16. Eficiencia de formación mamoesferas al tratar células Hs578T con lovastatina.	51
Figura 17. Evaluación de la actividad de ALDH en células MDA-MB-231 tratadas con diferentes concentraciones de lovastatina.	52
Figura 18. Evaluación de la actividad de ALDH en células Hs578T tratadas con diferentes concentraciones de lovastatina.	53
Figura 19. Evaluación de la expresión de la proteína SOX2.	54
Figura 20. Evaluación de la transactivación del promotor de SOX2, mediante un ensayo de gen reportero.	55
Figura 21. Western blot representativo de la evaluación de la expresión de SOX-2 y α -tubulina en MDA-MB-231 y Hs578T tratadas con lovastatina y/o mevalonato	56
Figura 22. Evaluación de la eficiencia de formación de mamoesferas en células MDA-MB-231.....	57
Figura 23. Evaluación de la eficiencia de formación de mamoesferas en células Hs578T.	58
Figura 24. Efectos inducidos por mevalonato en la acción de la lovastatina al tratar MDA-MB-231.....	59
Figura 25. Efectos inducidos por mevalonato en la acción de la lovastatina al tratar Hs578T.....	60
Figura 26. Análisis de enriquecimiento de tumores mamarios en ratones tratados con lovastatina.....	62

INDICE DE TABLAS

Tabla 1. Clasificación según subtipos moleculares.....	15
Tabla 2. Fármacos con potencial para revertir el fenotipo de CTTMs.....	41

ABREVIATURAS

Abreviatura	Significado
%EFM	Eficiencia de Formación de Mamo esferas
ABCB1	Miembro 1 de la subfamilia B de unión a ATP*
ADN	Ácido desoxirribonucleico
AKT	Cinasa serina-treonina*
ALDH	Aldehído Deshidrogenasa
ANOVA	Análisis de Varianza*
BAA	BODIPY-aminoacetato
BAAA	BODIPY-aminoacetaldehído
BrCa	<i>Breast cancer</i>
BSCS	<i>Breast Cancer Stem Cells</i>
CaMa	Cáncer de mama
CD133	Glicoproteína 133 transmembranal*
CD24	Sialoglicoproteína 24 de la membrana unida a glicosil-fosfatidilinositol*
CD44	Glicoproteína 44 de la superficie celular*
CDK	Cinasas dependientes de ciclinas*
Cmap	Mapa de conexión*
CSC	<i>Cancer Stem Cells</i>
CSR	Clasificación Troncal Consenso*
CT	Células troncales
CTT	Células Troncales Tumorales
CTTM	Células Troncales Tumorales de mama
DEAB	Dietilaminobenzaldehído
DEMEM-Alta glucosa	Medio Eagle modificado de Dulbecco – Alta glucosa
DMSO	Dimetilsulfóxido
DRD2/4	Receptor de Dopamina 2/4*
EDTA	Ácido etilendiaminotetraacético
EGTA	Ácido egtazico
EMT	Transición epitelio-mesénquima*
ER	Receptor de estrógeno*
ERK	Cinasas reguladas por señales extracelulares*
ESA	Antígeno Epitelial Específico*
FDA	Administración de alimentos y bebidas*
FGF4	Factor de crecimiento de fibroblastos 4*
GEO	Expresión génica Omibus*
GFP	Gen que codifica para una proteína verde fluorescente*
GSEA	Análisis de Enriquecimiento del Conjunto de Genes*
HER2	Receptor de crecimiento epidérmico humano 2*
HMG	Grupo de alta movilidad
HMG-CoA reductasa	Hidroximetilglutaril coenzima-A reductasa

HMGCR	3-hidroxi-3-metil-glutaril-coenzima A reductasa
HTRA2A	Miembro 2 de la familia serin-proteosa HtrA*
INEGI	Instituto Nacional de Estadística y Geografía
KFL4	Factor de transcripción con dedos dezinc similar a Kruppel*
KNIME	Plataforma de datos que permite el desarrollo de modelos en un entorno visual
MAPK	Cinasa activada por mitógenos*
mTor	Proteína serin-treonin cinasa*
MTT	Bromuro de 3(4,5 dimetil-2-tiazolil)-2,5-difeniltetrazólio
MYC	Familia de genes y proto-oncogenes que codifica para factores de transcripción*
NANOG	Factor de transcripción con una unica homeobox*
NOD/SCID	Marca de ratones inmunodeficientes
OCT4	Octámero de unión al factor de transcripción 4*
PBP2	Proteína de unión a penicilina 2*
PBS	Buffer salino de fosfato*
PGE2	16,16- dimetilprostaglandina E2*
PI3K	Cinasa fosfatidil-inositol 3 fosfatos*
PTEN	Homólogo de fosfatasa y tensina*
PTGER3	Receptor 3 de prostaglandina, por sus siglas en inglés
ROCK1	Proteína serin-treonin cinasa 1 asociada con rho*
ROCK2	Proteína serin-treonin cinasa 2 asociada con rho*
RPMI-1640	Instituto en memoria de Roswell Park 1640*
SEM	Desviación estándar de la media*
SFB	Suero Fetal Bovino*
SOX2	Gen de la región determinante del sexo Y-box 2*
STAT3	Transductor de señal y activador de la transcripción 3*
ZEB1	Proteína con estructura de dedo de zinc con union E-box 1*
Zfp42/Rex1	Proteína con estructura de dedo de zinc 42*
ZNF32	Proteína con estructura de dedo de zinc 32*

* Por sus siglas en inglés

AGRADECIMIENTOS

Al Posgrado en Ciencias Químicas de la UNAM.

A CONACyT por la beca que me permitió realizar mis estudios de doctorado (294393) y por el financiamiento parcial a la investigación (INFR-2014-01-225313).

A PAPIIT UNAM por el apoyo económico recibido mediante los proyectos IN228616 e IN219719.

Al Dr. Marco Velasco Velázquez quien fungió como mi tutor durante mis estudios de doctorado.

Al Dr. Ignacio Camacho y al Dr. José Luis Medina quienes formaron parte de mi comité tutor.

ARTÍCULOS

Vásquez-Bochm LX, Velázquez-Paniagua M, Castro-Vázquez SS, Guerrero-Rodríguez SL, Mondragon-Peralta A, De La Fuente-Granada M, Pérez-Tapia SM, González-Arenas A, Velasco-Velázquez MA. 2019. Transcriptome-based identification of lovastatin as a breast cancer stem cell-targeting drug.

Velasco-Velázquez MA, Velázquez-Quesada I, **Vásquez-Bochm LX**, Pérez-Tapia SM. 2019. Targeting Breast Cancer Stem Cells: A Methodological Perspective.

Salinas-Jazmín N, González-González E, **Vásquez-Bochm LX**, Pérez-Tapia SM, Velasco-Velázquez MA. 2017. In Vitro Methods for Comparing Target Binding and CDC Induction Between Therapeutic Antibodies: Applications in Biosimilarity Analysis.

RESUMEN

El cáncer de mama (CaMa) es una enfermedad neoplásica con una alta mortalidad y morbilidad en mujeres en todo el mundo. La teoría de las células troncales tumorales (CTT) propone que existe una subpoblación de células cancerosas que dirige la iniciación, mantenimiento y respuesta a la terapia en el cáncer de mama. Por lo tanto, las CTT de mama (CTTM) han sido consideradas como un nuevo blanco para el desarrollo de terapias novedosas. Con el objetivo de reposicionar fármacos contra las CTTM comparamos una firma de expresión que define a las CTTM contra los cambios transcripcionales inducidos por más de 1300 compuestos bioactivos que se encuentran en la plataforma de Connectivity map (CMap). Encontramos 5 fármacos (fasudil, pivmecilinam, ácido ursólico, 16,16-dimetilprostaglandina E2 (PGE2) y lovastatina) capaces de inducir una anticorrelación con la firma de expresión de CTTM. Empleando un modelo *in vitro*, evaluamos la capacidad de los fármacos seleccionados para inducir cambios fenotípicos en la población de CTTM. Lovastatina y fasudil son capaces de inhibir la transactivación del promotor de SOX2 en las células MDA-MB-231, pero solo lovastatina es capaz de disminuir la eficiencia de formación de mamoesferas, el porcentaje de células ALDH⁺ y la expresión de genes que controlan la troncalidad. Descubrimos que la adición de mevalonato revierte los efectos generados por lovastatina, lo cual sugiere que la lovastatina afecta a la población de CTTM a través de la inhibición de su blanco reportado, la 3-hidroxi-3-metil-glutaril-coenzima A reductasa (HMGCR). Nuestros resultados identifican a la lovastatina como un fármaco que reduce la fracción de CTTM mediante la inhibición de la HMGCR. Tras profundizar en su mecanismo de acción, este fármaco podría ser utilizado como una terapia adyuvante para el CaMa.

ABSTRACT

Breast cancer (BrCa) is a neoplastic disease with high mortality and morbidity in women worldwide. The theory of cancer stem cells (CSC) proposes that a subpopulation of cancer cells drives the initiation, maintenance and response to therapy in breast cancer. Therefore, breast CSC (BCSC) are considered targets for the development of new therapies against BrCa. With the aim of repositioning drugs against BCSC, we compare an expression signature that defines such population against the transcriptional changes induced by more than 1300 bioactive compounds using the Connectivity map platform. We found 5 drugs (fasudil, pivmicillinam, ursolic acid, 16, 16-dimethylprostaglandin E2 (PGE2) and lovastatin) that induces transcriptional responses that anticorrelate with the BCSC expression signature. Thus, those drugs may reduce the BCSC population.

Using an *in vitro model*, we evaluate the ability of the selected drugs to induce phenotypic changes in the BCSC population. Lovastatin and fasudil can inhibit transactivation of SOX2 promoter in MDA-MB-231 cells, but only lovastatin is capable to decreasing the efficiency of formation mammospheres, percentage of ALDH⁺ cells and expression of genes that control stemness. We found that the addition of mevalonate reverses the effects generated by lovastatin, which suggests that lovastatin affects the BCSC population through the inhibition of its canonical target, 3-hydroxy-3-methyl-glutaryl-coenzym A reductase (HMGCR). Our results indicate that lovastatin is a drug that reduces the fraction of BCSC by inhibiting HMGCR. A better knowledge of the mechanism of action of this drug, could cause the consideration of lovastatin as an adjuvant therapy for BrCa.

1. INTRODUCCIÓN

1.1. CÁNCER

El cáncer es un conjunto de enfermedades caracterizadas por presentar una proliferación descontrolada [1]. Se desarrolla a través de la acumulación progresiva de mutaciones genéticas y alteraciones epigenéticas que activan oncogenes e inactivan genes supresores de tumores.

Hanahan y Weinberg describieron las alteraciones esenciales que se desarrollan durante el incremento en la malignidad de un tumor. Estas alteraciones son: mantenimiento de la señalización proliferativa, evasión de los supresores de crecimiento, evasión de la respuesta inmune, presentan inmortalidad replicativa, promueven la inflamación, inestabilidad genómica, resistencia a la muerte celular, desregulación metabólica, inducción de la angiogénesis, activación de la invasión y metástasis (**Figura 1**) [2].

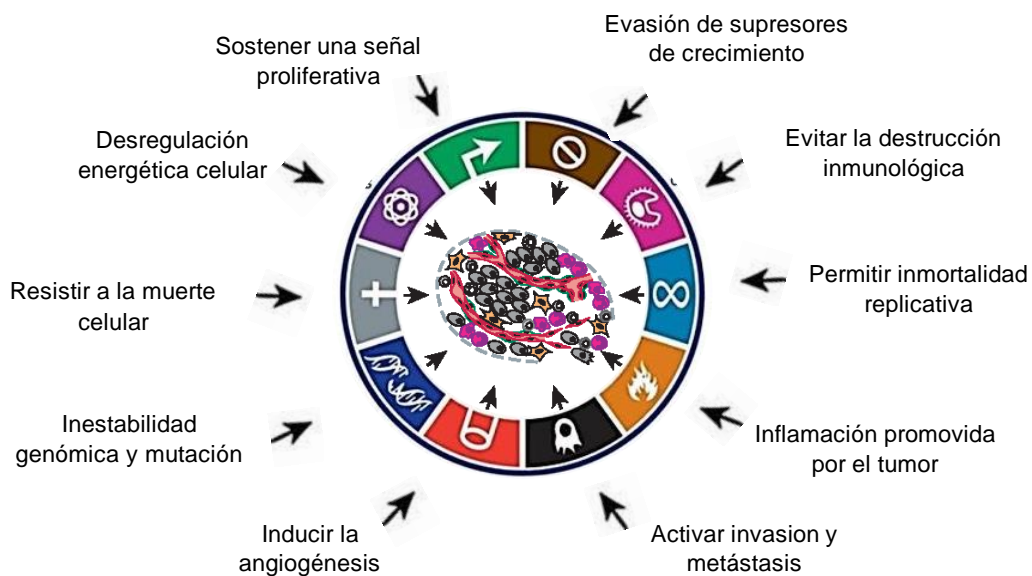


Figura 1. Alteraciones esenciales. Modificado de Hanahan y Weinberg 2011 [2]

1.2. CLASIFICACIÓN DE CÁNCER

La clasificación más común del cáncer es según el tejido en el cual se origina:

- Epitelial/Carcinoma: Representan del 80 al 90 % de todos los casos de cáncer [1, 3]. Se encuentran compuestos de células epiteliales, sin embargo, no mantienen el arreglo estructural de los tejidos epiteliales sanos. Se pueden subdividir en:
 - Adenocarcinoma. Consiste en células epiteliales especializadas en la secreción de sustancias en los ductos o cavidades. Por ejemplo, los adenocarcinomas de seno se originan en los conductos o en los lobulillos.
 - Carcinoma de células escamosas. Se origina en los epitelios que forman capas protectoras como: piel, cérvix, pulmón [4].
- Sarcoma. Cáncer de origen mesenquimal, puede derivar de fibroblastos, tejido conectivo o de soporte (huesos, tendones, cartílagos, músculos), adipocitos y osteoblastos.
- Hematopoyético. Compuesto por células de tipo linfóide o por células destinadas a formar eritrocitos.

Existe un subgrupo denominado linfoma que se desarrolla específicamente en glándulas o ganglios del sistema linfático y se encuentra constituido por linfocitos T y/o B. Este a su vez se subclasifica en linfoma de Hodgkin y linfoma de no Hodgkin [5].
- Melanoma. Tipo de cáncer que se origina en los melanocitos.
- Sistema Nervioso Central. Proceden de células de la glía (gliomas), células de Schwann (Schwannomas), astrocitos (astrocitomas), entre otros [6].

1.3. EPIDEMIOLOGÍA

El cáncer de mama (CaMa) tiene una alta morbilidad y mortalidad en mujeres en todo el mundo (**Figura 2**) [7]. Se estima que aproximadamente 3.2 millones de nuevos casos serán diagnosticados para el 2050 [8]. A pesar de recibir quimioterapia, radioterapia, cirugía o la combinación de éstos, se estima que la recurrencia se presenta en más del 40% de los pacientes, provocando que un tercio de los pacientes diagnosticados con CaMa mueren debido a la resistencia tumoral, recurrencia y metástasis [9].

En las mujeres mexicanas, a partir del año 2006 hasta el 2018, el CaMa se convirtió en la primera causa de muerte por cáncer al presentarse 6 884 fallecimientos [10]. El INEGI ha determinado que en el 2009 se presentaba la muerte de 14 mujeres por día, a causa del CaMa [11]. Según datos del Departamento de Epidemiología de la Secretaría de Salud la incidencia se incrementó de 2000 al 2013, cambiando de 10.76 a 26.1 casos por cada 100 000 habitantes. Por lo que se estima que durante 2013 se generaron 23 873 nuevos casos en México [12].

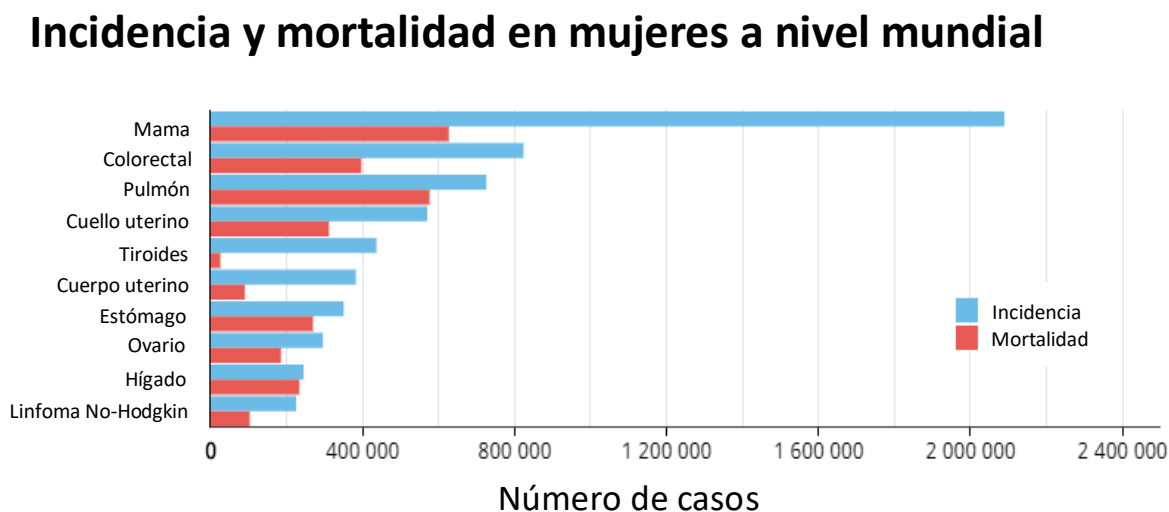


Figura 2. Estadísticas de incidencia y mortalidad de las principales neoplasias a nivel mundial. Modificada de Globocan 2018 [10].

1.4. CÁNCER DE MAMA

El CaMa es un adenocarcinoma que se cataloga como una enfermedad heterogénea y compleja que se desarrolla en las células de la glándula mamaria. Se encuentra asociado con diferentes características histopatológicas, biológicas y clínicas importantes para determinar el pronóstico y el tratamiento de los pacientes [13].

Existen diversas formas de clasificar el cáncer de mamá dentro de las que destacan:

- Subtipo histológico: La organización Mundial de la Salud ha reconocido al menos 17 tipos distintos [14].
- Subtipo molecular. Involucra la expresión o ausencia de marcadores como son: receptor de progesterona, receptor de estrógeno (ER), o el receptor de crecimiento epidérmico humano 2 (HER2). Utilizando estos marcadores como referencia se elaboró la clasificación expresada en la **Tabla 1** [15].

Tabla 1. Clasificación según subtipos moleculares

Subtipo de carcinoma mamario	Receptores
Luminal A	PR ⁺ , ER ⁺ , HER2 ⁻
Luminal B	PR ⁺ , ER ⁺ , HER2 ^{+/-}
HER2	PR ⁻ , ER ⁻ , HER2 ⁺
Triple negativo	PR ⁻ , ER ⁻ , HER2 ⁻

Esta clasificación ha sido la más utilizada debido a que estos biomarcadores son factores pronósticos y predictivos ya validados, por lo que su expresión en los carcinomas de mama resulta fundamental para guiar el tratamiento de los pacientes como se muestra en la **Figura 3**. Además de considerarse como pronóstico para la

recurrencia de la enfermedad después de la conservación de la mama o mastectomía [16, 17].

En México el 60 % de los casos de CaMa son positivos a receptores hormonales (Luminal A o B), mientras que para HER2 representa el 17 % de los casos y el triple negativo el 23 % [18].




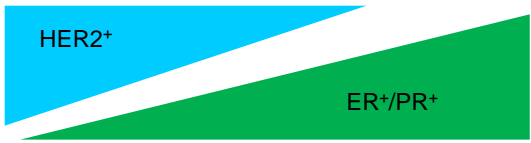


Fenotipo de la célula cancerosa	 Basal	 Basal luminal	 Luminal
Subtipo molecular	Triple negativo	HER2 ⁺	Luminal B Luminal A
Frecuencia en pacientes	15 - 23 %	10 - 15 %	20% 40%
Expresión de receptores			
Pronóstico			
Terapia			

Figura 3. Pronóstico según subtipo molecular [18]

1.5. DETECCIÓN

La detección temprana es representada, en la mayoría de los casos, un buen pronóstico. Por esto, la identificación temprana es uno de los principales objetivos de los programas de salud pública en el mundo.

Los principales métodos de diagnósticos son:

- Autoexploración mamaria
- Estudios de imagen: mastografía, ultrasonido mamario, resonancia magnética y tomografía por emisión de positrones
- En caso de presentar lesiones sospechosas se realizan biopsias y estudios histopatológicos [19]

La mayoría de las personas a las que se les ha diagnosticado algún cáncer viven en países de ingresos bajos o medios, tal es el caso de México. Se ha reportado que menos del 30% de estos países disponen de servicios de diagnóstico y tratamiento de acceso general, y a menudo carecen de sistemas de derivación de los presuntos casos de cáncer lo que retrasa y fragmenta la atención [20]. Provocando en el caso de nuestro país que la incidencia a etapas avanzadas aumente.

1.6. TRATAMIENTO CONTRA EL CÁNCER DE MAMA

Los métodos terapéuticos en la actualidad se clasifican en:

- Cirugía
 - Conservadora. Resección del tumor y tejido sano circundante. Utilizada cuando los tumores localizados son primarios y se encuentran encapsulados.
 - Mastectomía radical. Cuando el cáncer se presenta en más de un sitio de la mama.

- Radioterapia
 - Adyuvante. Administrada cuando los pacientes han recibido un tratamiento quirúrgico.
 - Neoadyuvante. Antes de un tratamiento quirúrgico, con el objetivo de reducir el tamaño del tumor.
- Quimioterapia. Existen diversos fármacos en el mercado dentro de los que destacan:
 - Tamoxifeno y derivados
 - Inhibidores de aromatasas
- Hormonoterapia (antagonistas de receptores a hormonas esteroides)
- Biotecnológicos (anticuerpos terapéuticos)

La cirugía y la radioterapia son de acción local, mientras que, en la quimioterapia, la hormonoterapia y los tratamientos biotecnológicos son de acción sistémica [21]. Todos estos tratamientos deben ir acompañados de algún tipo de rehabilitación que puede incluir fisioterapia, uso de prótesis, reconstrucción de la mama y/o tratamiento de linfedema [22].

1.7. CÉLULAS TRONCALES TUMORALES

1.7.1. Definición y características de las células troncales tumorales

Las células troncales tumorales (CTT) son células cancerosas con capacidad para generar tumores. Han sido reportadas en casi todos los tipos de leucemias [1] y en todos los tumores sólidos [9]. Estas células comparten características con las células troncales normales (CT), por ejemplo: tienen el potencial de proliferarse de forma indefinida lo que ayuda a la iniciación y propagación de los tumores. Otra característica es que son capaces de autorrenovarse, en donde la célula se puede dividir de forma simétrica o asimétrica. Adicionalmente estas células cuentan con la propiedad de poder diferenciarse en diversos tipos de células funcionales, que

usualmente, son las que generan la heterogeneidad de un tumor como se muestra en la **Figura 4** [1, 23].

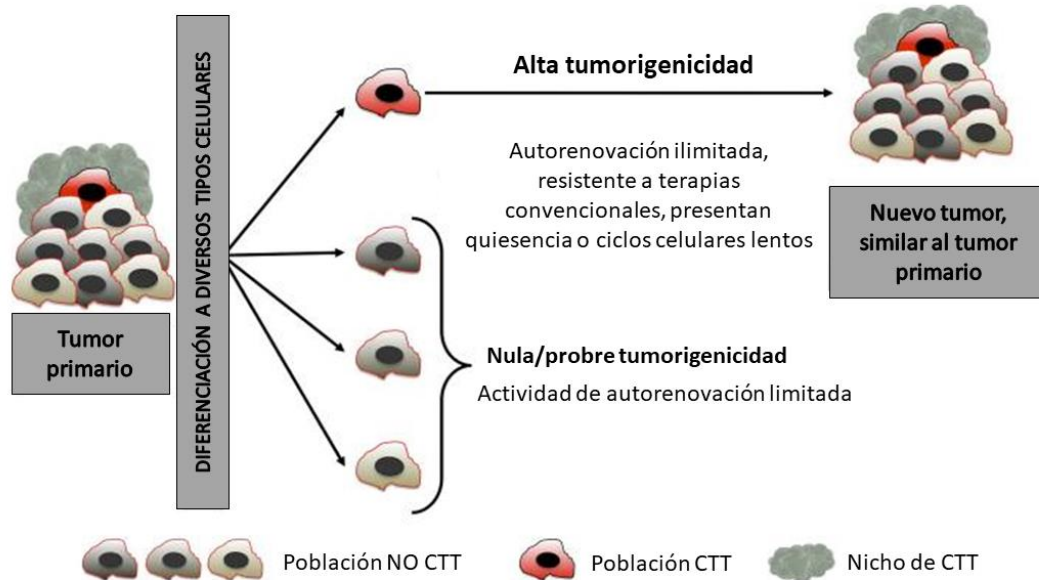


Figura 4. Heterogeneidad tumoral. Los tumores se encuentran conformados por células cancerosas con diferentes propiedades. Las características de las CTT son: inducción de la citotoxicidad, autorrenovación, y promoción de la diferenciación. Modificado de Baccelli et al [24].

Lo anterior explica las observaciones clínicas como son el fenómeno de quiescencia y el proceso de metástasis, la recurrencia después de una radio o quimio terapia efectiva, que puede deberse un transporte alterado en la membrana, y a que cuentan con mecanismos de reparación de ADN [25].

1.7.2. Teorías del inicio de las células troncales tumorales

Existen 2 teorías reportadas del origen de este tipo de células. La primera conocida como “modelo de evolución clonal”, explica que cada célula cancerosa en el tumor podría ganar la capacidad de autorrenovarse y desdiferenciarse en los numerosas y heterogéneos linajes de células cancerosas que comprenden un tumor [26]. La otra teoría denominada como “modelo de jerarquía” hace la suposición que cada

tumor es un conglomerado heterogéneo de células cancerosas y solo una minoría de ellas posee estas propiedades, se menciona que las CTT son generadas por la mutación de células troncales adultas o células progenitoras adultas [1]. Ambas teorías siguen vigentes debido a que existe evidencias que las sustentan tanto *in vitro* como *in vivo*.

1.7.3. Evidencia de las CTT en tumores

La aproximación más usada para confirmar la presencia de CTT en tumores humanos consiste en su separación utilizando marcadores celulares únicos y posteriormente realizar el trasplante de un pequeño número de células en un ratón inmunocomprometido [1, 27]. Esta estrategia se conoce como xenotransplante a dilución limitante.

En la última década del siglo XX y la primera del XXI se han reportado la identificación de CTT en diferentes tipos de cáncer entre los que destacan: leucemia [28], colorrectal [29], mama [30] y cerebro [31].

Las CTT representan una pequeña fracción del tumor total. Por lo que con el objetivo de encontrar nuevas terapias y distinguir esta pequeña población de las demás células su identificación es esencial. Actualmente los marcadores de CTT se han clasificado en diferentes categorías entre los que destacan: i) los llamados marcadores de superficie como son CD44, CD24 y CD133; ii) los marcadores de pluripotencia como son SOX2, Nanog, OCT4 y MYC; iii) los del grupo que promueve la resistencia a fármacos como son los transportadores ABC y la enzima aldehído deshidrogenasa (ALDH).

1.7.4. Células troncales en cáncer de mama

Las células troncales de cáncer de mama (CTTM) fueron identificadas con el uso de los marcadores de superficie CD44⁺/CD24⁻/ESA⁺ [30]. Al-Hajj y colaboradores describieron que la presencia de 200 de estas células es suficiente para formar tumores al ser inyectadas en ratones NOD/SCID. Cuando se aíslan células CD44⁺/CD24^{-/low} de los tumores generados y estas se inyectan en nuevos ratones,

las células que cuentan con dicho fenotipo son capaces de formar tumores con mayor eficiencia.

El análisis de CTTM utilizando el inmunofenotipo CD44⁺/CD24⁻ ha sido ampliamente reportado. Wang *et al* demostraron que aislar esa población a partir de la línea luminal MCF-7 incrementa la eficiencia de formación de tumores y metástasis [32]. Para esa misma línea celular Yan *et al* corroboraron la capacidad tumorigénica del inmunofenotipo, así como un incremento en la invasión [33].

Cuando Liu *et al* evaluaron la correlación del porcentaje de células CD44⁺/CD24⁻ con su efecto sobre las CTT en diversas líneas celulares, no encontraron diferencias estadísticamente significativas en la eficiencia formadora de colonias al clasificarlas según su perfil de expresión de CD44⁺/CD24⁻. Junto con Fillmore *et al* reportaron que la expresión de este inmunofenotipo no siempre correlaciona con el potencial de generar tumores o la susceptibilidad a agentes quimioterapéuticos [34, 35].

Adicionalmente, se ha publicado por diversos autores que existe una falta de consistencia entre la expresión de este inmunofenotipo y los cuadros clínicos que presentan los pacientes [36, 37]. Con lo anterior ahora se sabe que este inmunofenotipo es útil para tener una aproximación de la cantidad de CTTM, sin embargo, no es un marcador universal, lo que ha generado la necesidad de buscar nuevos marcadores para complementar la caracterización de las CTTM.

1.7.5. Marcadores de CTT en cáncer de mama

Se ha descrito que las CTTM cuentan con la capacidad de autorrenovación, y expresan proteínas y factores de transcripción que promueven la pluripotencia [30, 38] , por lo que se han reportado el uso de los marcadores mencionados a continuación.

1.7.5.1. Factor de transcripción SOX2

SOX2 es un miembro de la familia de genes de la región determinante del sexo Y-box 2. Las proteínas de esta familia comparten un dominio de unión al ADN del grupo de alta movilidad (HMG) altamente conservado, y se dividen en subgrupos,

de acuerdo con el grado de homología con este dominio. Se conoce que los miembros de esta familia son factores de transcripción resultando cruciales para el desarrollo normal, el mantenimiento de la troncalidad y la autorrenovación; así como la inhibición de la diferenciación [39, 40].

Las funciones de SOX2 tienen una dependencia del contexto biológico, ya que se ha demostrado que muchas proteínas influyen con la unión a sus genes objetivos [41]. La interacción con tantos cofactores confiere una gran flexibilidad a SOX2 convirtiéndolo en un factor clave para el desarrollo embrionario [42], el mantenimiento de la pluripotencia y la autorrenovación en CT embrionarias de ratón [43].

Se ha encontrado que SOX2 tiene una alta expresión en CT de melanoma. Su eliminación disminuye drásticamente la autorrenovación de esferas de melanoma, y su silenciamiento inhibe significativamente la capacidad de iniciar tumores [44]. Al silenciar SOX2 en CaMa es posible disminuir la proliferación de células tumorales y la formación de tumoresferas [45], así como la tumorigenicidad en modelos animales [46].

SOX2 se expresa en una variedad de carcinomas de mama posmenopáusicos en etapa temprana y en ganglios linfáticos metastásicos, por lo que diversos investigadores sugieren que SOX2 desempeña un papel temprano en la carcinogénesis de mama y su alta expresión promueve el potencial metastásico [47, 48].

En el 2012 Sachlos *et al*, desarrollaron una herramienta que consiste en la medir la intensidad de GFP que se encuentra correlacionada con la expresión de SOX2 y OCT4, permitiendo comparar la diferenciación resultante de la adición de un fármaco sobre las CTT y las CT. Encontrando que la tioridazina se dirige selectivamente contra las células neoplásicas, alterando las CTT capaces de iniciar leucemia sin tener un efecto sobre las CT sanguíneas normales [49].

1.7.5.2. Factor de transcripción OCT4

OCT4 es un factor de transcripción también conocido como Oct-3, Oct-3/4, Otf3 o NF-A3, esta codificado por el gen POU5F1 y pertenece a la POU familia de proteínas de unión al ADN [50].

La expresión de OCT4 está asociada con las propiedades pluripotentes de las CT, es un factor esencial que controla las etapas tempranas de la embriogénesis de mamíferos [51-53]. Estudios en células troncales embrionarias reportaron que su diferenciación depende de los niveles de OCT4 [54]. OCT4 suele formar complejos con otros factores de transcripción como c-MYC, KLF4, y SOX2 [55]. El complejo de OCT4 con SOX2 y NANOG, regula la expresión de varios genes, trabajando cooperativamente en una red transcripcional interdependiente que estimula la transcripción no solo de sus propios genes, sino también la expresión de genes clave necesarios para la embriogénesis, incluidos FGF4 y Zfp42 / Rex1 [56]. Otra de las funciones reportada de los complejos formados por OCT4 es activar y mantener la expresión de genes involucrados en la autorrenovación, y simultáneamente reprimir genes que median la diferenciación [57].

La presencia de niveles altos de OCT4 aumentan el potencial maligno con un fenotipo tumoral más agresivo, mientras que la inactivación de OCT4 induce la regresión del fenotipo maligno con una morfología más diferenciada [58]. La alta expresión de OCT4 y NANOG se ha asociado con carcinogénesis pancreática, mientras que silenciar ambos genes resultó en una disminución de la proliferación, migración, invasión, quimiorresistencia y tumorigénesis en cáncer de páncreas *in vitro* e *in vivo* [56] [59].

En un estudio con la línea celular de cáncer de mama 4T1, las células positivas para Oct4 fueron más tumorigénicas que las Oct4 negativo [60]. Recientemente se reportó que la regulación al alza de la expresión de Oct4, KLF4 y Nanog es debido a la sobreexpresión ZNF32. La alta expresión de ZNF32 y por ende lo altos niveles de OCT4 predicen una pobre supervivencia, la promoción de las propiedades similares a troncalidad y a la progresión del cáncer de mama [61].

Estudios clínicos han demostrado que los tumores con una alta expresión de OCT4 están asociados con una mayor progresión de la enfermedad, una mayor metástasis y una supervivencia más corta relacionada con el cáncer en comparación con los tumores con expresión moderada y baja de OCT4 [62] [63].

1.7.5.3. ALDH

Las aldehído deshidrogenasas (ALDH) son un grupo de enzimas intracelulares que oxidan aldehídos y convierten el retinol en ácido retinoico, que interviene en el control de las vías de diferenciación [64]. Se ha reportado que ALDH se expresa de forma elevada en células CTT y proporciona protección contra el agente alquilante ciclofosfamida [65-67].

La actividad de ALDH puede usarse de forma independiente o en combinación con marcadores de superficie para identificar CTT en neoplasias malignas hematopoyéticas y en tumores sólidos, incluidos los de mama, colón, próstata, pulmón, ovario [66, 68].

En CaMa, ALDH1A3 ha demostrado ser la principal isoforma responsable de la actividad de ALDH [69, 70]. La presencia de una alta actividad de ALDH en CTTM, les confiere la capacidad de con tan solo 20 células con fenotipo CD44⁺/CD24⁻/ALDH⁺ es posible formar tumores en ratones NOD/SCID, lo que ha sugerido que aquellas células con una alta actividad de ALDH es una población enriquecida en CTTM [66, 71]. La presencia de este marcador se encuentra relacionado con un mal pronóstico en pacientes con CaMa [70].

Para la determinación de la actividad de esta enzima se utiliza frecuentemente un kit (ALDEFLUOR[®]) que contiene un aldehído fluorescente que es sustrato de ALDH, llamado BAAA (BODIPY-aminoacetaldehído). Este sustrato es convertido por la ALDH a un producto fluorescente BAA⁻ (BODIPY-aminoacetato), que al presentar una carga negativa, se retiene dentro de las células [72]. Al aumentar la cantidad de acetato fluorescente dentro de las células es posible analizarlas mediante citometría de flujo.

Sin embargo, la fracción de ALDH⁺ en diferentes líneas celulares de CaMa es variable. Aquellas líneas celulares que representan un fenotipo triple negativo (MDA-MB-468) o que son HER2 positivas (SKBR-3), presentan un alto porcentaje de células ALDH⁺. En contraste los porcentajes de células ALDH⁺ en células positivas a ER (MCF7, T47D) es bajo, llegando a presentar valores menores al 1% de la población. Por lo que la actividad de ALDH, así como la determinación del inmunofenotipo CD44⁺/CD24⁻, no puede ser considerado como un marcador universal para las CTTM [71, 73].

1.7.6. Importancia clínica de las células troncales tumorales en cáncer de mama

Las CTTM representan un papel importante en la resistencia, recurrencia y progresión de los tumores de CaMa [23, 38]. Se ha reportado que las CTTM generan una resistencia a fármacos citotóxicos [74], presentan una hiperactivación de vías de señalización implicadas en el control de troncalidad [75], y un aumento en la reparación de ADN [76].

La metástasis, y no el tumor primario, suele ser la principal causa de muerte en pacientes con cáncer. El proceso de metástasis consiste en que las células deben migrar del tumor primario, transportarse por el torrente sanguíneo y llegar a un nuevo nicho donde serán capaces de formar nuevos tumores [77]. Se ha reportado que las CTTM son esenciales para el proceso de diseminación de tumores, siendo encargadas de formar tumores secundarios en órganos distantes y promoviendo la proliferación y heterogeneidad el nuevo tumor [78]. Lo anterior debido a que se ha identificado que las CTT se pueden diseminar a la médula ósea u otros sitios como pulmón e hígado y promover metástasis [75, 79].

Existe evidencia que muestra que el proceso de transición epitelial a mesenquimal (EMT) es necesario para el proceso de metástasis, y que los marcadores de EMT se encuentran expresados en CTT [80]. Un ejemplo es el marcador de fenotipo

mesenquimatoso Zeb1 que puede facilitar el proceso de que células cancerosas tengan propiedades similares a las CT [81, 82].

A la fecha se han identificado firmas genéticas, obtenidas de CTT, que predicen la recurrencia tumoral y la metástasis [38, 83]. Aunado a lo anterior, la presencia de CTT ha comenzado a plantearse como una posible herramienta de pronóstico en pacientes con CaMa metastásico [84]. Se ha encontrado que metástasis pleurales de pacientes con CaMa que ya han recibido quimioterapia presentan un enriquecimiento en la subpoblación CD44⁺/CD24⁻ [85].

Reafirmando el vínculo existente entre la quimioresistencia de las CTT y la metástasis, Creighton *et al*, publicaron que aquellas células resistentes de CaMa a la terapia endocrina o terapia citotóxica muestran características de CT y viceversa [86].

1.7.7. Desarrollo de terapias contra las CTT

Como se ha mencionado hasta el momento muchas de las estrategias terapéuticas actuales intentan eliminar las células cancerosas mediante quimioterapia antiproliferativa, la cual suele tener beneficios limitados.

Las células tumorales con características de troncalidad son más resistentes a los medicamentos quimioterapéuticos que las demás células del tumor [1]. Sin embargo, es una necesidad la búsqueda de blancos terapéuticos contra esta pequeña población celular dentro de la masa tumoral por lo que se han desarrollado diferentes estrategias que terminen con este tipo de células. Entre las que destacan Gupta *et al* identificaron que la salinomicina, un fármaco usualmente utilizado como antibacteriano o coccidiostático, inhibe el crecimiento tumoral en CaMa, induce la diferenciación epitelial de las CTT y regula a la baja genes CTT en las células tumorales [87].

Utilizando un cribado de moléculas pequeñas Sachlos *et al* encontraron que la tioridazina, un fármaco utilizado comúnmente como antipsicótico, era capaz de

inducir de forma selectiva la diferenciación de las CTT y no así a las CT somáticas humanas [49].

En julio del 2019 se completó la fase III del primer inhibidor del factor de transcripción STAT3 específico contra CTT en cáncer de páncreas. Este fármaco llamado BBI608 desarrollado por Boston Biomedical fue administrado en combinación con un anticancerígeno en pacientes con cáncer de páncreas avanzado, sin embargo, ni la FDA ni ninguna otra autoridad la ha aprobado [88]. Esto sugiere que en el futuro se desarrollarán terapias específicas contra CTT, incluyendo las de mama.

1.8. REPOSICIONAMIENTO DE FÁRMACOS

1.8.1. Definición

El reposicionamiento de fármacos es el proceso de encontrar una nueva indicación terapéutica para un fármaco previamente aprobado [89]. Este proceso ha comenzado a tener más interés al compararlo con el método tradicional del descubrimiento de fármacos, debido a que reduce el riesgo de la presencia de efectos tóxicos, tiene un tiempo de validación clínica menor y el nuevo uso es susceptible a ser patentado [90]. El reposicionamiento de fármacos cuenta con la ventaja de que se cuenta con estudios preclínicos y clínicos para la evaluación de seguridad en humanos; lo que genera que la aprobación del nuevo uso terapéutico sea más rápida. A largo plazo esto es una ventaja para los pacientes porque tienen el beneficio de que se reducen los riesgos y se acelera el acceso a un tratamiento [89].

Sin embargo, el reposicionamiento de fármacos no se encuentra libre de riesgos, porque debe demostrar la actividad terapéutica, aprobar parámetros farmacológicos y observaciones clínicas que deben ser perfectamente analizadas para disminuir los riesgos en la fase clínica.

1.8.2. Estrategias transcriptómicas para el reposicionamiento de fármacos

Para descubrir conexiones no explícitas o no reconocidas previamente entre los fármacos, los blancos y las enfermedades, se han reportado diversas estrategias, que incluyen modelos computacionales, métodos basados en los mecanismos de acción, revisión de efectos secundarios en común, y evaluación de perfiles de expresión genética [91].

Los estudios de perfiles transcripcionales se realizan utilizando firmas de expresión diferencial de genes, que son un conjunto de genes que es expresado diferencialmente en dos condiciones experimentales; por ejemplo tejido sano vs. tejido enfermo, o células que han sido expuestas a un fármaco vs. células control [92-94]. La idea central de esta estrategia es que el nivel de expresión de un gen se puede modificar según las circunstancias de la célula y, por lo tanto, el conjunto de genes subexpresado o sobrepresado representa un estado biológico en específico. Realizar la comparación de los cambios en la expresión de genes que genera una enfermedad contra los cambios que genera la exposición de cultivos de células expuestas a un fármaco, podría identificar nuevas correlaciones entre fármacos y enfermedades. Teóricamente, los fármacos que inducen un cambio en la transcripción opuesto al que se produce en una enfermedad tendrían que ser capaces de revertir el fenotipo de la enfermedad, con lo que se encontraría una nueva aplicación terapéutica para dicho fármaco [95]. Por esto, diferentes bases de datos y programas en línea han sido desarrollados con el objetivo de trasladar los análisis de la transcripción de genes en el descubrimiento de nuevos fármacos [96-98].

1.8.3. CMap

Connectivity Map (CMap) es una base de datos pública desarrollada por el *Broad Institute*, que contiene diferentes firmas de expresión diferencial, que son el

resultado del tratamiento de líneas celulares con una colección de 1300 compuestos bioactivos. Estas firmas de expresión diferencial son comparadas con otras firmas que son de interés a través de un algoritmo que utiliza un análisis estadístico similar al de Kolmogorov-Smirnov como se muestra en la **Figura 5** [99].

CMap ha sido útil para el reposicionamiento de fármacos, para descubrir estructuras líderes para nuevos compuestos, y analizar mecanismos de acción [100]. CMap se ha utilizado en la identificación de nuevas actividades de fármacos en diversas neoplasias. Por ejemplo: Manzotti *et al* determinaron que la amantadina, un fármaco aprobado como antiviral, inducía una diferenciación del tipo monocito-macrófago al tratar líneas celulares de leucemia mieloide (HL60, U937 y Kasumi-1) [101]. Mientras que en el estudio de Jade *et al*, CMap resultó una herramienta clave, ya que permitió el descubrimiento de que la withaferin A (un aislado de la planta *Withania somnifera*) induce apoptosis celular y autofagia en líneas celulares de cáncer de pulmón.

El uso de CMap no se encuentra limitado a las neoplasias, por lo que también ha sido empleado para reposicionar fármacos en otras enfermedades. Tal es el caso de Zonggui *et al*, que descubrieron que el pirivinio, un antihelmíntico clásico, podría ser un anti-adipogénico útil en la terapia contra la obesidad.

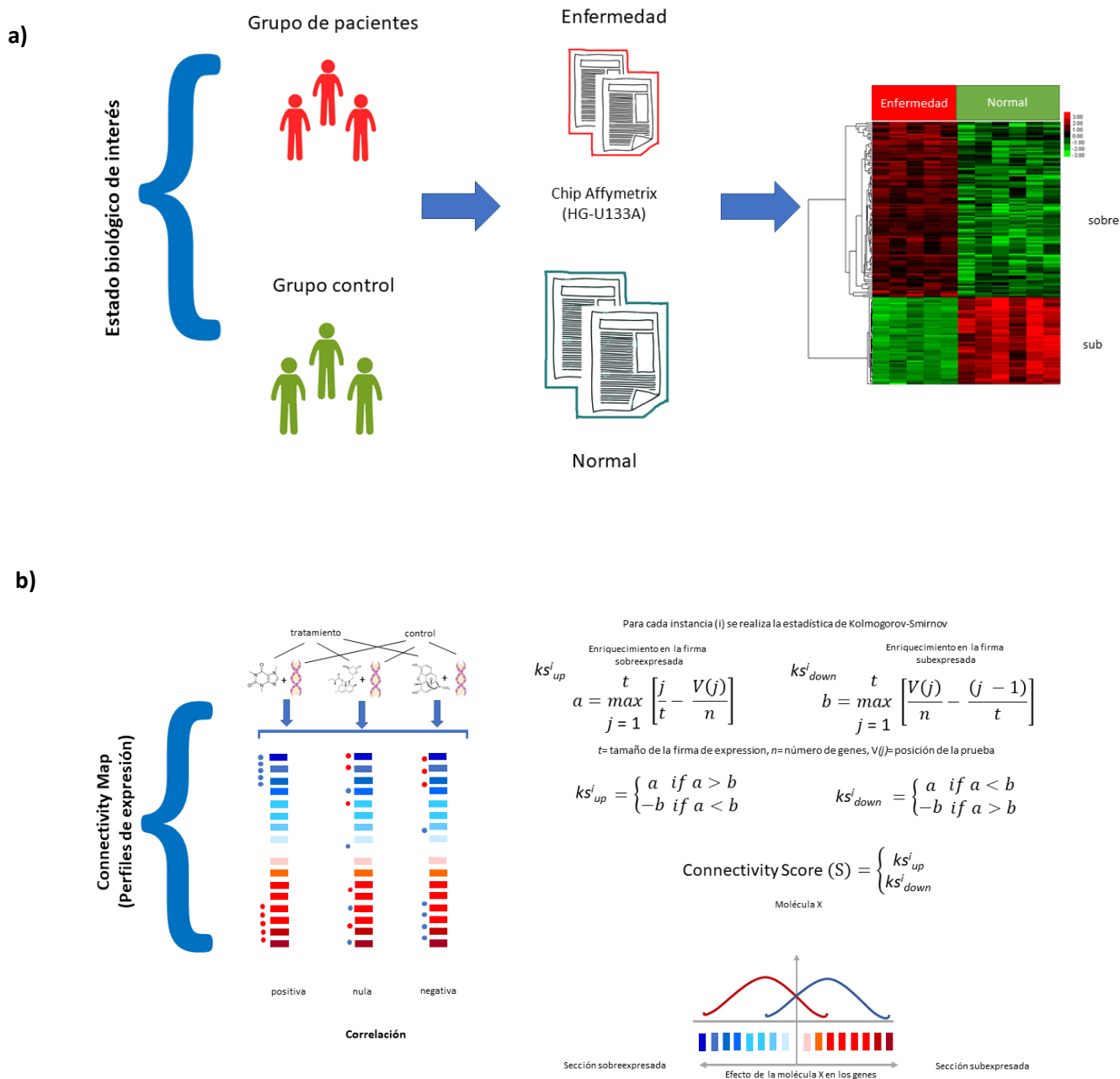


Figura 5. Flujo de trabajo en Connectivity Map. a) Obtención de una firma de expresión diferencial que defina el problema biológico de interés. b) Asignación de un valor según similitud encontrada entre las firmas contenidas en la base de datos y la firma de expresión diferencial de interés. [102].

1.9. ESTATINAS

Las estatinas son medicamentos potentes empleados en la clínica para reducir el colesterol y prevenir enfermedades cardiovasculares. Son moléculas de origen fúngico que gracias al desarrollo farmacéutico posterior han logrado un mejor potencial terapéutico.

Las siete estatinas aprobadas por la FDA son: lovastatina, simvastatina, pravastatina, fluvastatina, atorvastatina, rosuvastatina y pitavastatina. Estas presentan diferencias en la biodisponibilidad, proporción lipofílica/hidrofílica, metabolismo regulado por el citocromo 450, y su mecanismo de transporte celular. Dentro de sus principales efectos adversos se destacan la toxicidad hepática y el riesgo de sufrir diabetes o cataratas [103].

El mecanismo de acción reportado para este grupo de medicamentos es a través de la inhibición competitiva y reversible de la enzima hidroximetilglutaril coenzima-A reductasa (HMG-CoA reductasa), encargada de generar el mevalonato para realizar la síntesis de colesterol [104].

Recientemente las estatinas han atraído la atención como potenciales agentes terapéuticos en varios tipos de cáncer. De hecho un estudio epidemiológico danés mostró una reducción del 15% en la mortalidad por cualquier tipo de cáncer al comparar usuarios de estatinas contra no usuarios [105]. Se cuenta con reportes específicos del efecto que generan las estatinas contra la mortalidad relacionada con CaMa [106, 107].

Estudios preclínicos han demostrado que las estatinas juegan un papel importante en inhibir la angiogénesis en células de cáncer colorrectal que sobre expresan HER2 [108], en suprimir la vía PI3K/AKT/mTor y la ruta MAPK/ERK [109] y, en alterar la glicosilación de ABCB1 en células de neuroblastoma [110].

Existen reportes *in vitro* de que en CaMa fluvastatina y simvastatina aumentan la citotoxicidad, y que este efecto es revertido por la adición de mevalonato [111]. También se ha reportado que la atorvastatina es capaz de inhibir la proliferación,

invasión, EMT, la vía PTEN/AKT y promover la apoptosis en células de CaMa al promover la inactivación de RhoB [112].

Lovastatina cuenta con reportes *in vitro* de que en CaMa es capaz inhibir la proliferación [113] e inducir apoptosis [114, 115] . Así mismo existen reportes de su efecto sobre la acción en las CTT en carcinoma nasofaríngeos [116], leucemia [117] y CaMa [118].

2. JUSTIFICACIÓN

Los tratamientos existentes no son efectivos en todas las pacientes con cáncer de mama. La eficacia limitada de esas terapias, así como la generación de resistencia, se explica parcialmente porque esos tratamientos no actúan sobre las CTT. El reposicionamiento de fármacos podría identificar nuevos fármacos que presenten una actividad inhibitoria contra las CTT.

3. OBJETIVO

Reposicionar fármaco(s) con capacidad para revertir el fenotipo troncal tumoral en cáncer de mama.

4. HIPÓTESIS

El uso combinado de firmas transcripcionales que definen a las CTT y de bases de datos que contienen información de los cambios transcripcionales inducidos por compuestos bioactivos permitirá seleccionar y reposicionar fármacos con capacidad de inducir una reducción en el número de CTTM.

5. MATERIALES Y MÉTODOS

5.1. SELECCIÓN DE LA FIRMA DE EXPRESIÓN DEFERENCIAL EN CÉLULAS TRONCALES DE CÁNCER DE MAMA

La firma de expresión diferencial que se utilizó para la búsqueda de fármacos es una firma consenso de CTTM previamente reportada [87]. Esta firma contiene 39 genes (25 sobre y 14 subexpresados), los cuales cambian consistentemente en cada una de 3 firmas biológicas que comparan la expresión de CT contra células no troncales mamarias: i) genes de células de CaMa HMLER tratadas con salinomycin (tratamiento que erradica CTT) contra genes de células tratadas con paclitaxel (tratamiento que erradica células no troncales); ii) genes de cultivos primarios de células epiteliales mamarias de humano bajo condiciones que favorecen la expansión de CT epiteliales mamarias contra genes de cultivos celulares bajo condiciones que favorecen la diferenciación; iii) genes de una población CD44⁺ de células epiteliales mamarias humanas normales y neoplásicas (troncales), contra genes de células CD24⁺ (no troncales).

5.2. SELECCIÓN DE FÁRMACOS

Para la identificación de fármacos candidatos para revertir el fenotipo troncal se empleó la plataforma CMap versión 02, que contiene perfiles de expresión diferencial de genes, generados a partir de cultivos de células humanas tumorales tratadas con 1,309 compuestos activos, a diferentes concentraciones y tiempos [99]. Los parámetros utilizados fueron a) asociación negativa con la firma de expresión de CTTM ($p < 0.5$); b) tener un score ≤ 0.5 ; c) valor específico < 0.1 y d) porcentaje nulo-no nulo $\geq 75\%$. La comparación de la respuesta transcripcional global inducida por los compuestos candidatos fue realizada utilizando Modelo de acción de NeTwoRk Analysis (MANTRA) [96] con una distancia de corte (*threshold*) de 0.7.

5.3. RELACIÓN ESTRUCTURA ACTIVIDAD

La relación estructura actividad de cada uno de los fármacos candidatos fue analizado generando huellas digitales (*fingerprints*) utilizando dos representaciones moleculares (MACS y circular [119] [120]). Estas representaciones moleculares se compararon con el programa KNIME con el módulo CDK utilizando la métrica del coeficiente de Tanimoto [121].

5.4. FÁRMACOS

Los siguientes fármacos fueron adquiridos de la compañía Sigma-Aldrich: Clorhidrato de fasudil (número de catálogo HA-1077); pivmecilian (número de catálogo SML0817); ácido ursólico (número de catálogo 89797); 16-16-dimetil-prostaglandina E2 (PEG2) (número de catálogo D2250000); lovastatina (número de catálogo PHR1285). Las soluciones stock de los fármacos fueron preparadas en dimetilsulfóxido (DMSO) y almacenadas a - 70 °C, protegidas de la luz, hasta su uso. La solución stock de mevanolactona con número de catálogo M4667 de Sigma Aldrich se preparó en agua, y se resguardó a - 70 °C hasta su uso.

5.5. LÍNEAS CELULARES

Se utilizaron dos líneas celulares en este trabajo, ambas corresponden al subtipo basal, triple negativo. La primera fue la línea celular de CaMa MDA-MB-231, obtenida de ATCC. Las células se cultivaron en medio *Roswell Park Memorial Institute* 1640 (RPMI-1640, GIBCO) suplementado con 10 % de suero fetal bovino (SFB, GIBCO), en 5 % de CO₂, a 37 °C. La segunda línea, Hs578T, se obtuvo de ATCC, se cultivaron en medio *Dulbecco's Modified Eagle's Medium – High glucose* (DEMEM-Alta glucosa, GIBCO), suplementado con 10 % de suero fetal bovino (SFB, GIBCO), en 5 % de CO₂, a 37 °C.

Las sublíneas celulares de MDA-MB-231 que expresan de forma estable al gen reportero luciferasa (*luc*) bajo el control de los promotores de SOX2 u OCT4

(POU5F1), se generaron por cotransfección utilizando el vector pGL3 y los plásmidos pSOX2-luc o p-OCT4-luc (donados por Richard Pestell, Baruch S. Blumberg Institute, PA USA). Las transfecciones se realizaron utilizando lipofectamina 3000 (Invitrogen) como indica el fabricante. Las sublíneas que expresaron de forma estable la construcción del reportero fueron seleccionadas y mantenidas en medio RPMI, 10 % SFB con 0.5 µg/mL de puromicina.

Para realizar los experimentos las células se despegaron del plástico de cultivo al que se encontraban adheridas utilizando tripsina 0.05 % EDTA (GIBCO).

5.6. ENSAYOS DE VIABILIDAD

Los cambios en la viabilidad celular se analizaron empleando el ensayo colorimétrico de Bromuro de 3(4,5 dimetil-2-tiazolil)-2,5-difeniltetrazólio (MTT) [122]. Para este ensayo se sembraron 5 000 células MDA-MB-231 o 3 000 células Hs578T por cada pozo de una placa de 96 pozos (Nunc) en 100 µL de medio. Se expusieron durante 24 h a 100 µL de fármaco a diferentes concentraciones, y como control se expusieron al disolvente correspondiente. Transcurrido ese tiempo las células tratadas se incubaron con 1 mg/mL de MTT durante 90 min. El formazán formado se disolvió en DMSO y se cuantificó en un espectrofotómetro a 570 nm (Epoch, BioTeK). El ensayo se realizó por triplicado para cada uno de los fármacos en concentraciones diferentes.

Para realizar el análisis, las lecturas de absorbancia obtenidas en cada experimento se normalizaron contra el control de solvente. Con estos datos se calculó la concentración inhibitoria 50, utilizando una regresión no lineal con un modelo de dosis-respuesta de inhibición (log vs respuesta de 3 parámetros) con el programa GraphPad Prism 6. El análisis estadístico se determinó mediante ANOVA seguido de una comparación múltiple de Dunnet.

5.7. ENSAYO DE GEN REPORTERO DEPENDIENTE DE LA TRANSACTIVACIÓN DE LOS PROMOTORES DE SOX2 U OCT4

Se sembraron 30 000 células MDA-MB-231 transfectadas con el promotor del factor de pluripotencia de SOX2 u OCT4, en placas de 24 pozos. Las células se expusieron a diferentes fármacos y diferentes concentraciones durante 24 h, se colocaron 2 pozos para la evaluación de la viabilidad y dos pozos para la evaluación de la transactivación de los promotores, por cada fármaco. Transcurrido este tiempo se adicionó MTT a los pozos correspondientes para determinar la viabilidad. Para determinar la expresión del gen reportero dependiente de la transactivación de los promotores (proporcional a la transactivación del promotor), se retiró todo el medio del pozo y se adicionaron 100 µL de buffer de lisis (1 % tritón X-100, 1 mM DTT en GME buffer (25 mM Gly-Gly, 15 mM MgSO₄, 4 mM EGTA)) a cada pozo. Se agitó a 100 rpm durante 10 min a temperatura ambiente. Se recolectó todo el volumen y se transfirió a un tubo eppendorf ultratransparente. A cada tubo se adicionaron 300 µL de Mix de ATP (17 mM K₂PO₄, 1 mM DTT y 2 mM ATP en GME buffer). Se adicionaron 100 µL de luciferina (GOLDBIO) justo antes de leer en el luminómetro GLOMAX® 20/20 (Promega).

Los resultados de luminiscencia se obtuvieron al restar el valor del blanco a cada lectura. Los valores se normalizaron contra el promedio de la viabilidad, para obtener la actividad del transgen por el número de células vivas.

5.8. ENSAYO DE FORMACIÓN DE MAMOESFERAS

Se sembraron 100 células MDA-MB-231 o 120 células Hs578T en una placa de ultra baja adherencia (Corning Costar) de 96 pozos. Las células se colocaron en 100 µL de medio MammoCult (StemCell Technologies) suplementado con factores de crecimiento como indica el fabricante.

Los fármacos fueron evaluados a diferentes concentraciones por octuplicado. Al tercer día se adicionaron 50 µL de medio con fármaco. Después de 7 días se toman fotografías de cada pozo con el objetivo 4 x de un microscopio Eclipse Ti-U Nikon.

La cuantificación se realizó con el software NIS Elements Imaging Software 4.13 (Nikon). Se consideraron mamoesferas a las colonias con diámetro mayor a 80 μm . En algunos experimentos las células se trataron durante 24 h con el fármaco a diferentes concentraciones en condiciones adherentes. Posteriormente, las células se recolectaron y se sembraron en placas de ultra baja adherencia en ausencia de fármaco, siguiendo el protocolo descrito en el párrafo anterior.

Los resultados se presentan como eficiencia de formación de mamoesferas (% EFM), y fue calculado con la siguiente ecuación:

$$\% \text{ EFM} = \frac{(\text{número de mamoesferas por pozo})}{(\text{número de células sembradas por pozo})} \times 100$$

5.9. ENSAYO DE ACTIVIDAD DE LA ENZIMA ALDEHÍDO DESHIDROGENASA

Se sembraron 400 000 células MDA-MB-231 o 350 000 células Hs578T en un pozo de placa de 6 para cada condición experimental. Se dejaron en adhesión durante toda la noche. Se adicionó lovastatina (2.5, 5 o 10 μM) y/o mevalonato (100 μM) y las células se cultivaron durante 24 h. Transcurrido este tiempo, se lavaron los pozos con PBS para retirar las células muertas, posteriormente se adicionaron 300 μL de tripsina y se incubó durante 5 min. La tripsina se inactivó con 600 μL de RPMI (10 % SFB) o DEMEM (10 % SFB) según corresponda al tipo de células, todo el volumen del pozo se recuperó y colocó en un tubo para centrifugarlo a 800 g durante 5 min. Se contaron las células y se colocaron 250 000 células vivas en 900 μL de buffer de ensayo del kit de ALDH. Se adicionó a la suspensión celular 5 μL de sustrato, se mezcló e inmediatamente se trasladó la mitad del volumen total, al tubo que contiene 7 μL de inhibidor dietilaminobenzaldehído (DEAB; control negativo de tinción). Se incubó durante 45 min a 37 $^{\circ}\text{C}$, en oscuridad, agitando manualmente cada 10 min. Terminado este tiempo se centrifugó durante 5 min a 3 000 rpm y retiró el sobrenadante. Las células se resuspendieron en 250 μL de buffer de ensayo y se analizaron en el citómetro Attune Nxt (Life Technologies). Se estableció como señal

negativa la obtenida en la muestra de DEAB. Los datos fueron analizados con FlowJo 8.7 (Tree Star Inc).

5.10. ANÁLISIS DE ENRIQUECIMIENTO DE GENES

Se obtuvieron de la base Gene Expression Omnibus (GEO) los datos de microarreglos provenientes de tumores de mama de ratón que fueron tratados con lovastatina junto con sus correspondientes controles (clave es GSE42787) [123]. Estos datos fueron normalizados utilizando R studio (v1.1.383) utilizando una normalización robusta promedio de múltiples conjuntos. El Análisis de Enriquecimiento del Conjunto de Genes (GSEA, por sus siglas en inglés) fue realizado utilizando el software GSEA (v2.2.3, Broad) [124]. Las firmas moleculares empleadas en el análisis incluyen: i) firma consenso de troncalidad *Consensus Stemness Ranking* (CSR por sus siglas en inglés), la cual contiene genes sobreexpresados en CTT y ha sido asociada con tumores en etapas avanzadas y pobre pronóstico en múltiples tipos de cáncer [125]; ii) firma de CT mamarias en ratón y humano [126]; iii) firma de EMT, que contiene los genes con cambios sustantivos durante dicho proceso (obtenida de la base de datos GSEA) [127]; y iv) firma que contiene los genes expresados diferencialmente en carcinomas ductuales invasivos [128].

5.11. WESTERN BLOT

Las células tratadas a diferentes condiciones se lisaron con buffer RIPA (50 mM Tris-HCl, 0.1 % SDS, 150 mM NaCl) suplementado con inhibidores de proteasas (5 µg/mL leupeptina, 1 µg/mL pepstatina, 2 µg/mL aprotinina). Las concentraciones de los lisados fueron determinadas utilizando el kit Pierce BCA Protein Assay Kit (Thermo Fisher Scientific). Para cada condición, 30 µg de proteína total fueron separados utilizando SDS-PAGE y transferidos a una membrana de PVDF mediante un electroblotted. Se realizó un bloqueo con leche al 5 % en PBS, después del cual

las membranas fueron incubadas con anticuerpo anti-SOX2 (Abcam 97959; 1:1000). Como anticuerpo secundario se usó un anticuerpo de cabra anti-conejo conjugado con HRP (Santa Cruz Biotechnology sc-2004; 1:5000). Las mismas membranas fueron sometidas a stripped como se ha reportado [129] e incubadas con un anticuerpo anti- α -tubulina (Santa Cruz Biotechnology sc- 398103; 1:500), seguido de una incubación con el anticuerpo secundario de cabra anti-ratón conjugado con HRP.

Las bandas de proteína se detectaron utilizando *SuperSignal West Femto Maximum Sensitivity Substrate Pierce ECL Western Blotting Substrate* (Thermo Fisher Scientific). La intensidad de las bandas fue determinada utilizando el Image J [130], los datos fueron normalizados contra la señal obtenida en las células tratadas con el vehículo correspondiente (DMSO).

6. RESULTADOS

6.1. PREDICCIÓN *IN SILICO* DE FÁRMACOS CONTRA CTTM

La firma de expresión diferencial seleccionada se empleó para realizar una búsqueda en la plataforma de CMap. Como resultado, los 1,309 compuestos que se encuentran en dicha plataforma se jerarquizaron, basados en la probabilidad de que induzcan cambios transcripcionales semejantes u opuestos a los de la firma de interés. Utilizando los criterios de selección descritos en la metodología, se identificaron 6 fármacos con potencial para revertir la firma empleada para la búsqueda (**Tabla 2**). En todos esos casos el valor de *P* fue significativo y las respuestas generadas son específicas, es decir el fármaco no induce cambios que puedan asociarse con otras firmas seleccionadas de forma aleatoria.

Tabla 2. Fármacos con potencial para revertir el fenotipo de CTTMs

Compuesto	Actividad farmacológica/Indicación terapéutica	Valor promedio de CMap	Valor de p	Especificidad
Fasudil	Vasoespasma cerebral	-0.71	0.02382	0
Espiperona	Esquizofrenia	-0.677	0.00592	0.0088
Pivmecilinam	Antibiótico	-0.606	0.00438	0.0111
Ácido ursólico	Antimicrobiano	-0.601	0.00203	0.0073
16, 16-dimetil prostaglandina E2	Prevención de úlceras en el estómago	-0.572	0.00877	0.0138
Lovastatina	Anticolesterolemiantes	-0.527	0.0118	0.0155

Como se muestra en la **Figura 6a**, los fármacos seleccionados muestran una estructura distinta. Lo anterior se corrobora al compararlos mediante un análisis de huella estructural utilizando las representaciones moleculares de MACS y circular, ya que es posible apreciar que aún entre los fármacos con mayor similitud los valores de comparación están por debajo de 0.7 (**Figura 6b**).

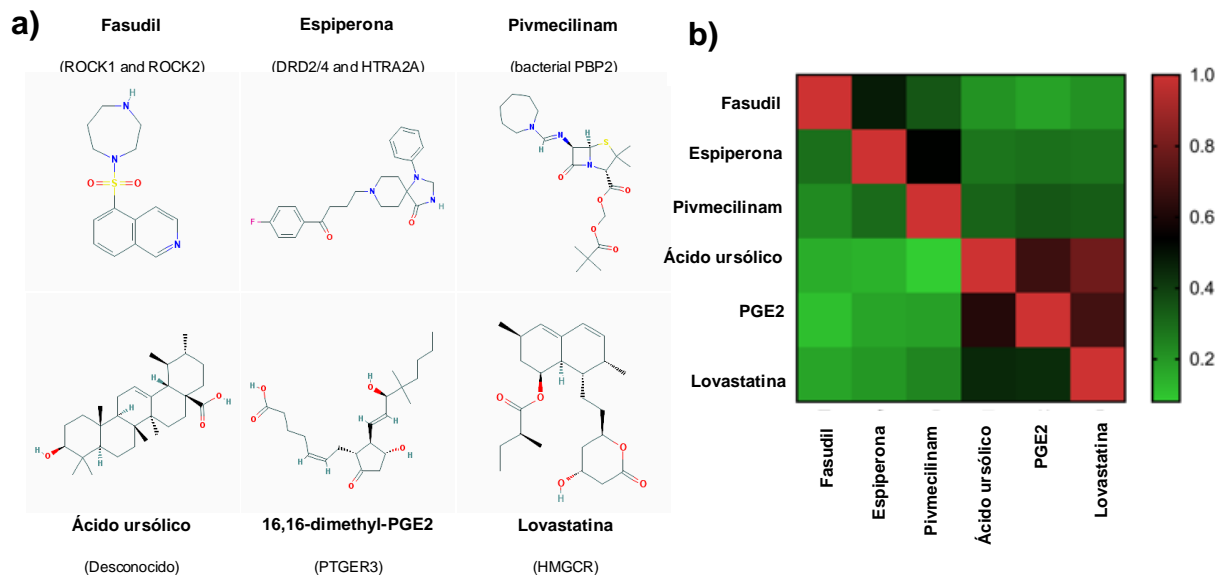


Figura 6. Evaluación de la similitud estructural. a) Estructuras de los 6 fármacos y su blanco de acción reportado. b) Comparación estructural utilizando la representación molecular circular (parte inferior) y la representación molecular MACS (parte superior).

Con el objetivo de comparar los cambios transcriptómicos globales (es decir, no sólo en los genes de interés) de los 6 fármacos identificados, realizamos un análisis en el servidor MANTRA (<http://mantra.tigem.it>). Dicho análisis permite identificar si los cambios globales en la expresión de genes inducidos por los fármacos seleccionados son similares a los generados por otros fármacos dentro de la base de datos. Como se observa en la **Figura 7**, los cambios inducidos por espiperona y ácido ursólico son similares a los inducidos por otros compuestos bioactivos. En contraste, el perfil transcriptómico que genera el tratamiento con fasudil no tiene similitud con ningún otro compuesto en la base de datos. Este análisis también demuestra que la actividad en el transcriptoma de los 6 candidatos (triángulos rosas

en la **Figura 7**) es disimilar entre sí. En conjunto, la información de los blancos canónicos de los fármacos candidatos, sus diferencias estructurales, y su distinta actividad en el transcriptoma, sugieren que cada uno de los candidatos tendría un mecanismo de acción diferente para revertir la firma de CTT seleccionada, por lo que decidimos que todos debían estudiarse *in vitro*. En nuestro estudio no realizamos ensayos en cultivo con espiperona pues su alto costo impidió su adquisición, por lo que los ensayos posteriores sólo se realizaron con 5 de los fármacos de interés.

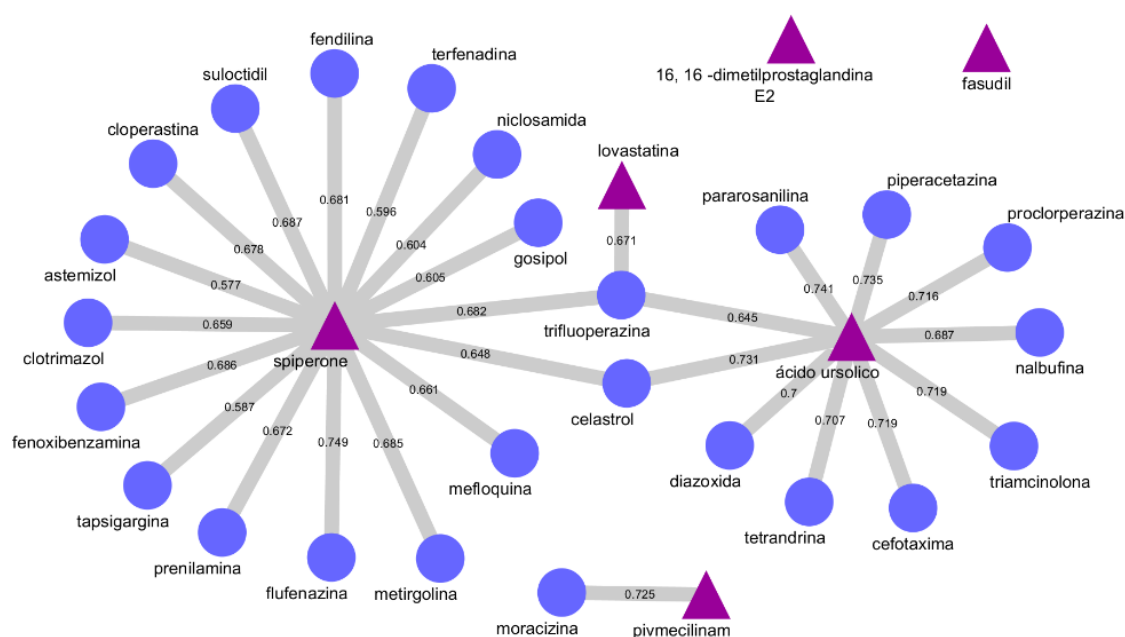


Figura 7. Evaluación en el servidor MANTRA. Los triángulos rosas representan los fármacos candidatos provenientes de la selección en CMap. Los círculos morados representan aquellos fármacos cuyo mecanismo de acción podría estar relacionado. Los valores anotados sobre las líneas corresponden a un puntaje de similitud transcripcional entre fármacos.

6.2. EFECTO DE LOS FÁRMACOS EN LA VIABILIDAD

La evaluación de la viabilidad se realizó para descartar que las concentraciones a utilizar en los demás estudios produzcan muerte celular en alto porcentaje. La viabilidad se determinó en tres replicados biológicos empleando el ensayo colorimétrico de MTT. En la **Figura 8** se muestra un ejemplo de las curvas-

concentración obtenidas para cada fármaco, en donde es posible observar que Lovastatina tiene una IC50 de 16.9 μM (**Figura 8b**), mientras que para Fasudil (**Figura 8a**) solo se observa una reducción modesta en la viabilidad al disminuir aproximadamente el 10.5 % a la concentración máxima. La **Tabla 3** resume los datos obtenidos mediante estos ensayos.

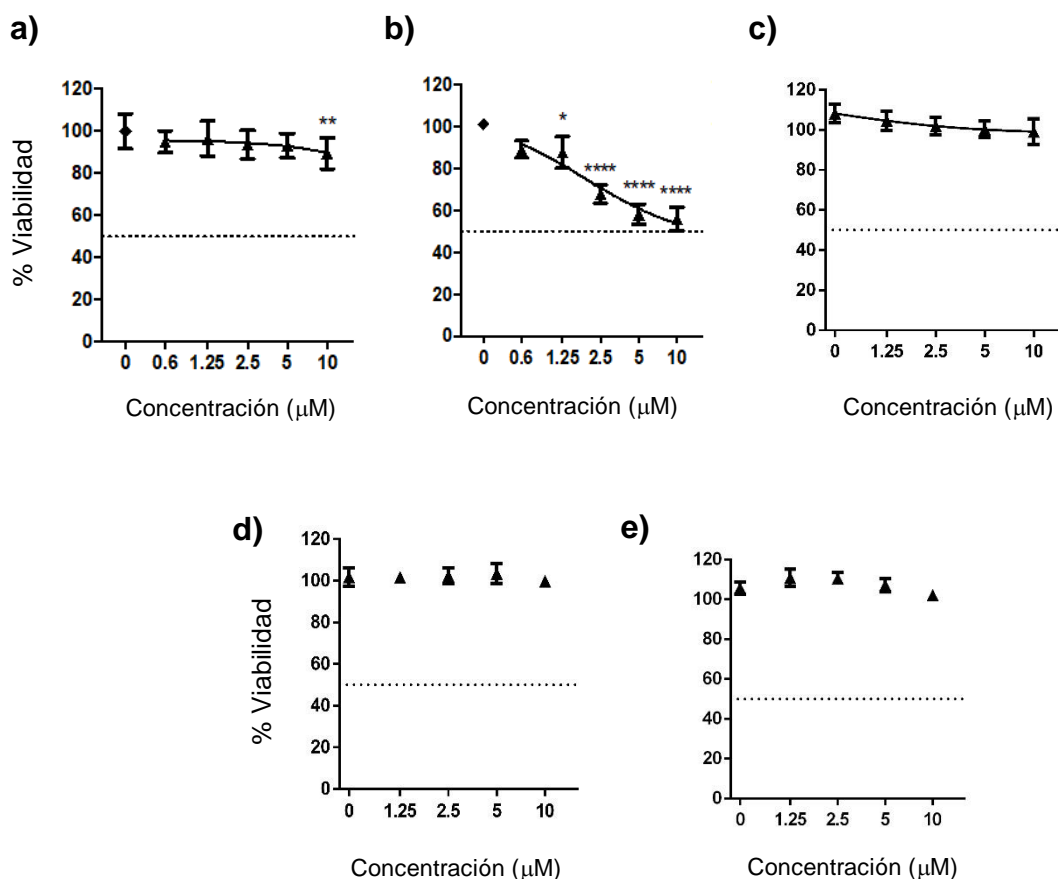


Figura 8. Curvas-concentración representativas del porcentaje de viabilidad obtenidas para cada fármaco contra la respuesta observada en el control. $p < 0.05$ (*), < 0.0001 (****). a) Fasudil. b) Lovastatina. c) PGE2. d) Pivmecilinam. e) Ácido ursólico.

Tabla 3. Valor de IC50 para cada uno de los fármacos seleccionados en células MDA-MB-231

Fármaco	IC50 (μM)
Fasudil	>10
Pivmecilinam	>10
Ácido ursólico	>10
16, 16-dimetil prostaglandina E2	>10
Lovastatina	16.9

6.3. ENSAYO DE GEN REPORTERO PARA DETERMINAR LA TRANSACTIVACIÓN DEL PROMOTOR DE SOX2 U OCT4

SOX2 y OCT4 son reguladores esenciales en la auto renovación celular y mantenimiento de pluripotencia de CTT [46]. Se han reportado construcciones basados en porciones de los promotores para monitorear troncalidad en células de CaMa [131, 132]. Por lo que, como una primera aproximación para evaluar la actividad de los candidatos sobre la subpoblación de CT, se estudió el efecto de los fármacos candidatos (10 μM) sobre la transactivación de los promotores SOX2 y OCT4. Como se puede observar en la **Figura 9** fasudil y lovastatina disminuyeron 60 y 95 % la transactivación del promotor de SOX2, respectivamente. Por otra parte, como se puede apreciar en la **Figura 10**, no se observó que existiera un efecto de forma estadísticamente significativa sobre la transactivación del promotor de OCT4 por parte de ninguno de los fármacos candidatos.

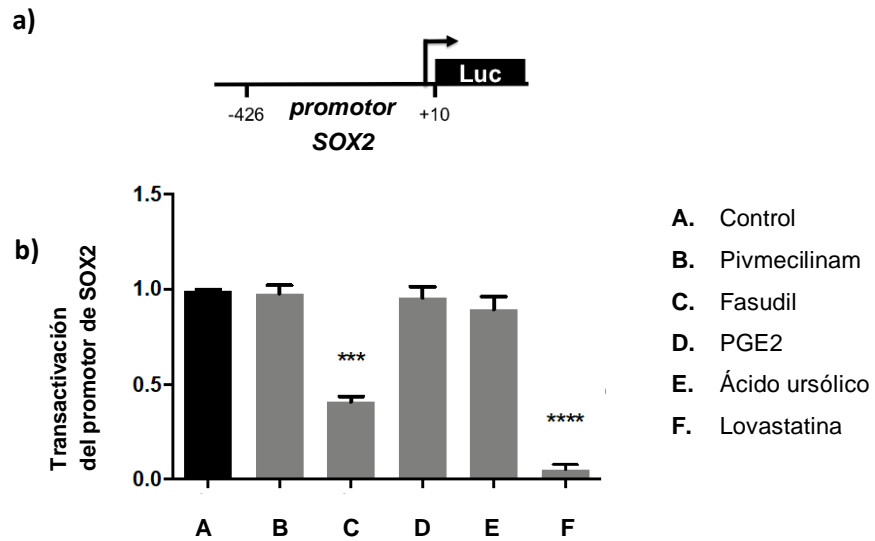


Figura 9. Transactivación del promotor de SOX2. a) Esquema que muestra el tamaño del promotor de SOX2 en la construcción. b) La transactivación del promotor SOX2 fue medida mediante un ensayo de gen reportero, se presenta la gráfica de evaluación de todos los fármacos a una concentración de 10 μ M. La gráfica presenta el promedio \pm SEM de 3 experimentos independientes. $p < 0.001$ (***), < 0.0001 (****) contra el valor del control.

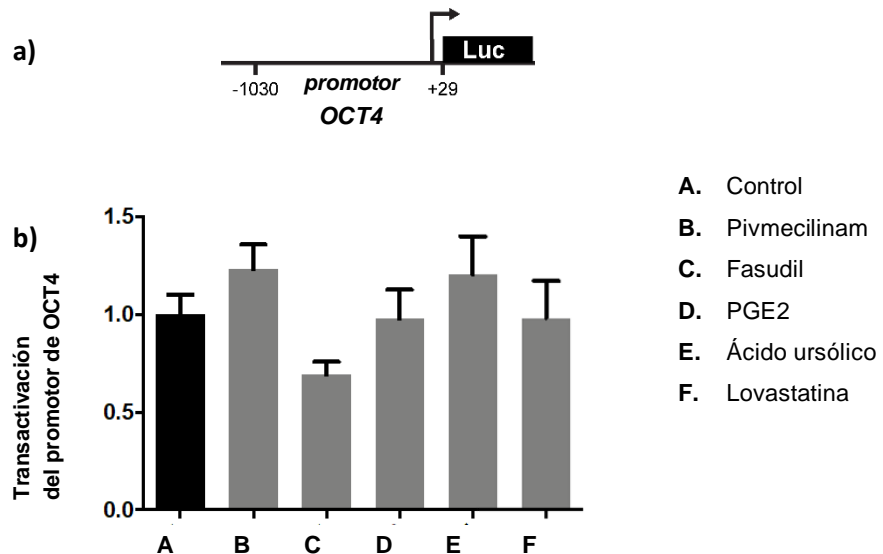


Figura 10. Transactivación del promotor de OCT4. a) Esquema que muestra el tamaño del promotor de OCT4 en la construcción. b) La transactivación del promotor OCT4 fue medida mediante un ensayo de gen reportero, se presenta la gráfica de evaluación de todos los fármacos a una concentración de 10 μ M. La gráfica presenta el promedio \pm SEM de 3 experimentos independientes.

Estos resultados indican que fasudil y lovastatina fueron los mejores candidatos para disminuir el número de CTT, por lo que decidimos enfocarnos en estos dos fármacos en los experimentos posteriores. Para determinar si existía una relación concentración-respuesta se realizó el ensayo de gen reportero a diferentes concentraciones de fármaco, encontrando que lovastatina y fasudil disminuyen la transactivación del promotor de SOX2 de forma concentración dependiente como se observa en las **Figuras 11 y 12**, incluso a la concentración de 0.6 μM .

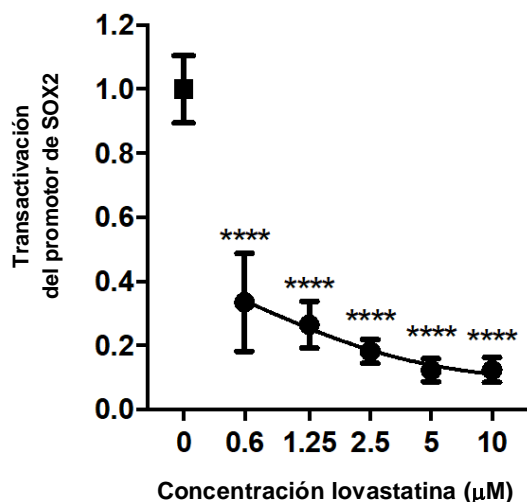


Figura 11. Curva concentración respuesta de la transactivación del promotor de SOX2 a diferentes concentraciones de lovastatina. La gráfica presenta el promedio \pm SEM de 3 experimentos independientes. $p < 0.0001$ (****) contra el valor del control (vehículo).

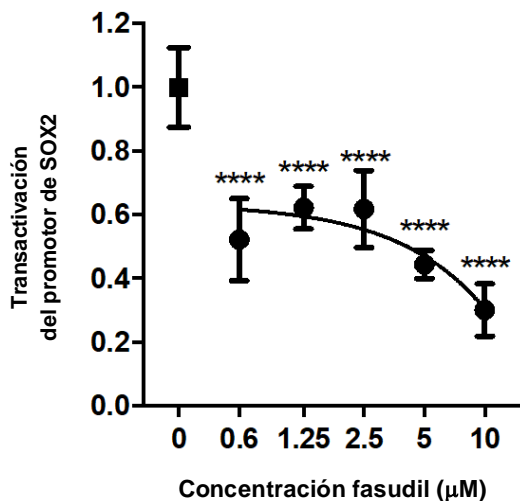


Figura 12. Curva concentración respuesta de la transactivación del promotor de SOX2 a diferentes concentraciones de fasudil. La gráfica presenta el promedio \pm SEM de 3 experimentos independientes. $p < 0.0001$ (****) contra el valor del control (vehículo).

6.4. ENSAYO DE FORMACIÓN DE MAMOESFERAS

La formación de mamoesferas es un ensayo que permite la propagación de células troncales y progenitoras de CaMa. La capacidad de formar mamoesferas correlaciona con la capacidad de iniciar tumores [80, 133, 134]. Por esto, analizamos la eficiencia de formación de mamoesferas (% EFM) en células MDA-MB-231 tratadas con lovastatina o fasudil. La **Figura 13** muestra que diferentes concentraciones de lovastatina disminuyen la eficiencia de formación de mamoesferas, con una IC₅₀ de 2.2 μ M.

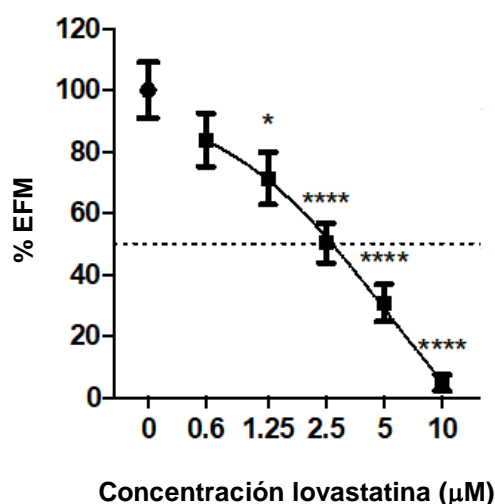


Figura 13. Eficiencia de formación mamoesferas al tratar células MDA-MB-231 con lovastatina durante 7 días. La gráfica presenta el promedio \pm SEM de 3 experimentos independientes. $p < 0.05$ (*), < 0.0001 (****) contra el valor del control. % EFM = Eficiencia de formación de mamoesferas, en porcentaje con respecto al control.

Cuando comparamos este dato con la IC₅₀ obtenida en ensayos de viabilidad, es posible decir que se requiere una concentración 7.7 veces menor para inhibir la formación de mamoesferas que para reducir el número total de un cultivo en 2D. Esto sugiere que la lovastatina puede afectar selectivamente a la población de CTT.

Al realizar este ensayo con fasudil a diferentes concentraciones, no se observa el mismo efecto que con lovastatina (**Figura 14**). Por esta razón, no se realizaron más experimentos con fasudil.

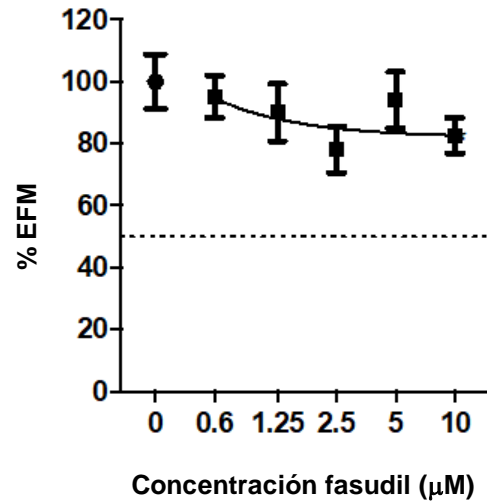


Figura 14. Eficiencia de formación mamoesferas al tratar células MDA-MB-231 con fasudil durante 7 días. La gráfica presenta el promedio \pm SEM de 3 experimentos independientes. % EFM = Eficiencia de formación de mamoesferas, en porcentaje con respecto al control.

Con el objetivo de corroborar la disminución de la población troncal, empleamos un protocolo publicado previamente [87] que consiste en tratar los cultivos en 2D durante un corto periodo de tiempo (24h), colectar las células viables, y evaluar la eficiencia de la formación de mamoesferas en ausencia de fármaco. Se encontró que la lovastatina es capaz de evitar la formación de mamoesferas de forma estadísticamente significativa lo que sugiere que el fármaco disminuye la población troncal de forma irreversible en la línea celular MDA-MB-231 como se muestra en la **Figura 15**.

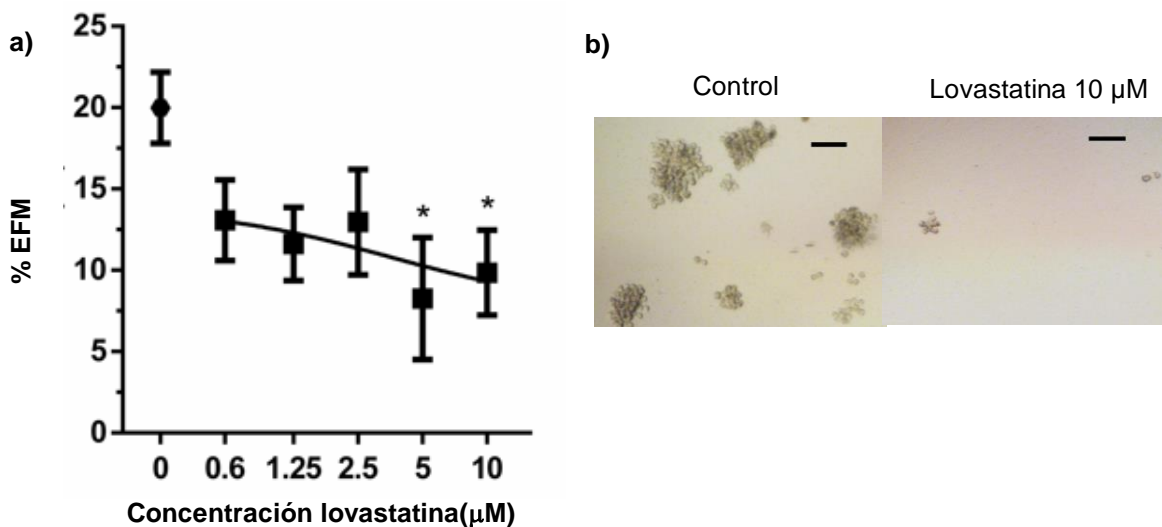


Figura 15. Eficiencia de formación mamoesferas al tratar células MDA-MB-231 con lovastatina durante 24 h. a) La gráfica presenta el promedio \pm SEM de 3 experimentos independientes. $p < 0.05$ (*) contra el valor del control b) Imágenes representativas, la barra representa una escala de 100 μm .

La actividad de lovastatina sobre las CTTM se corroboró empleando una segunda línea celular del mismo subtipo que MDA-MB-231. Los experimentos con células Hs578T identificaron que lovastatina también disminuye la eficiencia de formación de mamoesferas en esta línea celular (**Figura 16**).

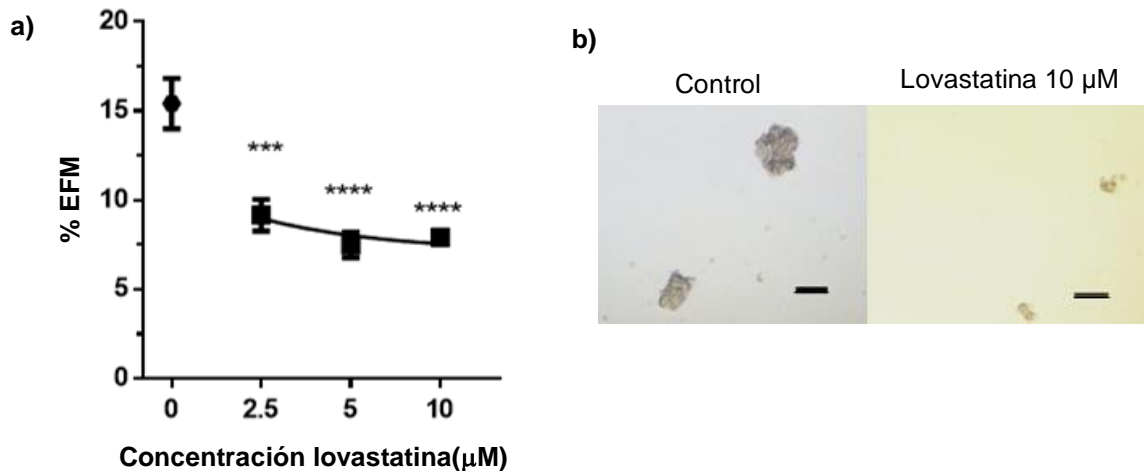


Figura 16. Eficiencia de formación mamoesferas al tratar células Hs578T con lovastatina. a) La gráfica presenta el promedio \pm SEM de 3 experimentos independientes, $p < 0.001$ (***) , < 0.0001 (****) contra el valor del control b) Imágenes representativas, la barra representa una escala de 100 μm .

6.5. ENSAYO DE ACTIVIDAD DE LA ENZIMA ALDEHÍDO DESHIDROGENASA

La actividad de la enzima ALDH ha sido utilizada ampliamente para la caracterización de la población de CT en CaMa [66, 131, 135]. Por lo que con las células tratadas durante 24 h se realizó un ensayo de evaluación de actividad de ALDH. Encontramos que la lovastatina disminuye de forma estadísticamente significativa a la mayor concentración, la actividad de ALDH tanto para células MDA-MB-231 (**Figura 17**), como para Hs578T (**Figura 18**).

Es posible apreciar que el porcentaje de células ALDH⁺ en cada línea celular es diferente. Sin embargo, la tendencia en la respuesta a la presencia de lovastatina se mantiene a una concentración de 10 μM en ambas líneas celulares.

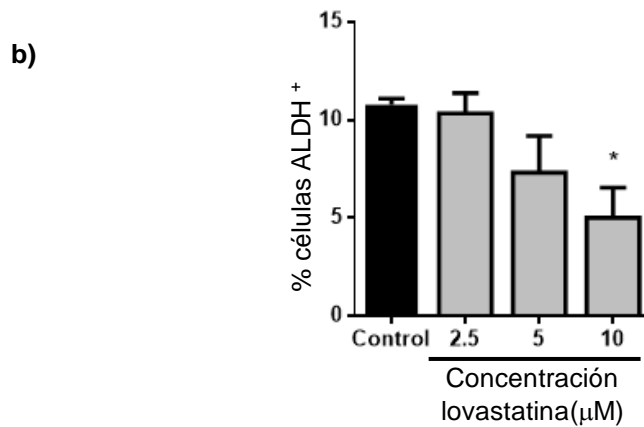
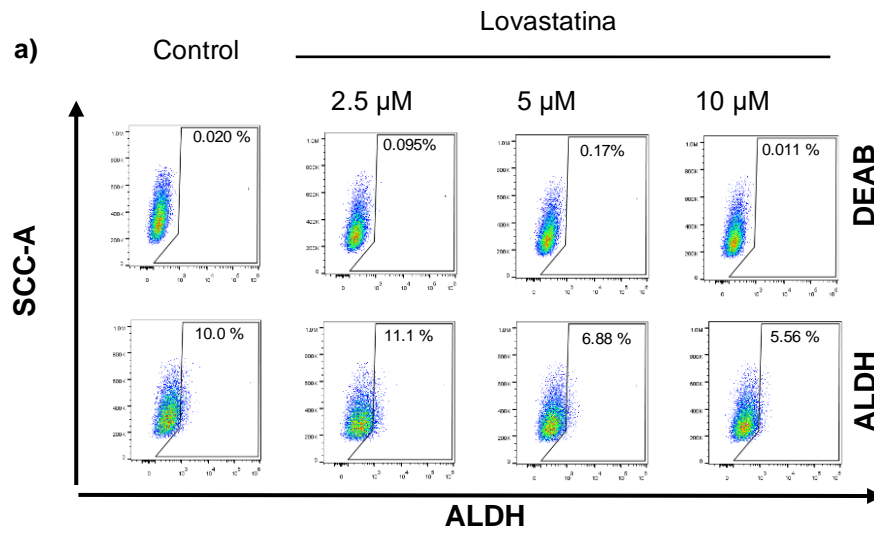


Figura 17. Evaluación de la actividad de ALDH en células MDA-MB-231 tratadas con diferentes concentraciones de lovastatina. a) Dot plot representativos de la fracción ALDH+ en células MDA-MB-231. b) Cuantificación de la fracción celular ALDH+ en cinco experimentos independientes $p < 0.05$ (*) contra el valor del control.

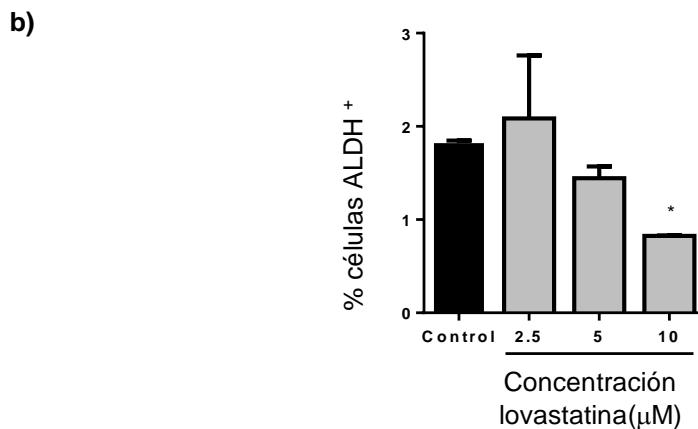
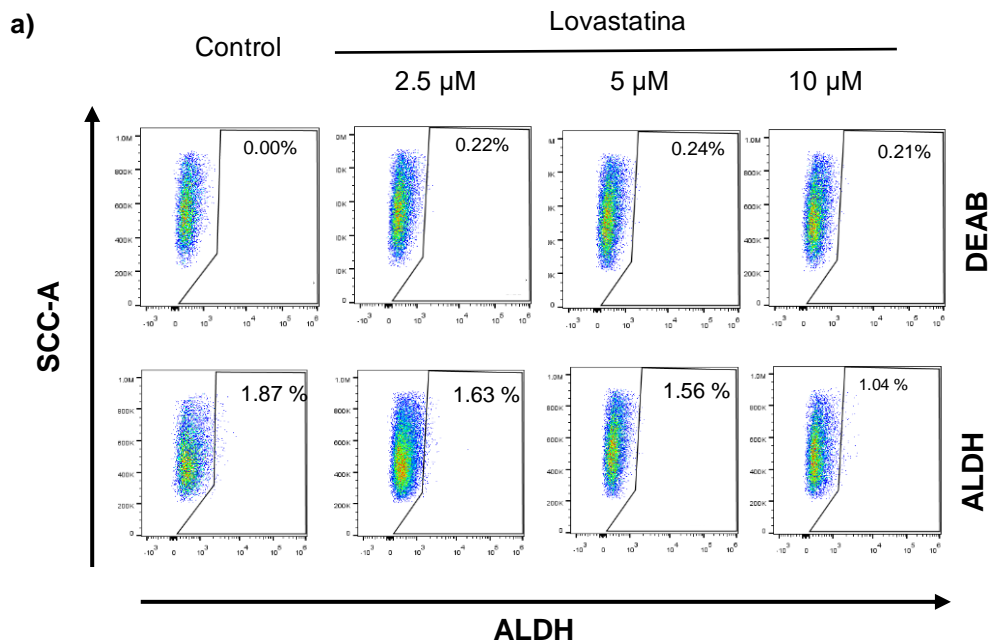


Figura 18. Evaluación de la actividad de ALDH en células Hs578T tratadas con diferentes concentraciones de lovastatina. A. Dot plot representativos de la fracción ALDH⁺ en células Hs578T. B. Cuantificación de la fracción celular ALDH⁺ en dos experimentos independientes. $p < 0.05$ (*) contra el valor del control.

6.6. EVALUACIÓN DE LA EXPRESIÓN DE LA PROTEÍNA SOX2

Para determinar si lo observado mediante el ensayo de gen reportero, sobre la transactivación de SOX2 coincidía con la expresión de la proteína, se decidió realizar ensayos de *western blot*. Como se puede apreciar en la **Figura 19** se

observa una disminución en la expresión de SOX2 de forma estadísticamente significativa. Este efecto que ocurre tanto para la línea celular MDA-MB-231, como para la línea Hs578T, después de tratar ambas líneas con lovastatina a una concentración de 10 μ M.

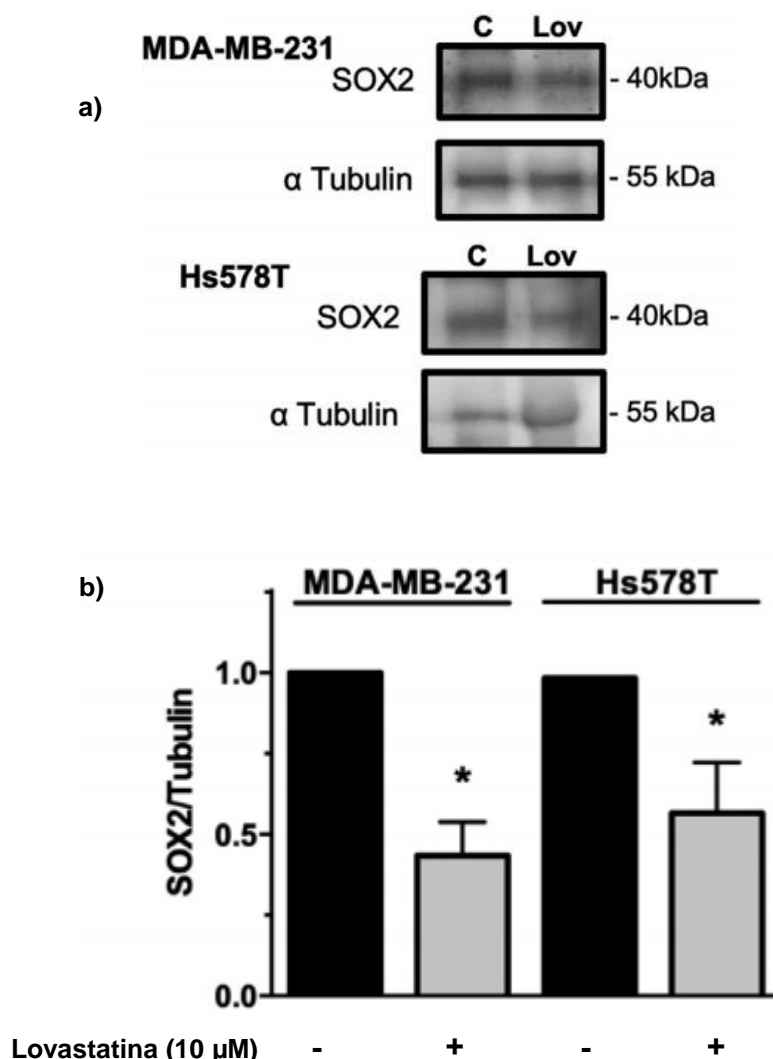


Figura 19. Evaluación de la expresión de la proteína SOX2. a) Se muestra una imagen representativa del western blot utilizado para evaluar la expresión de SOX2 en las líneas celulares MDA-MB-231 y Hs578T. b) Cuantificación de la relación de la expresión de SOX2 contra α -tubulina de tres experimentos independientes. Análisis estadístico determinado por un análisis de t-student $p < 0.05$ (*).

6.7. PARTICIPACIÓN DE LA ENZIMA 3-HIDROXI-3-METIL-GLUTARIL-COA REDUCTASA EN LOS EFECTOS DE LOVASTATINA

Para analizar si los efectos observados al tratar las células con lovastatina se deben a su blanco reportado se repitieron los experimentos descritos previamente, con la siguiente modificación: algunas células se trataron en forma conjunta con lovastatina y mevalonato, que es el producto generado por la 3-hidroxi-3-metil-glutaril-CoA-reductasa (HMGCR) [73]. La hipótesis en estos experimentos fue que, si el mevalonato era capaz de revertir lo efectos de la lovastatina, entonces dichos efectos habrían sido causados por la inhibición de la HMGCR.

En la **figura 20** observamos que el mevalonato no interfiere con la transactivación del promotor de SOX2 en las células MDA-MB-231. Sin embargo, al tratar con mevalonato y lovastatina se revierte parcialmente la inhibición de la transactivación del promotor de SOX2 de forma estadísticamente significativa.

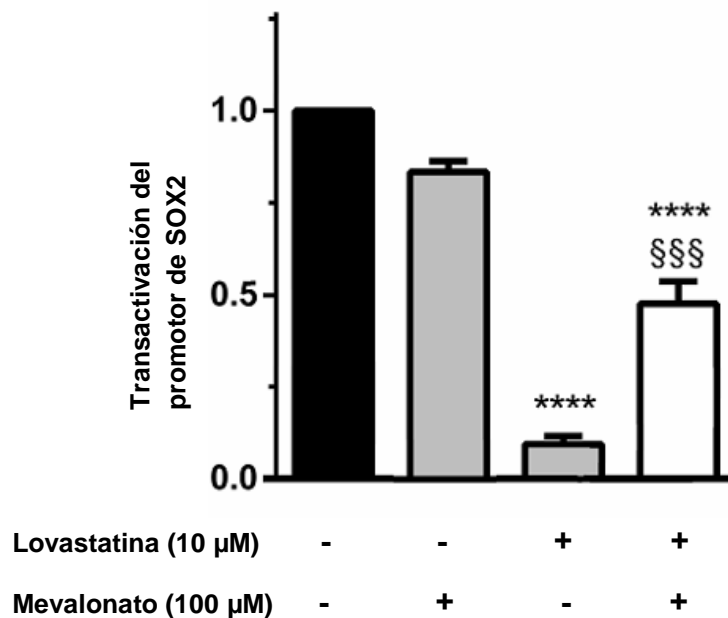


Figura 20. Evaluación de la transactivación del promotor de SOX2, mediante un ensayo de gen reportero. La gráfica representa el promedio de tres experimentos independientes \pm SEM $p < 0.0001$ (****) al comparar contra el control, mientras que $p < 0.001$ (\$\$\$) al comparar contra la respuesta obtenida al adicionar lovastatina.

En la **figura 21** podemos observar que cuando se realiza un *western blot* al tratar ambas líneas celulares con mevalonato no se presenta un aumento y/o disminución en la expresión de la proteína SOX2. Mientras que cuando se trata de forma conjunta con lovastatina y mevalonato se observa que aumenta la expresión de SOX2, es decir se revierte la disminución en la expresión de la proteína SOX2, provocada por tratar con lovastatina. Este efecto se presenta tanto para la línea MDA-MB-231, como para la línea Hs578T.

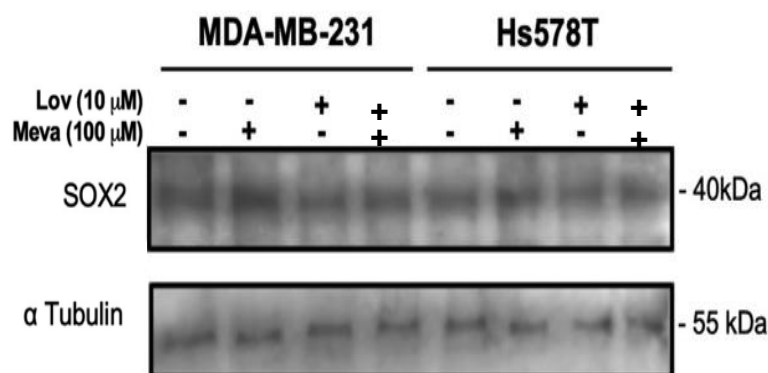


Figura 21. *Western blot* representativo de la evaluación de la expresión de SOX-2 y α -tubulina en MDA-MB-231 y Hs578T tratadas con lovastatina y/o mevalonato

Al realizar la evaluación sobre la población de CTT exponiendo a las células durante 24 horas a mevalonato y/o lovastatina y posteriormente realizando un ensayo de formación de mamoesferas, encontramos como se muestra en la **figura 22** que al tratar con mevalonato a la línea celular MDA-MB-231 esta no presenta una diferencia significativa contra el control. Al tratar con lovastatina se observó el efecto de disminución en el porcentaje de formación de mamoesferas identificado previamente. Cuando se realiza el tratamiento conjunto con lovastatina y mevalonato, se observa un incremento en el porcentaje de formación de mamoesferas superior al porcentaje formado por el control.

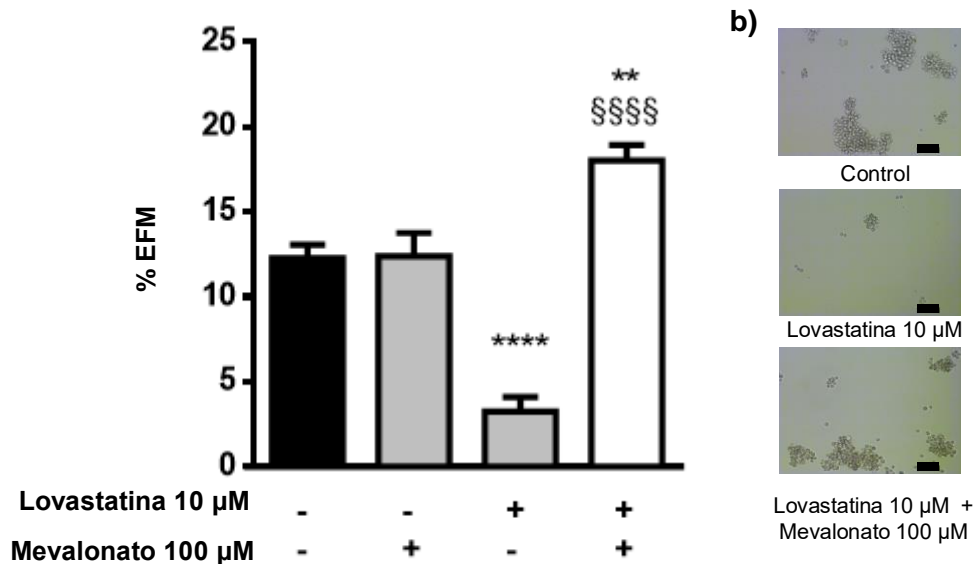


Figura 22. Evaluación de la eficiencia de formación de mamoesferas en células MDA-MB-231. a) La gráfica representa un experimento representativo realizado por octuplicado \pm SEM. $p < 0.01$ (**), < 0.0001 (****) al comparar contra el control, mientras que $p < 0.0001$ (\$\$\$\$) al comparar contra la respuesta obtenida al adicionar lovastatina. b) Imágenes representativas, la barra es igual a 100 μm

Por otro lado, al realizar este experimento con la línea celular Hs578T, encontramos como se muestra en la **figura 23** que cuando se adiciona mevalonato no se modifica la eficiencia en la formación de mamoesferas y cuando se adiciona lovastatina se observa una disminución estadísticamente significativa. Así mismo, es posible apreciar que dicha disminución se revierte cuando se adicionan a las células de forma conjunta la lovastatina y el mevalonato.

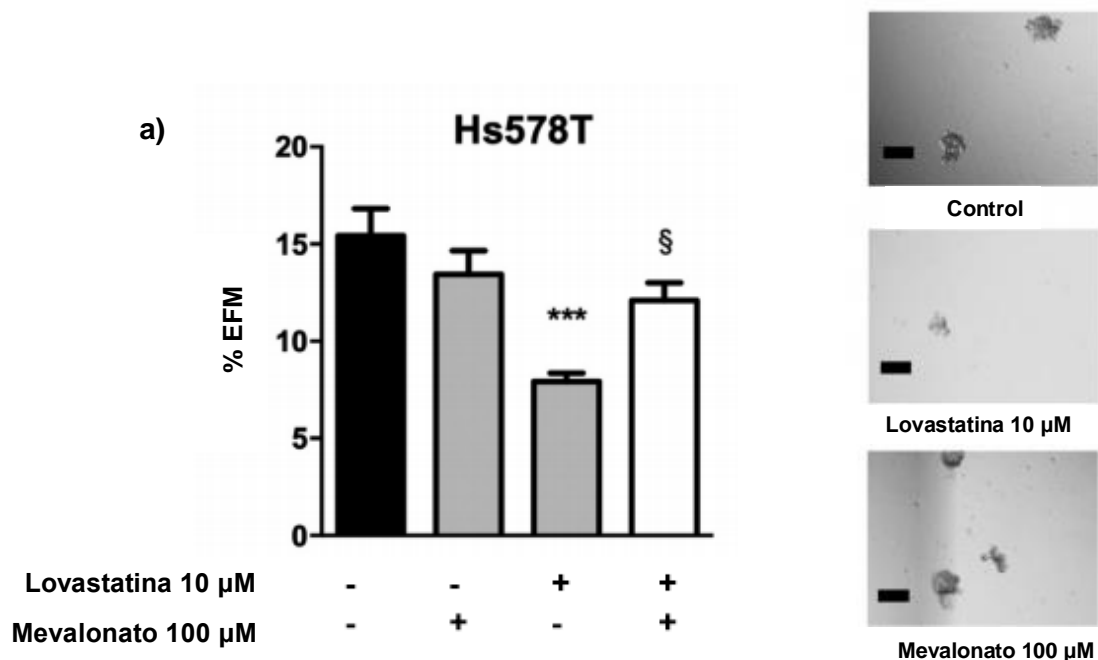


Figura 23. Evaluación de la eficiencia de formación de mamoesferas en células Hs578T. a) La gráfica representa un experimento representativo realizado por octuplicado \pm SEM. $p < 0.001$ (***) al comparar contra el control, mientras que $p < 0.05$ (§) al comparar contra la respuesta obtenida al adicionar lovastatina. b) Imágenes representativas, la barra es igual a 100 μ m

Para complementar lo observado en los ensayos de mamoesferas, se realizó la evaluación de la actividad de la enzima ALDH al tratar las líneas celulares (MDA-MB-231 y Hs578T) con lovastatina y mevalonato. Este experimento consistió en tratar las líneas celulares durante 24 horas con mevalonato 100 μ M y/o lovastatina 10 μ M. Encontrando para la línea celular MDA-MB-231 que la adición de mevalonato evita la disminución de células ALDH⁺ de forma estadísticamente significativa, como se muestra en la **Figura 24**. Estos efectos se mantienen cuando se evalúa con la línea celular Hs578T como se puede observar en la **Figura 25**.

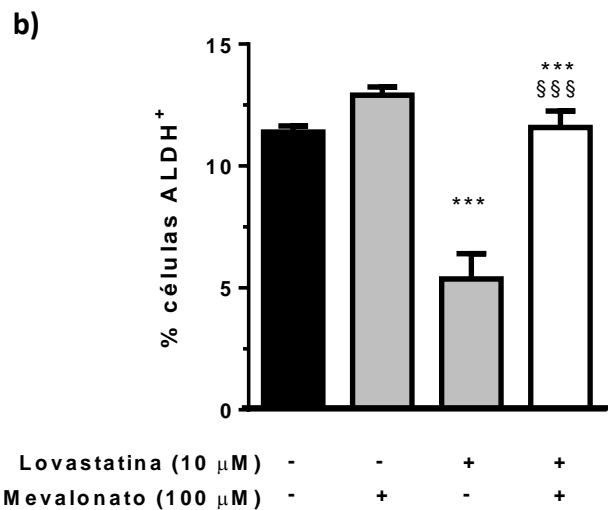
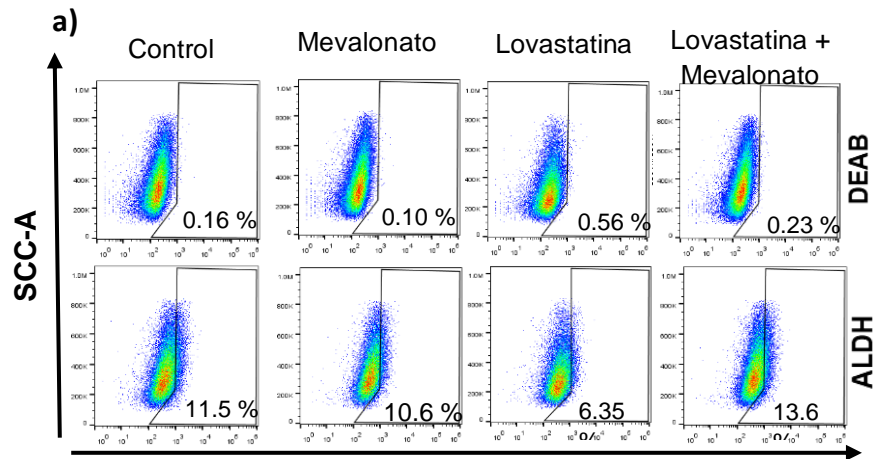
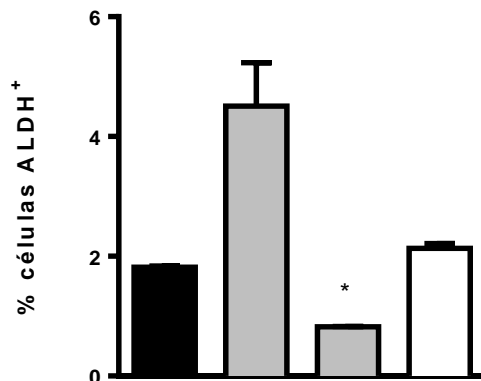
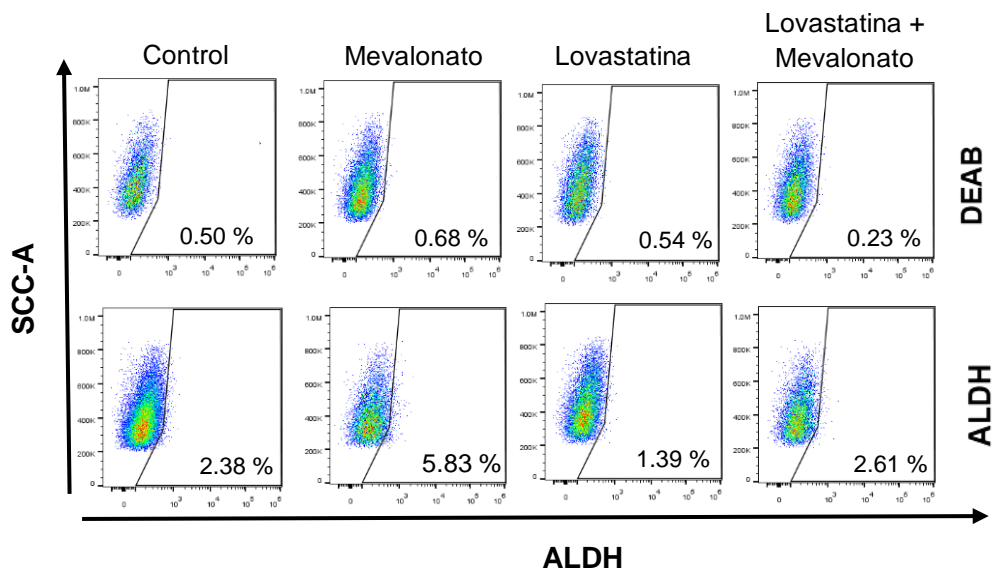


Figura 24. Efectos inducidos por mevalonato en la acción de la lovastatina al tratar MDA-MB-231. a) Dot plots representativos para la cuantificación de la fracción de ALDH+ en células MDA-MB-231 tratadas con lovastatina (10 μ M) y/o mevalonato (100 μ M). b) La gráfica representa el promedio de tres experimentos independientes \pm SEM. Prueba estadística de Turkey; $p < 0.001$ (***) al comparar contra el control, mientras que $p < 0.001$ (\$\$\$) al comparar contra la respuesta obtenida al adicionar lovastatina.



Lovastatina (10 μ M)	-	-	+	+
Mevalonato (100 μ M)	-	+	-	+

Figura 25. Efectos inducidos por mevalonato en la acción de la lovastatina al tratar Hs578T. A. Dot plots representativos para la cuantificación de la fracción de ALDH+ en células Hs578T tratadas con lovastatina (10 μ M) y/o mevalonato (100 μ M). B. Gráfica representativa de dos experimentos independientes \pm SEM. Prueba estadística de Turkey; $p < 0.05$ (*) al comparar contra el control.

6.8. VALIDACIÓN *IN VIVO* DE LOS EFECTOS DE LOVASTATINA

Para esta validación, tomamos datos de los cambios transcriptómicos inducidos en tumores mamarios de ratones tratados con lovastatina (GSE42787; [123]). Al comparar los datos contra diversas firmas reportadas, utilizando el software de GSEA, encontramos que los genes sobreexpresados en los tumores de ratones con el vehículo están enriquecidos en los genes contenidos en una firma consenso de CTT [125] o en una firma de células progenitoras mamarias [126] (**Figura 26a y 26b** respectivamente), lo que sugiere que *in vivo* la lovastatina genera una regulación a la baja de aquellos genes que se encuentra sobreexpresados en poblaciones celulares con propiedades troncales y/o progenitoras.

Cuando se realizó la comparación con la firma de EMT ([127]; **Figura 26c**) y la de células de CaMa con propiedades invasivas ([128]; **Figura 26d**), encontramos que lovastatina genera una regulación a la baja de estas firmas, lo que sugiere que este fármaco actúa sobre poblaciones con un fenotipo invasivo. Lo anterior provee una evidencia indirecta de que el tratamiento con lovastatina reduce la población de CTT cuando se administra *in vivo*.

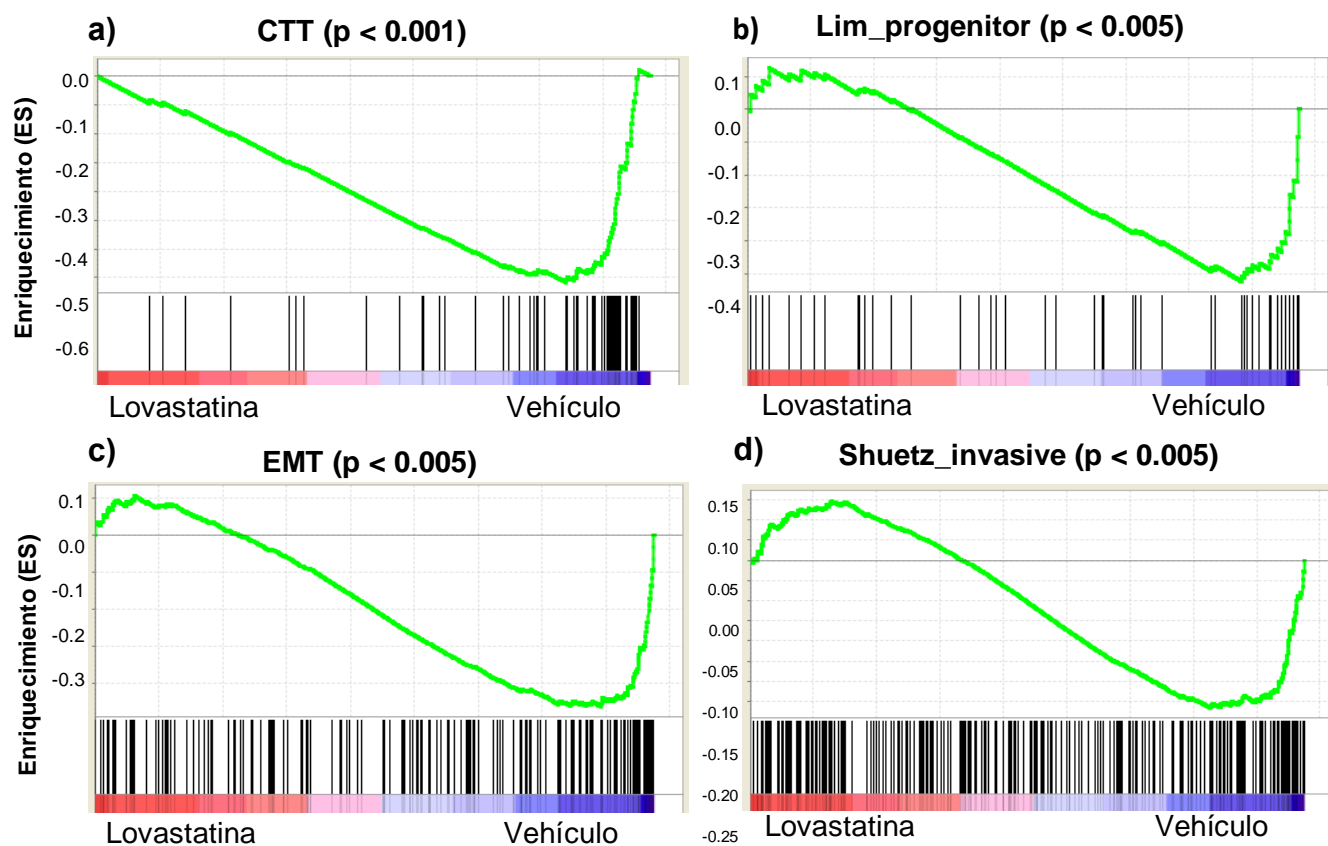


Figura 26. Análisis de enriquecimiento de tumores mamarios en ratones tratados con lovastatina. Las gráficas muestran un valor de enriquecimiento (eje y) y la posición (líneas negras) de los miembros de los genes sobreexpresados para a) CTT, b) progenitores luminales, c) EMT e d) invasividad.

7. DISCUSIÓN

El reposicionamiento de fármacos es una estrategia válida para identificar nuevos tratamientos contra el cáncer [99]. En particular, en este trabajo buscamos reposicionar fármacos como agentes que disminuyan la fracción de CTT en CaMa. Para la identificación de fármacos candidatos empleamos la plataforma de CMap, la cual permite la selección *in silico* basada en los efectos transcripcionales que induce un compuesto en múltiples líneas celulares. Entonces, CMap sirve como generador de hipótesis acerca de cuáles fármacos pueden revertir una firma de expresión, sin importar el contexto celular [133, 136]. Nuestro análisis utilizando una firma consenso de expresión diferencial para CTT identificó 6 fármacos candidatos con diferentes mecanismos de acción reportados. Dado que los fármacos son estructuralmente diferentes e inducen cambios transcripcionales globales disimilares entre sí, consideramos que, de generarse el efecto predicho por CMap, éste se generaría por mecanismos diferentes. Por lo tanto, se adquirieron la mayoría de los fármacos (5/6) para su estudio *in vitro* en células de CaMa.

La evaluación biológica inicial se realizó en la línea celular MDA-MB-231. Se encontró que lovastatina y fasudil disminuyen la transactivación del promotor de SOX2, pero ninguno de los fármacos candidatos afecta la transactivación del promotor OCT4.

Se ha reportado que la expresión de SOX2 correlaciona de forma significativa con tumores más grandes y la presencia de nodos linfáticos metastásicos en pacientes con CaMa [47]. Adicionalmente, el silenciamiento de SOX2 disminuye la formación de mamoesferas *in vitro* y la tumorigenicidad en modelos animales [46]. Dada la importancia de SOX2 en el mantenimiento de la troncalidad de células de CaMa, se seleccionaron lovastatina y fasudil para estudios posteriores. Al no existir estudios adicionales con el resto de los fármacos candidatos, no tenemos suficiente evidencia para descartarlos, por lo que se requieren estudios posteriores para estudiar a profundidad su actividad sobre CTTM.

Lovastatina, pero no fasudil, reduce la viabilidad celular en cultivos de MDA-MB-231 con una IC50 > 10 μ M. Nuestros resultados son consistentes con reportes previos que indican que la lovastatina induce muerte celular [114, 137] e inhibe la proliferación de múltiples líneas celulares de CaMa, incluida MDA-MB-231 [138] [139].

El efecto tóxico identificado en cultivos bidimensionales puede deberse a la muerte tanto de células no-troncales como de CTT. Para analizar la selectividad del efecto sobre CTT, realizamos ensayos de mamoesferas. En esos ensayos, el número de mamoesferas formadas es proporcional al número de CTT en un cultivo [140-143]. Fasudil no demostró efectos significativos, pero lovastatina inhibió totalmente la capacidad clonogénica. Esto sugiere que, aunque la lovastatina afecta la viabilidad de células no troncales, las CTT son más susceptibles al fármaco.

Para validar los efectos de lovastatina en las CTT se trataron las células durante 24 h y se analizaron los cambios de la población ALDH⁺. La actividad de ALDH como marcador de la población CTTM se correlaciona con la quimioresistencia, autorrenovación de CTT en tumores, un mal pronóstico en pacientes con CaMa [66] [144]. Encontramos que la lovastatina reduce la fracción de células ALDH⁺. Estos datos junto con la disminución en los niveles de la proteína SOX2 y la reducción irreversible de la eficiencia de formación de mamoesferas en condiciones libre de fármaco, corroboraron que la lovastatina reduce la población de CTT en la línea celular MDA-MB-231. Efectos similares se encontraron en una segunda línea celular de CaMa triple negativo Hs578T, lo cual sugiere que este efecto podría aparecer en pacientes con CaMa de ese subtipo.

CMap permite la selección de fármacos, pero no provee información sobre el mecanismo que causaría los cambios transcripcionales deseados. Por lo tanto, no se puede predecir el mecanismo de acción de los compuestos activos. Por esto, examinamos si los efectos observados en las CTTM se deben al blanco canónico reportado de la lovastatina, la enzima HMGCR. En esos experimentos, se adicionó mevalonato a cultivos tratados con lovastatina, con el fin de reponer el producto de

la reacción inhibida por el fármaco. Previamente se reportó que la adición de mevalonato revierte los efectos de la lovastatina en la viabilidad [114] y en el arresto en G1 [138] de células cancerosas.

La adición de mevalonato a las células MDA-MB-231 o Hs578T tratadas con lovastatina revierte el efecto observado sobre la fracción ALDH⁺, la transactivación del promotor de SOX2 y la eficiencia de formación de mamoesferas, sugiriendo que los cambios observados en la población troncal podrían ser atribuidos a la inhibición de HMGCR. Consistentemente, estudios previos mostraron que los efectos en las estatinas en la subpoblación troncal en cáncer pancreático podrían estar asociados con la inhibición de la vía del mevalonato [145]. Sin embargo, es necesario realizar más estudios para discernir que no existan otros mecanismos de acción que sean responsables de los efectos observados. Tal es el caso de Walther *et al*, que reportaron que la lovastatina induce la expresión de COX-2 y la subsecuente activación de PPAR causando citotoxicidad en las células de cáncer de pulmón [146].

Para estudiar si los efectos de lovastatina identificados en este trabajo se reproducen *in vivo*, analizamos los cambios transcripcionales que se inducen en ratones tratados con 10 mg/kg de lovastatina [147]. Mediante GSEA, encontramos que la lovastatina disminuye la expresión de grupos de genes que definen EMT, invasión, troncalidad, y apoptosis, incluyendo proteínas como Hippo, Notch, Wnt y la vía HIF [137, 148]. Adicionalmente, se sabe que las estatinas pueden tener efectos benéficos en pacientes con cáncer. La administración de atorvastatina en pacientes con CaMa genera cambios en la expresión de múltiples genes que participan en la proliferación y apoptosis que podrían depender de cambios en la activación de factores transcripcionales como CREB1, ATF, OCT y SRF [149]. Por lo tanto, es posible que los cambios transcripcionales que hacen que la lovastatina sea efectiva reduciendo la población de CTT, aparezcan en humanos.

Una de las limitaciones de este estudio es que nuestros experimentos fueron diseñados empleando concentraciones similares a las utilizadas para generar los

datos contenidos en CMap (10 μ M). Sin embargo, se ha demostrado que estas concentraciones son 100 o hasta 1000 veces mayores que las encontradas en el torrente sanguíneo de sujetos que consumen dosis terapéuticas de lovastatina [150, 151]. Por lo tanto, aún falta conocer si la administración clínica de lovastatina a pacientes con CaMa induce efectos similares a los generados en este trabajo.

8. CONCLUSIONES

La selección de una firma transcripcional que define a las CTTM fármaco junto con el análisis *in silico* para identificar fármacos capaces de revertir dicha firma permitieron la identificación de la lovastatina como un agente que afecta la población troncal en CaMa.

Los efectos observados podrían ser causados por la inhibición de la HMGCR lo que nos indica que estos efectos podrían observarse con otras estatinas. Determinar el mecanismo involucrado en los efectos de la lovastatina y estudiar si los mismos efectos aparecen a dosis tolerables clínicamente podría ayudar a proponer el uso de este fármaco como una terapia adyuvante terapéutico en pacientes con CaMa.

9. BIBLIOGRAFIA

1. Ahmad, G. and M.M. Amiji, *Cancer stem cell-targeted therapeutics and delivery strategies*. Expert Opin. Drug Delivery, 2017. **14**(8): p. 997-1008.
2. Hanahan, D. and R.A. Weinberg, *Hallmarks of cancer: the next generation*. Cell, 2011. **144**(5): p. 646-74.
3. Rogalla, S. and C.H. Contag, *Early Cancer Detection at the Epithelial Surface*. Cancer J, 2015. **21**(3): p. 179-87.
4. Wang, C.-C., L. Jamal, and K.A. Janes, *Normal morphogenesis of epithelial tissues and progression of epithelial tumors*. Wiley Interdiscip. Rev.: Syst. Biol. Med., 2012. **4**(1): p. 51-78.
5. Cazzola, M., *Introduction to a review series: the 2016 revision of the WHO classification of tumors of hematopoietic and lymphoid tissues*. Blood, 2016. **127**(20): p. 2361-2364.
6. Zhuge, Y., et al., *Brain tumor segmentation using holistically nested neural networks in MRI images*. Med Phys, 2017. **44**(10): p. 5234-5243.
7. McGuire, S., *World Cancer Report 2014*. Geneva, Switzerland: World Health Organization, International Agency for Research on Cancer, WHO Press, 2015. Advances in Nutrition, 2016. **7**(2): p. 418-419.
8. Tao, Z., et al., *Breast Cancer: Epidemiology and Etiology*. Cell Biochemistry and Biophysics, 2015. **72**(2): p. 333-338.
9. Ahmad, A., *Pathways to breast cancer recurrence*. ISRN Oncol, 2013. **2013**: p. 290568.
10. Bray, F., et al., *Global cancer statistics 2018: GLOBOCAN estimates of incidence and mortality worldwide for 36 cancers in 185 countries*. CA Cancer J Clin, 2018. **68**(6): p. 394-424.
11. Salud, S.d., *NOM-041-SSA2-2011, Para la prevención, diagnóstico, tratamiento, control y vigilancia epidemiológica del cáncer de mama*. Diario Oficial 2011.
12. Mexico, G., *Anuario de Morbilidad 2018*.
13. Badve, S. and Y. Goekmen-Polar, *Tumor Heterogeneity in Breast Cancer*. Adv. Anat. Pathol., 2015. **22**(5): p. 294-302.
14. Weigelt, B., F.C. Geyer, and J.S. Reis-Filho, *Histological types of breast cancer: how special are they?* Mol. Oncol., 2010. **4**(3): p. 192-208.
15. Turashvili, G. and E. Brogi, *Tumor Heterogeneity in Breast Cancer*. 2017. **4**(227).
16. Lanceta, *Effects of chemotherapy and hormonal therapy for early breast cancer on recurrence and 15-year survival: an overview of the randomised trials*. Lancet, 2005. **365**(9472): p. 1687-717.
17. Harris, L.N., et al., *Use of Biomarkers to Guide Decisions on Adjuvant Systemic Therapy for Women With Early-Stage Invasive Breast Cancer: American Society of Clinical Oncology Clinical Practice Guideline*. J Clin Oncol, 2016. **34**(10): p. 1134-50.
18. Gonzalez, J.D., *Expresión de Biomarcadores pronósticos (P53, TOP2a) en biopsias de mujeres mexicanas con cáncer de mama*, in Instituto Estatal de Cancerología. 2019, Universidad Nacional Autónoma de México p. 67.
19. Bevers, T.B., et al., *NCCN clinical practice guidelines in oncology: breast cancer screening and diagnosis*. J Natl Compr Canc Netw, 2009. **7**(10): p. 1060-96.
20. Salud, O.M.d.I. *El diagnóstico temprano del cáncer salva vidas y reduce los costos de tratamiento 2017*; Available from: <https://www.who.int/es/news-room/detail/03-02-2017-early-cancer-diagnosis-saves-lives-cuts-treatment-costs>.
21. Gradishar, W.J., et al., *Invasive Breast Cancer Version 1.2016, NCCN Clinical Practice Guidelines in Oncology*. J Natl Compr Canc Netw, 2016. **14**(3): p. 324-54.

22. S Franco, S., et al., *In vitro models of cancer stem cells and clinical applications*. BMC cancer, 2016. **16**(Suppl 2): p. 738-738.
23. Luo, M., et al., *Breast Cancer Stem Cells: Current Advances and Clinical Implications*, in *Mammary Stem Cells: Methods and Protocols*, M.d.M. Vivanco, Editor. 2015, Springer New York: New York, NY. p. 1-49.
24. Baccelli, I. and A. Trumpp, *The evolving concept of cancer and metastasis stem cells*. J Cell Biol, 2012. **198**(3): p. 281-93.
25. Luqmani, Y.A., *Mechanisms of drug resistance in cancer chemotherapy*. Med Princ Pract, 2005. **14 Suppl 1**: p. 35-48.
26. Phi, L.T.H., et al., *Cancer Stem Cells (CSCs) in Drug Resistance and their Therapeutic Implications in Cancer Treatment*. Stem Cells Int, 2018. **2018**: p. 5416923.
27. Seymour, T., A.J. Twigger, and F. Kakulas, *Pluripotency Genes and Their Functions in the Normal and Aberrant Breast and Brain*. Int J Mol Sci, 2015. **16**(11): p. 27288-301.
28. Bonnet, D. and J.E. Dick, *Human acute myeloid leukemia is organized as a hierarchy that originates from a primitive hematopoietic cell*. Nat Med, 1997. **3**(7): p. 730-7.
29. O'Brien, C.A., et al., *A human colon cancer cell capable of initiating tumour growth in immunodeficient mice*. Nature, 2007. **445**(7123): p. 106-10.
30. Al-Hajj, M., et al., *Prospective identification of tumorigenic breast cancer cells*. Proc Natl Acad Sci U S A, 2003. **100**(7): p. 3983-8.
31. Singh, S.K., et al., *Identification of human brain tumour initiating cells*. Nature, 2004. **432**(7015): p. 396-401.
32. Wang, L., et al., *Smoothed activates breast cancer stem-like cell and promotes tumorigenesis and metastasis of breast cancer*. Biomed Pharmacother, 2014. **68**(8): p. 1099-104.
33. Yan, W., et al., *Increased invasion and tumorigenicity capacity of CD44+/CD24- breast cancer MCF7 cells in vitro and in nude mice*. Cancer Cell Int, 2013. **13**(1): p. 62.
34. Fillmore, C.M. and C. Kuperwasser, *Human breast cancer cell lines contain stem-like cells that self-renew, give rise to phenotypically diverse progeny and survive chemotherapy*. Breast Cancer Res, 2008. **10**(2): p. R25.
35. Liu, Y., et al., *Lack of correlation of stem cell markers in breast cancer stem cells*. Br J Cancer, 2014. **110**(8): p. 2063-71.
36. Ryspayeva, D.E., et al., *Are CD44(+)/CD24(-) cells the assumed cancer stem cells in breast cancer?* Exp Oncol, 2017. **39**(3): p. 224-228.
37. Ahmed, M.A., et al., *A CD44(-)/CD24(+) phenotype is a poor prognostic marker in early invasive breast cancer*. Breast Cancer Res Treat, 2012. **133**(3): p. 979-95.
38. Velasco-Velazquez, M.A., et al., *The role of breast cancer stem cells in metastasis and therapeutic implications*. Am J Pathol, 2011. **179**(1): p. 2-11.
39. Seo, E., et al., *Distinct functions of Sox2 control self-renewal and differentiation in the osteoblast lineage*. Mol Cell Biol, 2011. **31**(22): p. 4593-608.
40. Basu-Roy, U., et al., *Sox2 maintains self renewal of tumor-initiating cells in osteosarcomas*. Oncogene, 2012. **31**(18): p. 2270-82.
41. Zhang, S. and W. Cui, *Sox2, a key factor in the regulation of pluripotency and neural differentiation*. World J Stem Cells, 2014. **6**(3): p. 305-11.
42. Thomson, J.A., et al., *Embryonic stem cell lines derived from human blastocysts*. Science, 1998. **282**(5391): p. 1145-7.
43. Avilion, A.A., et al., *Multipotent cell lineages in early mouse development depend on SOX2 function*. Genes Dev, 2003. **17**(1): p. 126-40.

44. Santini, R., et al., *SOX2 regulates self-renewal and tumorigenicity of human melanoma-initiating cells*. *Oncogene*, 2014. **33**(38): p. 4697-708.
45. Stolzenburg, S., et al., *Targeted silencing of the oncogenic transcription factor SOX2 in breast cancer*. *Nucleic Acids Res*, 2012. **40**(14): p. 6725-40.
46. Leis, O., et al., *Sox2 expression in breast tumours and activation in breast cancer stem cells*. *Oncogene*, 2012. **31**(11): p. 1354-65.
47. Zheng, Y., et al., *Clinicopathological significance of Sox2 expression in patients with breast cancer: a meta-analysis*. *Int J Clin Exp Med*, 2015. **8**(12): p. 22382-92.
48. Lengerke, C., et al., *Expression of the embryonic stem cell marker SOX2 in early-stage breast carcinoma*. *BMC Cancer*, 2011. **11**: p. 42.
49. Sachlos, E., et al., *Identification of drugs including a dopamine receptor antagonist that selectively target cancer stem cells*. *Cell*, 2012. **149**(6): p. 1284-97.
50. Zhao, S., et al., *Expression of OCT4 pseudogenes in human tumours: lessons from glioma and breast carcinoma*. *J Pathol*, 2011. **223**(5): p. 672-82.
51. Nichols, J., et al., *Formation of Pluripotent Stem Cells in the Mammalian Embryo Depends on the POU Transcription Factor Oct4*. *Cell*, 1998. **95**(3): p. 379-391.
52. Scholer, H.R., *Octamania: the POU factors in murine development*. *Trends Genet*, 1991. **7**(10): p. 323-9.
53. Zeineddine, D., et al., *The Oct4 protein: more than a magic stemness marker*. *Am J Stem Cells*, 2014. **3**(2): p. 74-82.
54. Niwa, H., J. Miyazaki, and A.G. Smith, *Quantitative expression of Oct-3/4 defines differentiation, dedifferentiation or self-renewal of ES cells*. *Nat Genet*, 2000. **24**(4): p. 372-6.
55. Takahashi, K., et al., *Induction of pluripotent stem cells from adult human fibroblasts by defined factors*. *Cell*, 2007. **131**(5): p. 861-72.
56. Boer, B., et al., *Elevating the levels of Sox2 in embryonal carcinoma cells and embryonic stem cells inhibits the expression of Sox2:Oct-3/4 target genes*. *Nucleic Acids Res*, 2007. **35**(6): p. 1773-86.
57. Kashyap, V., et al., *Regulation of stem cell pluripotency and differentiation involves a mutual regulatory circuit of the NANOG, OCT4, and SOX2 pluripotency transcription factors with polycomb repressive complexes and stem cell microRNAs*. *Stem Cells Dev*, 2009. **18**(7): p. 1093-108.
58. Gidekel, S., et al., *Oct-3/4 is a dose-dependent oncogenic fate determinant*. *Cancer Cell*, 2003. **4**(5): p. 361-70.
59. Wei, Z., et al., *Klf4 interacts directly with Oct4 and Sox2 to promote reprogramming*. *Stem Cells*, 2009. **27**(12): p. 2969-78.
60. Kim, R.J. and J.S. Nam, *OCT4 Expression Enhances Features of Cancer Stem Cells in a Mouse Model of Breast Cancer*. *Lab Anim Res*, 2011. **27**(2): p. 147-52.
61. Li, Y., et al., *Zinc finger protein 32 promotes breast cancer stem cell-like properties through directly promoting GPER transcription*. *Cell Death Dis*, 2018. **9**(12): p. 1162.
62. Chang, C.C., et al., *Oct-3/4 expression reflects tumor progression and regulates motility of bladder cancer cells*. *Cancer Res*, 2008. **68**(15): p. 6281-91.
63. Rasti, A., et al., *Co-expression of Cancer Stem Cell Markers OCT4 and NANOG Predicts Poor Prognosis in Renal Cell Carcinomas*. *Sci Rep*, 2018. **8**(1): p. 11739.
64. Marchitti, S.A., et al., *Non-P450 aldehyde oxidizing enzymes: the aldehyde dehydrogenase superfamily*. *Expert Opin Drug Metab Toxicol*, 2008. **4**(6): p. 697-720.
65. Boonyaratanakornkit, J.B., et al., *Selection of tumorigenic melanoma cells using ALDH*. *J Invest Dermatol*, 2010. **130**(12): p. 2799-808.

66. Ginestier, C., et al., *ALDH1 is a marker of normal and malignant human mammary stem cells and a predictor of poor clinical outcome*. Cell Stem Cell, 2007. **1**(5): p. 555-67.
67. Moreb, J.S., *Aldehyde dehydrogenase as a marker for stem cells*. Curr Stem Cell Res Ther, 2008. **3**(4): p. 237-46.
68. Visvader, J.E. and G.J. Lindeman, *Cancer stem cells in solid tumours: accumulating evidence and unresolved questions*. Nat Rev Cancer, 2008. **8**(10): p. 755-68.
69. Croker, A.K., et al., *Differential Functional Roles of ALDH1A1 and ALDH1A3 in Mediating Metastatic Behavior and Therapy Resistance of Human Breast Cancer Cells*. Int J Mol Sci, 2017. **18**(10).
70. Marcato, P., et al., *Aldehyde dehydrogenase activity of breast cancer stem cells is primarily due to isoform ALDH1A3 and its expression is predictive of metastasis*. Stem Cells, 2011. **29**(1): p. 32-45.
71. Charafe-Jauffret, E., et al., *Breast cancer cell lines contain functional cancer stem cells with metastatic capacity and a distinct molecular signature*. Cancer Res, 2009. **69**(4): p. 1302-13.
72. Christ, O., et al., *Improved purification of hematopoietic stem cells based on their elevated aldehyde dehydrogenase activity*. Haematologica, 2007. **92**(9): p. 1165-72.
73. Croker, A.K., et al., *High aldehyde dehydrogenase and expression of cancer stem cell markers selects for breast cancer cells with enhanced malignant and metastatic ability*. J Cell Mol Med, 2009. **13**(8B): p. 2236-52.
74. Li, X., et al., *Intrinsic Resistance of Tumorigenic Breast Cancer Cells to Chemotherapy*. JNCI: Journal of the National Cancer Institute, 2008. **100**(9): p. 672-679.
75. Balic, M., et al., *Most Early Disseminated Cancer Cells Detected in Bone Marrow of Breast Cancer Patients Have a Putative Breast Cancer Stem Cell Phenotype*. Clinical Cancer Research, 2006. **12**(19): p. 5615.
76. Jiao, X., et al., *CCR5 Governs DNA damage repair and breast cancer stem cell expansion*. Cancer Research, 2018. **78**(7): p. 1657-1671.
77. S, S.F., et al., *In vitro models of cancer stem cells and clinical applications*. BMC Cancer, 2016. **16**(Suppl 2): p. 738.
78. Nguyen, D.X., P.D. Bos, and J. Massague, *Metastasis: from dissemination to organ-specific colonization*. Nat Rev Cancer, 2009. **9**(4): p. 274-84.
79. Baccelli, I., et al., *Identification of a population of blood circulating tumor cells from breast cancer patients that initiates metastasis in a xenograft assay*. Nature Biotechnology, 2013. **31**: p. 539.
80. Mani, S.A., et al., *The epithelial-mesenchymal transition generates cells with properties of stem cells*. Cell, 2008. **133**(4): p. 704-15.
81. Morel, A.-P., et al., *Generation of breast cancer stem cells through epithelial-mesenchymal transition*. PloS one, 2008. **3**(8): p. e2888-e2888.
82. Taube, J.H., et al., *Core epithelial-to-mesenchymal transition interactome gene-expression signature is associated with claudin-low and metaplastic breast cancer subtypes*. Proc Natl Acad Sci U S A, 2010. **107**(35): p. 15449-54.
83. Shiozawa, Y., et al., *Cancer stem cells and their role in metastasis*. Pharmacol Ther, 2013. **138**(2): p. 285-93.
84. Cristofanilli, M., et al., *Circulating tumor cells, disease progression, and survival in metastatic breast cancer*. N Engl J Med, 2004. **351**(8): p. 781-91.
85. Yu, F., et al., *let-7 regulates self renewal and tumorigenicity of breast cancer cells*. Cell, 2007. **131**(6): p. 1109-23.

86. Creighton, C.J., et al., *Residual breast cancers after conventional therapy display mesenchymal as well as tumor-initiating features*. Proc Natl Acad Sci U S A, 2009. **106**(33): p. 13820-5.
87. Gupta, P.B., et al., *Identification of selective inhibitors of cancer stem cells by high-throughput screening*. Cell, 2009. **138**(4): p. 645-659.
88. Europea, U., *Clinical Trials* 2006.
89. Wurth, R., et al., *Drug-repositioning opportunities for cancer therapy: novel molecular targets for known compounds*. Drug Discov Today, 2016. **21**(1): p. 190-199.
90. Cavalla, D., *Therapeutic switching: a new strategic approach to enhance R&D productivity*. IDrugs, 2005. **8**(11): p. 914-8.
91. Pritchard, J.E., T.A. O'Mara, and D.M. Glubb, *Enhancing the Promise of Drug Repositioning through Genetics*. Front Pharmacol, 2017. **8**: p. 896.
92. Lussier, Y.A. and J.L. Chen, *The emergence of genome-based drug repositioning*. Sci Transl Med, 2011. **3**(96): p. 96ps35.
93. Sirota, M., et al., *Discovery and preclinical validation of drug indications using compendia of public gene expression data*. Sci Transl Med, 2011. **3**(96): p. 96ra77.
94. Verbist, B., et al., *Using transcriptomics to guide lead optimization in drug discovery projects: Lessons learned from the QSTAR project*. Drug Discov Today, 2015. **20**(5): p. 505-13.
95. Iorio, F., et al., *Transcriptional data: a new gateway to drug repositioning?* Drug Discov Today, 2013. **18**(7-8): p. 350-7.
96. Iorio, F., et al., *Discovery of drug mode of action and drug repositioning from transcriptional responses*. Proc Natl Acad Sci U S A, 2010. **107**(33): p. 14621-6.
97. Mirza, N., et al., *Identifying new antiepileptic drugs through genomics-based drug repurposing*. Hum Mol Genet, 2017. **26**(3): p. 527-537.
98. de Anda-Jauregui, G., et al., *Exploration of the Anti-Inflammatory Drug Space Through Network Pharmacology: Applications for Drug Repurposing*. Front Physiol, 2018. **9**: p. 151.
99. Lamb, J., et al., *The Connectivity Map: using gene-expression signatures to connect small molecules, genes, and disease*. Science, 2006. **313**(5795): p. 1929-35.
100. Qu, X.A. and D.K. Rajpal, *Applications of Connectivity Map in drug discovery and development*. Drug Discov Today, 2012. **17**(23-24): p. 1289-98.
101. Manzotti, G., et al., *Monocyte-macrophage differentiation of acute myeloid leukemia cell lines by small molecules identified through interrogation of the Connectivity Map database*. Cell Cycle, 2015. **14**(16): p. 2578-89.
102. Musa, A., et al., *A review of connectivity map and computational approaches in pharmacogenomics*. Brief Bioinform, 2018. **19**(3): p. 506-523.
103. Sirtori, C.R., *The pharmacology of statins*. Pharmacol Res, 2014. **88**: p. 3-11.
104. Demierre, M.F., et al., *Statins and cancer prevention*. Nat Rev Cancer, 2005. **5**(12): p. 930-42.
105. Nielsen, S.F., B.G. Nordestgaard, and S.E. Bojesen, *Statin use and reduced cancer-related mortality*. N Engl J Med, 2012. **367**(19): p. 1792-802.
106. Borgquist, S., et al., *Statin use and breast cancer survival - a Swedish nationwide study*. BMC Cancer, 2019. **19**(1): p. 54.
107. Murtola, T.J., et al., *Statin use and breast cancer survival: a nationwide cohort study from Finland*. PLoS One, 2014. **9**(10): p. e110231.
108. Li, G., et al., *Simvastatin inhibits tumor angiogenesis in HER2-overexpressing human colorectal cancer*. Biomed Pharmacother, 2017. **85**: p. 418-424.

109. Wang, T., et al., *Simvastatin-induced breast cancer cell death and deactivation of PI3K/Akt and MAPK/ERK signalling are reversed by metabolic products of the mevalonate pathway*. *Oncotarget*, 2016. **7**(3): p. 2532-44.
110. Atil, B., et al., *In vitro and in vivo downregulation of the ATP binding cassette transporter B1 by the HMG-CoA reductase inhibitor simvastatin*. *Naunyn Schmiedebergs Arch Pharmacol*, 2016. **389**(1): p. 17-32.
111. Kanugula, A.K., et al., *Statin-induced inhibition of breast cancer proliferation and invasion involves attenuation of iron transport: intermediacy of nitric oxide and antioxidant defence mechanisms*. *Febs j*, 2014. **281**(16): p. 3719-38.
112. Ma, Q., et al., *Atorvastatin Inhibits Breast Cancer Cells by Downregulating PTEN/AKT Pathway via Promoting Ras Homolog Family Member B (RhoB)*. *Biomed Res Int*, 2019. **2019**: p. 3235021.
113. Wu, D., et al., *Synergistically Enhanced Inhibitory Effects of Pullulan Nanoparticle-Mediated Co-Delivery of Lovastatin and Doxorubicin to Triple-Negative Breast Cancer Cells*. *Nanoscale Res Lett*, 2019. **14**(1): p. 314.
114. Siddiqui, R.A., et al., *Characterization of lovastatin-docosahexaenoate anticancer properties against breast cancer cells*. *Bioorg Med Chem*, 2014. **22**(6): p. 1899-908.
115. Niknejad, N., et al., *Lovastatin-induced apoptosis is mediated by activating transcription factor 3 and enhanced in combination with salubrinal*. *Int J Cancer*, 2014. **134**(2): p. 268-79.
116. Peng, Y., et al., *Lovastatin Inhibits Cancer Stem Cells and Sensitizes to Chemo- and Photodynamic Therapy in Nasopharyngeal Carcinoma*. *J Cancer*, 2017. **8**(9): p. 1655-1664.
117. Hartwell, K.A., et al., *Niche-based screening identifies small-molecule inhibitors of leukemia stem cells*. *Nat Chem Biol*, 2013. **9**(12): p. 840-848.
118. Song, L., et al., *Cerasomal Lovastatin Nanohybrids for Efficient Inhibition of Triple-Negative Breast Cancer Stem Cells To Improve Therapeutic Efficacy*. *ACS Appl Mater Interfaces*, 2018. **10**(8): p. 7022-7030.
119. Hert, J., et al., *Comparison of Fingerprint-Based Methods for Virtual Screening Using Multiple Bioactive Reference Structures*. *Journal of Chemical Information and Computer Sciences*, 2004. **44**(3): p. 1177-1185.
120. Salim, N., J. Holliday, and P. Willett, *Combination of Fingerprint-Based Similarity Coefficients Using Data Fusion*. *Journal of Chemical Information and Computer Sciences*, 2003. **43**(2): p. 435-442.
121. KNIME, *CDK Nodes for KNIME*. 2019.
122. Prabst, K., et al., *Basic Colorimetric Proliferation Assays: MTT, WST, and Resazurin*. *Methods Mol Biol*, 2017. **1601**: p. 1-17.
123. Mira, E., et al., *A lovastatin-elicited genetic program inhibits M2 macrophage polarization and enhances T cell infiltration into spontaneous mouse mammary tumors*. *Oncotarget*, 2013. **4**(12): p. 2288-301.
124. Subramanian, A., et al., *Gene set enrichment analysis: a knowledge-based approach for interpreting genome-wide expression profiles*. *Proc Natl Acad Sci U S A*, 2005. **102**(43): p. 15545-50.
125. Shats, I., et al., *Using a stem cell-based signature to guide therapeutic selection in cancer*. *Cancer Res*, 2011. **71**(5): p. 1772-80.
126. Lim, E., et al., *Transcriptome analyses of mouse and human mammary cell subpopulations reveal multiple conserved genes and pathways*. *Breast Cancer Res*, 2010. **12**(2): p. R21.
127. Liberzon, A., et al., *The Molecular Signatures Database (MSigDB) hallmark gene set collection*. *Cell Syst*, 2015. **1**(6): p. 417-425.

128. Schuetz, C.S., et al., *Progression-specific genes identified by expression profiling of matched ductal carcinomas in situ and invasive breast tumors, combining laser capture microdissection and oligonucleotide microarray analysis*. *Cancer Res*, 2006. **66**(10): p. 5278-86.
129. Kar, P., et al., *A protocol for stripping and reprobing of Western blots originally developed with colorimetric substrate TMB*. *Electrophoresis*, 2012. **33**(19-20): p. 3062-5.
130. Schneider, C.A., W.S. Rasband, and K.W. Eliceiri, *NIH Image to ImageJ: 25 years of image analysis*. *Nat Methods*, 2012. **9**(7): p. 671-5.
131. Tang, B., et al., *A flexible reporter system for direct observation and isolation of cancer stem cells*. *Stem Cell Reports*, 2015. **4**(1): p. 155-169.
132. Wu, K., et al., *Cell fate determination factor Dachshund reprograms breast cancer stem cell function*. *J Biol Chem*, 2011. **286**(3): p. 2132-42.
133. Gao, L., et al., *Discovery of the neuroprotective effects of alvespimycin by computational prioritization of potential anti-Parkinson agents*. *FEBS J*, 2014. **281**(4): p. 1110-22.
134. Fiorillo, M., et al., *Bergamot natural products eradicate cancer stem cells (CSCs) by targeting mevalonate, Rho-GDI-signalling and mitochondrial metabolism*. *Biochim Biophys Acta Bioenerg*, 2018. **1859**(9): p. 984-996.
135. Nishi, M., et al., *Induction of cells with cancer stem cell properties from nontumorigenic human mammary epithelial cells by defined reprogramming factors*. *Oncogene*, 2014. **33**(5): p. 643-52.
136. Beck, A., et al., *Connectivity map identifies HDAC inhibition as a treatment option of high-risk hepatoblastoma*. *Cancer Biol Ther*, 2016. **17**(11): p. 1168-1176.
137. Yang, T., et al., *Effects of Lovastatin on MDA-MB-231 Breast Cancer Cells: An Antibody Microarray Analysis*. *J Cancer*, 2016. **7**(2): p. 192-9.
138. Rao, S., et al., *Lovastatin-mediated G1 arrest is through inhibition of the proteasome, independent of hydroxymethyl glutaryl-CoA reductase*. *Proc Natl Acad Sci U S A*, 1999. **96**(14): p. 7797-802.
139. Campbell, M.J., et al., *Breast cancer growth prevention by statins*. *Cancer Res*, 2006. **66**(17): p. 8707-14.
140. Dontu, G., et al., *In vitro propagation and transcriptional profiling of human mammary stem/progenitor cells*. *Genes Dev*, 2003. **17**(10): p. 1253-70.
141. Liao, M.J., et al., *Enrichment of a population of mammary gland cells that form mammospheres and have in vivo repopulating activity*. *Cancer Res*, 2007. **67**(17): p. 8131-8.
142. Ponti, D., et al., *Isolation and in vitro propagation of tumorigenic breast cancer cells with stem/progenitor cell properties*. *Cancer Res*, 2005. **65**(13): p. 5506-11.
143. Lombardo, Y., et al., *Mammosphere formation assay from human breast cancer tissues and cell lines*. *J Vis Exp*, 2015(97).
144. Magni, M., et al., *Induction of cyclophosphamide-resistance by aldehyde-dehydrogenase gene transfer*. *Blood*, 1996. **87**(3): p. 1097-103.
145. Brandi, J., et al., *Proteomic analysis of pancreatic cancer stem cells: Functional role of fatty acid synthesis and mevalonate pathways*. *J Proteomics*, 2017. **150**: p. 310-322.
146. Walther, U., et al., *Lovastatin lactone elicits human lung cancer cell apoptosis via a COX-2/PPARgamma-dependent pathway*. *Oncotarget*, 2016. **7**(9): p. 10345-62.
147. van de Steeg, E., et al., *Combined analysis of pharmacokinetic and efficacy data of preclinical studies with statins markedly improves translation of drug efficacy to human trials*. *J Pharmacol Exp Ther*, 2013. **347**(3): p. 635-44.

148. Koohestanimobarhan, S., et al., *Lipophilic statins antagonistically alter the major epithelial-to-mesenchymal transition signaling pathways in breast cancer stem-like cells via inhibition of the mevalonate pathway*. J Cell Biochem, 2018.
149. Bjarnadottir, O., et al., *Global Transcriptional Changes Following Statin Treatment in Breast Cancer*. Clin Cancer Res, 2015. **21**(15): p. 3402-11.
150. Neuvonen, P.J. and K.M. Jalava, *Itraconazole drastically increases plasma concentrations of lovastatin and lovastatin acid*. Clin Pharmacol Ther, 1996. **60**(1): p. 54-61.
151. Kyrklund, C., et al., *Plasma concentrations of active lovastatin acid are markedly increased by gemfibrozil but not by bezafibrate*. Clin Pharmacol Ther, 2001. **69**(5): p. 340-5.

ANEXO

ARTÍCULOS

Vásquez-Bochm LX, Velázquez-Paniagua M, Castro-Vázquez SS, Guerrero-Rodríguez SL, Mondragon-Peralta A, De La Fuente-Granada M, Pérez-Tapia SM, González-Arenas A, Velasco-Velázquez MA. 2019. Transcriptome-based identification of lovastatin as a breast cancer stem cell-targeting drug.

Velasco-Velázquez MA, Velázquez-Quesada I, **Vásquez-Bochm LX**, Pérez-Tapia SM. 2019. Targeting Breast Cancer Stem Cells: A Methodological Perspective.

Salinas-Jazmín N, González-González E, **Vásquez-Bochm LX**, Pérez-Tapia SM, Velasco-Velázquez MA. 2017. In Vitro Methods for Comparing Target Binding and CDC Induction Between Therapeutic Antibodies: Applications in Biosimilarity Analysis.



Contents lists available at ScienceDirect

Pharmacological Reports

journal homepage: www.elsevier.com/locate/pharep

Original article

Transcriptome-based identification of lovastatin as a breast cancer stem cell-targeting drug



Luz X. Vásquez-Bochm^{a,b}, Mireya Velázquez-Paniagua^{a,c}, Sandra S. Castro-Vázquez^a, Sandra L. Guerrero-Rodríguez^a, Abimael Mondragon-Peralta^a, Marisol De La Fuente-Granada^d, Sonia M. Pérez-Tapia^e, Aliesha González-Arenas^d, Marco A. Velasco-Velázquez^{a,f,*}

^a Department of Pharmacology, School of Medicine, National Autonomous University of Mexico (Universidad Nacional Autónoma de México; UNAM), Mexico City, Mexico

^b Graduate Program in Chemical Sciences, UNAM, Mexico City, Mexico

^c Department of Physiology, School of Medicine, UNAM, Mexico City, Mexico

^d Department of Genomic Medicine and Environmental Toxicology, Institute of Biomedical Research (IIB), UNAM, Mexico City, Mexico

^e Unit for Development and Research in Bioprocesses (UDIBI), National School of Biological Sciences, National Polytechnic Institute, Mexico City, Mexico

^f Unit for Research in Translational Biomedicine, Research Division, School of Medicine, UNAM, Mexico City, Mexico

ARTICLE INFO

Article history:

Received 7 August 2018

Received in revised form 27 January 2019

Accepted 15 February 2019

Available online 16 February 2019

Keywords:

Breast cancer stem cells

Drug repurposing

Lovastatin

HMGR inhibitor

ABSTRACT

Background: Breast cancer is a neoplastic disease with high morbidity and mortality in women worldwide. Breast cancer stem cells (CSCs) have a significant function in tumor growth, recurrence, and therapeutic resistance. Thus, CSCs have been pointed as targets of new therapies for breast cancer. Herein, we aimed to repurpose certain drugs as breast CSC-targeting agents.

Methods: We compared a consensus breast CSC signature with the transcriptomic changes that were induced by over 1300 bioactive compounds using Connectivity Map. The effects of the selected drugs on SOX2 promoter transactivation, SOX2 expression, viability, clonogenicity, and ALDH activity in breast cancer cells were analyzed by luciferase assay, western blot, MTT assay, mammosphere formation assay, and ALDEFUOR[®] test, respectively. Gene Set Enrichment Analysis (GSEA) was performed using the gene expression data from mammary tumors of mice that were treated with lovastatin.

Results: Five drugs (fasudil, pivmecillinam, ursolic acid, 16,16-dimethylprostaglandin E2, and lovastatin) induced signatures that correlated negatively with the query CSC signature. *In vitro*, lovastatin inhibited SOX2 promoter transactivation, and reduced the efficiency of mammosphere formation and the percentage of ALDH⁺ cells. Mevalonate mitigated the effects of lovastatin, suggesting that the targeting of CSCs by lovastatin was mediated by the inhibition of its reported target, 3-hydroxy-3-methyl-glutaryl-coenzyme A reductase (HMGR). By GSEA, lovastatin down-regulated genes that are involved in stemness and invasiveness in mammary tumors, corroborating our *in vitro* findings.

Conclusion: Lovastatin is a breast CSC-targeting drug. The inhibition of HMGR might develop new adjuvant therapeutic strategies for breast tumors.

© 2019 Institute of Pharmacology, Polish Academy of Sciences. Published by Elsevier B.V. All rights reserved.

Introduction

Breast cancer (BC) has a high incidence and causes significant mortality in women worldwide [1]. It is estimated that

approximately 3.2 million new cases of BC will develop annually by 2050 [2]. Despite the implementation of new therapies and treatments, approximately one-third of BC patients die due to tumor resistance, recurrence, and metastasis [3].

The cancer stem cell (CSC) hypothesis proposes that a subpopulation at the top of the tumor cell hierarchy contributes to tumor heterogeneity and is uniquely able to seed new tumors. Breast cancer stem cells (BCSCs) can self-renew, express signaling

* Corresponding author.

E-mail address: marcovelasco@unam.mx (M.A. Velasco-Velázquez).

proteins and transcription factors that promote pluripotency, generate non-stem tumor cells, and initiate tumors when implanted into immunocompromised mice [4,5].

BCSCs play key roles in the therapeutic resistance, recurrence, and progression of human breast tumors [6,7]. BCSCs display resistance to cytotoxic drugs [8], hyperactivation of signaling pathways that control stemness [9], and heightened DNA repair [10]. Further, breast cancer cells that disseminate to bone marrow and metastasis-initiating cells [9,11] have a stem phenotype, indicating that the CSC pool drives metastasis. Thus, CSCs are targets for new therapies in BC [12,13].

Drug repurposing is the identification of new therapeutic indications for approved drugs [14]. This strategy has several advantages, including a lower risk of toxic effects, accelerated clinical validation, and the ability to patent its new use [15]. There are many approaches for detecting unrecognized or non-explicit connections between drugs, targets, and diseases, including computational modeling, studying the mechanism of action-based methods, genetic profiling, and translational bioinformatics [16].

Transcriptional profiling studies identify gene sets that are differentially expressed in diseases or cells that have been exposed to drugs [17–19]. The comparison of a disease-induced gene signature against the expression profiles that are generated by drug exposure can reveal new connections between drugs and the disease. Theoretically, the drugs that induce transcriptional changes that are opposite to those in the disease could revert the phenotype [20]. Thus, several databases and user interfaces have been developed to translate genomewide transcriptional analyses into drug discovery [21–23].

Connectivity Map (CMap) [24] is a public database that contains genomewide expression profiles of human cancer cell lines that have been treated with bioactive compounds. These profiles can be compared with gene sets of interest by a matching algorithm, based on Kolmogorov-Smirnov statistical analysis. CMap has been useful for drug repurposing, lead discovery, mechanism of action analyses, and systems biology [25]. For example, it has been used to identify new activities of drugs in various neoplastic [26,27] and non-cancerous diseases [28].

To repurpose drugs that target BCSCs, we used a consensus gene signature that defines BCSCs to query CMap. The candidates that we identified were evaluated *in vitro* in triple-negative breast cancer cells. We found that the drug lovastatin reduced the CSC pool and that this effect was attributed to the inhibition of 3-hydroxy-3-methyl-glutaryl-coenzyme A reductase (HMGCR). By bioinformatic analysis of an independent dataset, mammary cancer cells from lovastatin-treated mice downregulated genes that control stemness and invasiveness, corroborating our *in vitro* findings. Our results agree with previously identified effects of statins [29–31] and support the repurposing of lovastatin as a drug with efficacy against BCSCs.

Materials and methods

Chemical transcriptomics

We used build 02 of the CMap database [24]. As a query signature, we selected a reported consensus BCSC signature [12] that comprised 39 genes (25 upregulated and 14 downregulated) and was generated from 3 biologically validated signatures, comparing: i) paclitaxel- versus salinomycin-treated HMLER breast cancer cells [12]; ii) primary human mammary epithelial cells that were cultured under conditions that favor mammary epithelial stem cell expansion versus cells that were cultured under conditions that favor differentiation [32]; and iii) CD44⁺ normal and neoplastic human mammary epithelial populations versus CD24⁺ cells [33].

Candidate drugs were selected from the CMap results, based on: a) significant negative association with the query signature ($p < 0.5$); b) a mean score < -0.5 ; c) specificity value < 0.1 ; and d) percentage non-null $\geq 75\%$. The global transcriptional responses that were induced by the candidate drugs were compared using Mode of Action by NeTwoRk Analysis (MANTRA) [21] with a computed distance threshold of 0.7.

Compounds

Fasudil hydrochloride (HA-1077), pivmecillinam (SML0817), ursolic acid (89797), 16,16-dimethyl-prostaglandin E2 (PGE2) (D2250000), and lovastatin (PHR1285) were purchased from Sigma-Aldrich. The stock solutions were prepared in DMSO and stored at -70°C under light-protected conditions until use. (\pm)-Mevalonolactone (Sigma-Aldrich M4667) solutions were prepared in water. The structural similarity of the candidate drugs was analyzed by generating fingerprints by circular and MACCS methods and comparing them using the Tanimoto coefficient, with the KNIME program in the CDK module.

Cell lines and culture

The triple-negative cell lines MDA-MB-231 and Hs578T were obtained from ATCC. The cells were grown in RPMI-1640 (MDA-MB-231) or DMEM (Hs578T) (Gibco) that was supplemented with 10% fetal bovine serum (FBS), at 5% CO₂ atmosphere. We used cell cultures from passage 6 to 16.

Luciferase assay

MDA-MB-231 cells were cotransfected with pGL3-SOX2-luc or pGL3-OCT4-luc plasmid [34] (generously donated by Dr. Richard Pestell, Baruch S. Blumberg Institute, PA, USA) and pNEG-PG04 using lipofectamine 3000 (Invitrogen) per the manufacturer's guidelines. Sublines that stably expressed the reporter constructions were selected and maintained in complete medium plus 0.5 $\mu\text{g}/\text{ml}$ puromycin. Cells were incubated with drugs for 24 h; then, the medium was removed, and the cells were incubated with lysis buffer (1% Triton X-100, 1 mM DTT in GME buffer) for 10 min at room temperature with shaking. Homogenates were mixed with 3 volumes of assay buffer (17 mM K₂PO₄, 1 mM DTT, and 2 mM ATP in GME buffer). Luminescence was quantified immediately after the addition of luciferin (GOLDBIO) on a GloMax[®] 20/20 luminometer (Promega). The fraction of viable cells at each concentration of drug was quantified in the same experiment and used for normalization.

Cell viability

5,000 MDA-MB-231 or 3,000 Hs578T cells were seeded in 96-well microplates and exposed to drugs for 24 h. The effect of the drugs on cell viability was estimated by MTT [3-(4,5-dimethylthiazol-2-yl)-2,5-diphenyltetrazolium bromide] assay. Reduced tetrazolium salt was measured spectrophotometrically at 570 nm (Epoch, BioTeK). Two to three independent experiments, each with six technical replicates, were performed (see figure legends for details).

Mammosphere formation assay

Sphere formation assay was performed as reported [32]. Briefly, 100 viable cells/well were plated in 96-well ultra-low attachment plates (Corning Costar) with MammoCult medium and growth factors (StemCell Technologies). The spheres were quantified on Day 7 in micrographs (Eclipse Ti-U microscopy, Nikon) and analyzed with NIS-Elements Imaging Software 4.13 (Nikon). Each

independent experiment was performed in octuplicate. In some experiments, the drug was present throughout the 7-d incubation, whereas in others, the cells were pretreated for 24 h and cultured in drug-free medium (see figure legends for details). The results are presented as mammosphere-forming efficiency (MFE%), which was calculated with the following equation: $MFE\% = (\text{number of mammospheres per well}) / (\text{number of cells seeded per well}) \times 100$.

ALDH staining

Treated cells were analyzed with the ALDEFLUOR® assay kit (StemCELL Technologies) per the manufacturer's guidelines. Briefly, cells were harvested with 0.05% trypsin-EDTA (Gibco), washed, counted, and suspended in ALDEFLUOR® buffer (2.5×10^6 cells/mL). ALDH substrate was added to the sample, which was then divided immediately into 2, to one half of which 7 μ L of the ALDH inhibitor DEAB was added. Both samples were incubated for 45 min at 37 °C before being analyzed on an Attune-NxT cytometer (Life Technologies). Data were analyzed in FlowJo 8.7 (Tree Star

Table 1
Potential drugs targeting the BCSC phenotype.

Compound	P	Mean cMap score	Specificity
Fasudil	0.02382	-0.71	0
Spiperone	0.00592	-0.677	0.0088
Pivmecillinam	0.00438	-0.606	0.0111
Ursolic acid	0.00203	-0.601	0.0073
16,16-dimethylprostaglandin E2	0.00877	-0.572	0.0138
Lovastatin	0.0118	-0.527	0.0155

Inc.) using DEAB-treated controls to establish the negative fluorescence signal.

Western blot

Treated cells were lysed in RIPA buffer (50 mM Tris-HCl, 0.1% SDS, 150 mM NaCl) supplemented with protease inhibitors (5 μ g/mL leupeptin, 1 μ g/mL pepstatin, 2 μ g/mL aprotinin). Protein

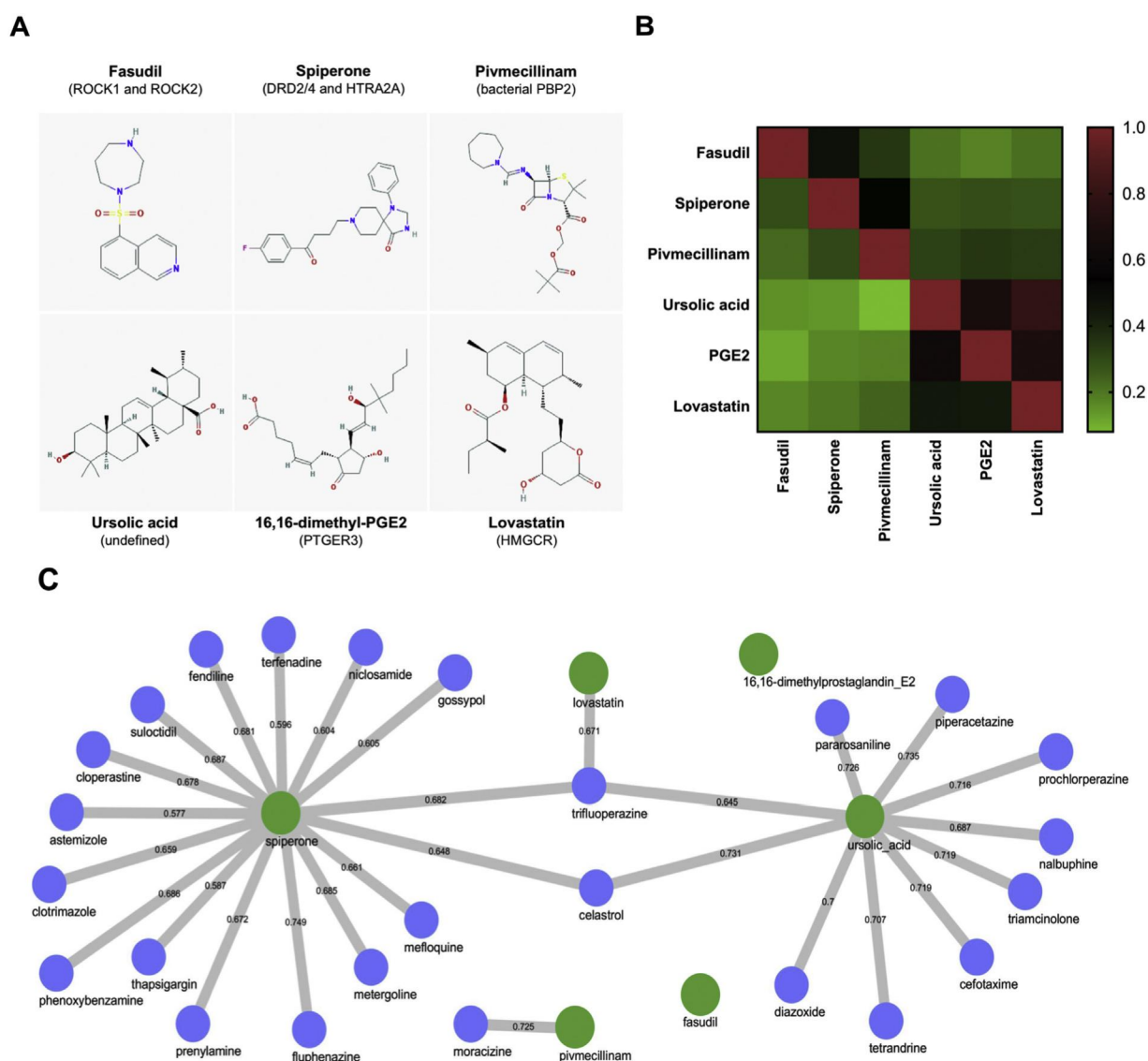


Fig. 1. Comparison of candidate drugs. A) Structure and reported targets of the six drugs selected in CMap. B) Chemical similarity evaluation by Tanimoto coefficient. Upper half of the matrix corresponds to the analysis based on fingerprint generation by MACCS, whereas the lower part shows the comparison using fingerprint generation by circular method. C) Comparison of global transcriptional changes induced by the candidate drugs (green circles). Drugs with significant associations are shown as blue circles. (For interpretation of the references to colour in this figure legend, the reader is referred to the web version of this article).

concentrations in the lysates were determined using the Pierce BCA Protein Assay Kit (Thermo Fisher Scientific). Samples that contained 30 µg of total protein were separated by SDS-PAGE and electroblotted onto PVDF membranes. After being blocked, the membranes were incubated with anti-SOX2 (Abcam ab97959; 1:1000), followed by a HRP-conjugated goat anti-rabbit secondary antibody (Santa Cruz Biotechnology sc-2004). The same membranes were stripped and reprobed with anti- α -tubulin (Santa Cruz Biotechnology sc-398103; 1:500), followed by a HRP-conjugated goat anti-mouse antibody (Abcam ab6789). Protein bands were detected using SuperSignal West Femto Maximum Sensitivity Substrate Pierce ECL Western Blotting Substrate (Thermo Fisher Scientific). Band intensities were measured in ImageJ [35] and data were normalized against vehicle (DMSO).

Enrichment analysis

Microarray data on 5 mouse mammary tumors that were treated with lovastatin and 5 controls were obtained from the Gene Expression Omnibus dataset GSE42787 [36]. Data were normalized in R studio (v1.1.383) using robust multi-array average normalization. Gene Set Enrichment Analysis (GSEA) [37] was performed using GSEA (v2.2.3). The following molecular signatures were used in the analysis: i) the Consensus Stemness Ranking (CSR) signature, [38]; ii) the oncogenic signature in mouse and human mammary stem cells [39]; iii) a hallmark gene set of the epithelial-to-mesenchymal transition (EMT) [40]; and iv) a signature from invasive ductal carcinomas [41]. Enrichment analysis for transcription factor targets was performed by feeding the top 250 differentially expressed genes into the ChIP-X Enrichment Analysis (ChEA) tool [42].

Statistical analysis

IC₅₀ values were calculated by nonlinear regression. Unless otherwise noticed, statistical significance was determined by one-way ANOVA, followed by Dunnett's multiple comparisons test against the vehicle control. Graphs were constructed and statistical analyses were performed in Prism (GraphPad).

Results

In silico prediction of drugs targeting BCSCs

Using a BCSC gene expression signature [12], we ranked the 1309 compounds in the CMap platform. Based on the selection

criteria (see "Materials and methods"), we identified several drugs that induced gene expression signatures that correlated negatively with those of BCSCs and thus represented potential therapeutic candidates (Table 1). The drugs were structurally distinct, had diverse canonical targets, and induced dissimilar global transcriptional signatures (Fig. 1). Of these candidates, we examined fasudil, pivmecillinam, ursolic acid, 16,16-dimethylprostaglandin E2 (PGE2), and lovastatin with regard to their activity in breast cancer cell cultures.

Lovastatin and fasudil reduce SOX2 promoter transactivation

SOX2 and OCT4 are essential regulators of cellular self-renewal and the maintenance of pluripotency in CSCs [43,44], and reporter constructs that harbor portions of their promoters have been used to monitor stemness in breast cancer cells [34,45]. In a primary screen, we measured the effects of the selected drugs on the transactivation of the SOX2 and OCT4 promoters at the concentration employed in CMap development (10 µM). Fasudil and lovastatin reduced SOX2 promoter transactivation by 60% and 95%, respectively (Fig. 2A). Conversely none of the drugs had a significant effect on transactivation of the OCT4 promoter (Fig. 2B). Based on these results, we focused on fasudil and lovastatin in subsequent analyses.

Lovastatin but not fasudil impairs clonogenicity

Using fasudil and lovastatin, we generated concentration-response curves to analyze their: i) cytotoxic effects in 2D cultures, ii) effects on mammosphere formation efficiency, and iii) impact on SOX2 promoter transactivation at various concentrations. Lovastatin reduced the viability of MDA-MB-231 to 56% of that of the control at the highest concentration. In contrast, fasudil had a modest effect on cell viability (Fig. 3A). Lovastatin but not fasudil decreased the number of mammospheres (IC₅₀ = 2.2 µM; Fig. 3B). Finally, both drugs impaired SOX2 promoter transactivation (Fig. 3C), supporting the findings in the primary screen and indicating that lovastatin is more potent. Based on the effects of lovastatin on clonogenicity and SOX2 promoter transactivation, we subjected it to additional analysis.

Short-term exposure of breast cancer cells to lovastatin irreversibly affects the CSC pool

Aldehyde dehydrogenase (ALDH) activity has been used extensively to quantify the CSC population in triple-negative

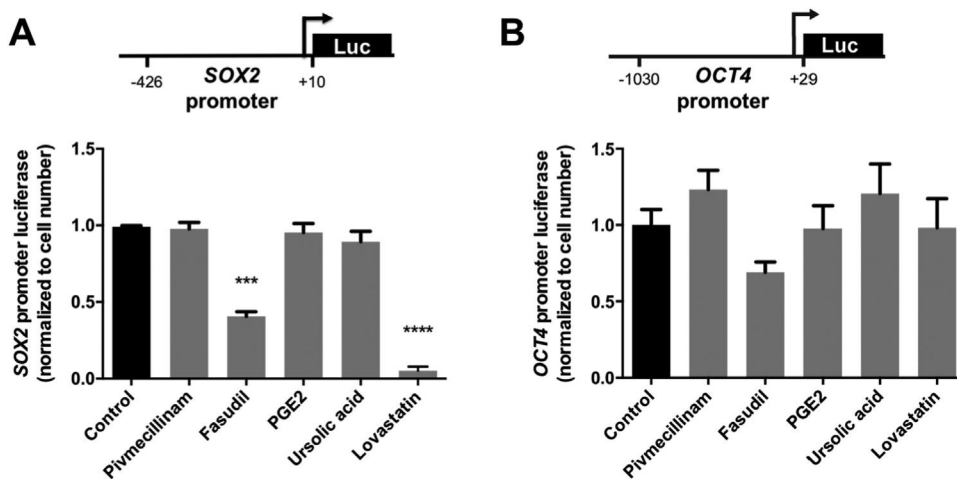


Fig. 2. Effects of the selected drugs on transactivation of the SOX2 (A) and OCT4 (B) promoters. Schemes above graphs show the size of the promoters in the constructs. Transactivation was measured by luciferase reporter assay. Values are mean \pm SEM from 4 independent experiments; $p < 0.05$ (*), < 0.01 (**), < 0.001 (***), < 0.0001 (****).

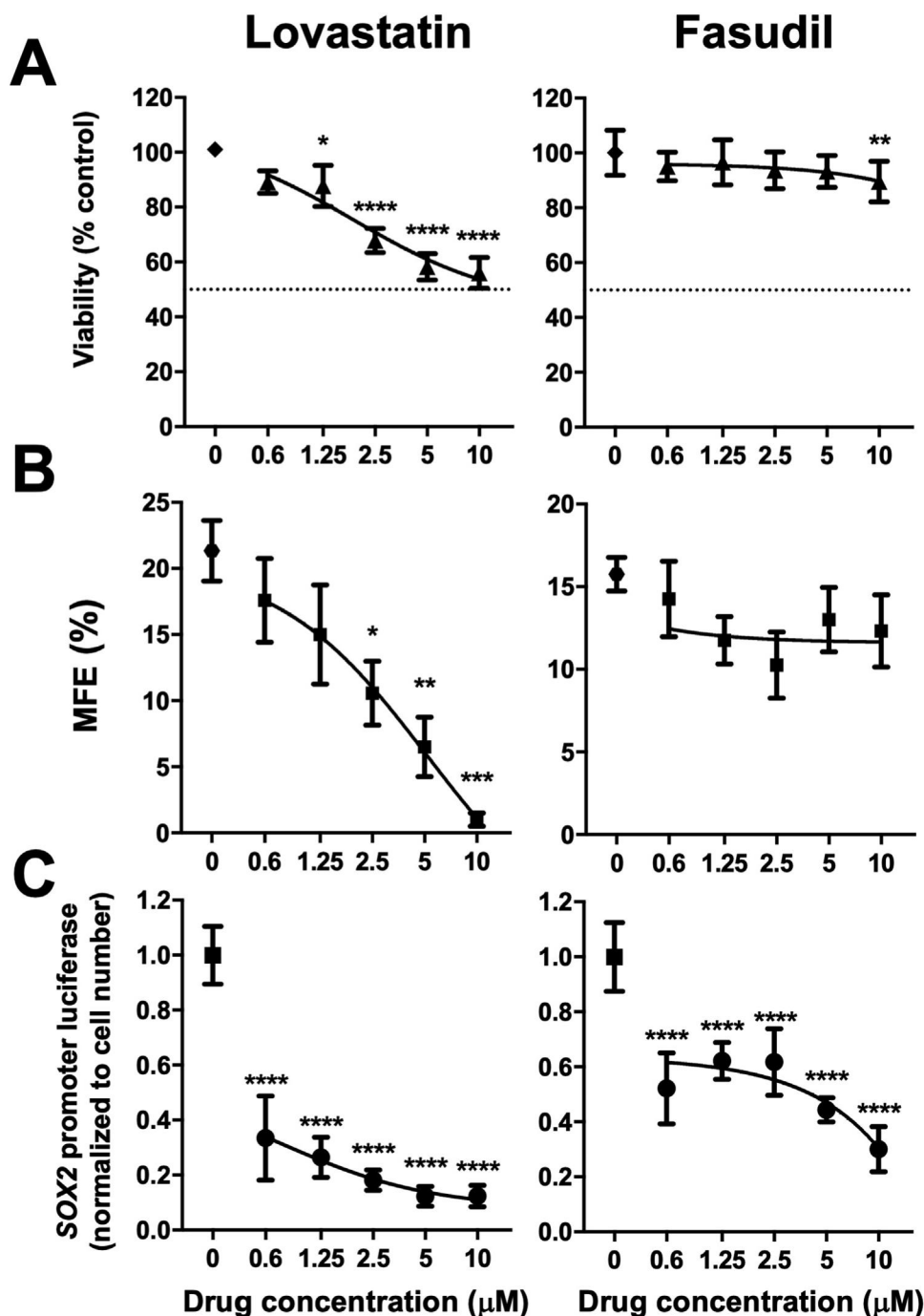


Fig. 3. Activity of presumed BCSC-targeting drugs. Effects of lovastatin or fasudil on MDA-MB-231 cell viability (A) and mammosphere-initiating capacity (B). The effects of the drugs on SOX2 promoter transactivation were corroborated in dose-response curves (C). Graphs show mean \pm SEM of a compilation of 3 independent experiments; $p < 0.05$ (*), < 0.01 (**), < 0.001 (***), < 0.0001 (****) against the vehicle control.

breast cancer cells [46–48]. Lovastatin significantly reduced the ALDH⁺ fraction in a concentration-dependent manner in MDA-MB-231 cells (Fig. 4B–C) and Hs578T cells (Fig. 4D and Suppl. Fig. 1B). The effects correlated with reductions in SOX2 protein expression in both cell lines (Fig. 4E). Together, these results supported the hypothesis that lovastatin decreases the CSC pool.

To confirm the CSC-targeting effects of lovastatin, we followed the strategy reported by Gupta and collaborators [12]. Cells were pre-incubated with lovastatin, collected and cultured to evaluate their mammosphere formation capacity under drug-free

conditions (Fig. 4A). Pre-incubation significantly lowered the number of mammospheres in the two studied cell lines (Fig. 4F, G), supporting that lovastatin irreversibly reduces the CSC pool.

Effects of lovastatin on CSC are mediated by HMGCR inhibition

To determine whether the effects of lovastatin are mediated by its canonical target, we treated cells simultaneously with lovastatin and/or mevalonate, the latter of which is generated by HMGCR [49]. Mevalonate reverted the lovastatin-induced

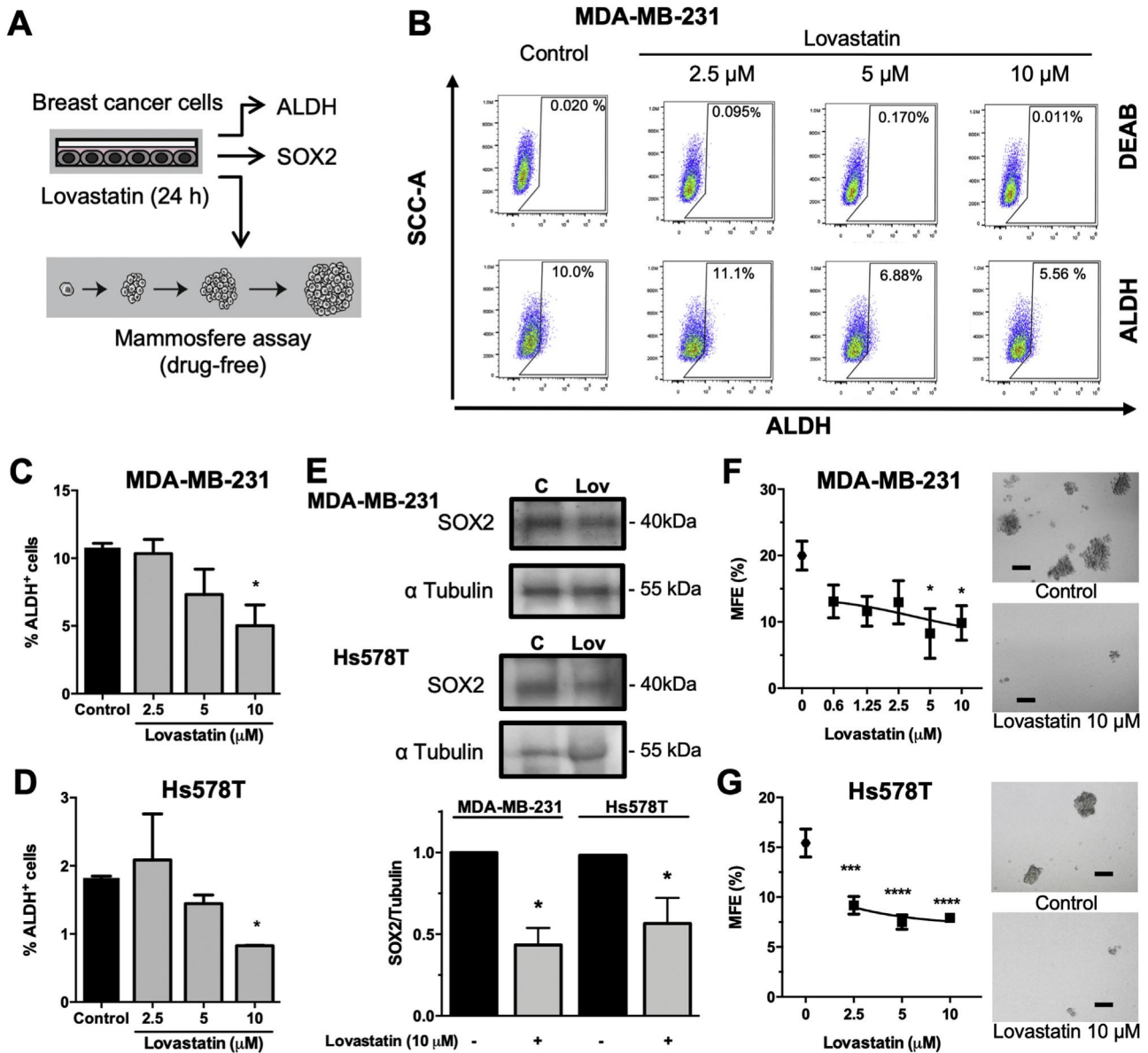


Fig. 4. Effects of lovastatin on the breast cancer stem cell pool. A) Experimental strategy for analyzing stemness after short exposure of breast cancer cells to lovastatin. B) Representative dot plots quantifying the ALDH⁺ fraction in lovastatin-treated MDA-MB-231 cells. C, D) Analysis of ALDH⁺ cells in MDA-MB-231 (C) and Hs578T (D) cells. Graphs show mean \pm SEM from 5 (C) or 2 (D) independent experiments. E) Representative western blot evaluating the expression of SOX2 and the corresponding analysis of the SOX2/ α -tubulin ratio from 3 independent experiments. Statistical significance was determined by Student's *t*-test. F, G) Viable MDA-MB-231 (F) or Hs578T (G) cells that had been exposed to lovastatin for 24 h were seeded to test their capacity to grow mammospheres in drug-free medium. Graphs show the mean number of mammospheres \pm SEM from 4 independent experiments (F) or from a representative experiment performed in octuplicate (G). Representative pictures are shown; bar = 100 μ m; *p* < 0.05 (*), < 0.01 (**), < 0.001 (***), < 0.0001 (****).

decrease in the fraction of ALDH⁺ cells (Fig. 5A) and mammosphere formation (Fig. 5B). Mevalonate also partially restored SOX2 promoter transactivation, which was completely inhibited by lovastatin (Fig. 5C), and SOX2 protein expression (Fig. 5F). Notably, mevalonate alone did not alter cell viability (Suppl. Fig. 2C).

Lovastatin reverts CSC and invasiveness signatures in mice bearing breast tumors

GSEA revealed that gene sets from a CSR signature (Fig. 6A) and a mammary progenitor cell signature (Fig. 6B) were enriched in mammary tumors of mice that had been treated with vehicle, indicating that *in vivo*, lovastatin downmodulates key genes that are upregulated in the stem/progenitor population of cancer cells.

We also queried the dataset with a hallmark set of genes that are upregulated in the EMT (Fig. 6C) and in invasive breast cancer cells (Fig. 6D), given that induction of the EMT promotes the acquisition of CSC features in breast cancer cells [50]. Lovastatin also downregulated these gene sets, suggesting that it shrinks the population with an invasive phenotype and providing indirect evidence of a reduction in the CSC pool.

Finally, the 250 genes with highest differential expression between tumors of lovastatin-treated and vehicle-treated mice were analyzed with regard to enrichment in putative targets of transcription factors (Suppl. Fig. 3). We found that such subset of genes was significantly enriched in targets of transcription factors that control the pluripotency of stem cells or participate in the differentiation of hematopoietic stem cells.

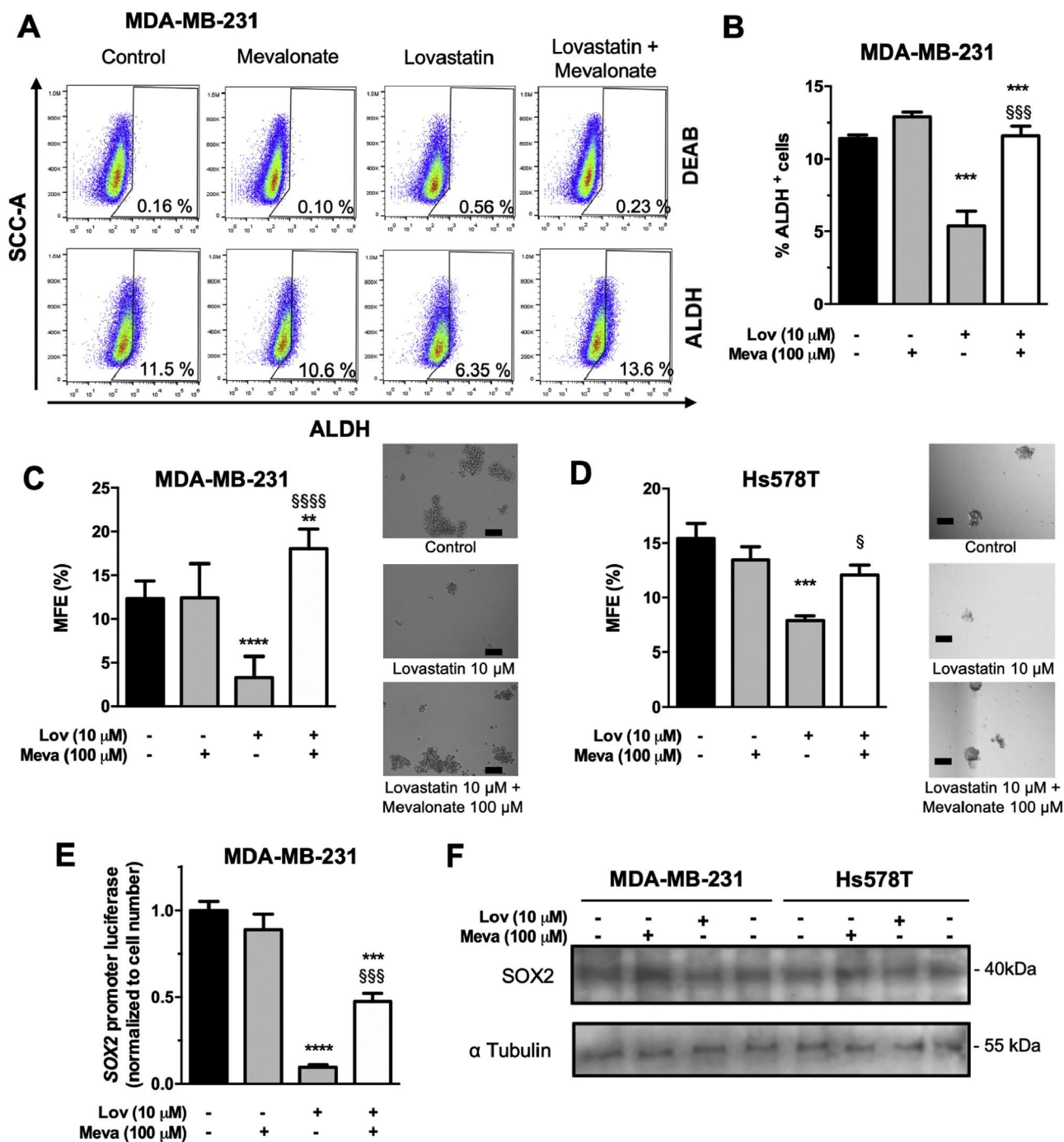


Fig. 5. Effects of mevalonate on lovastatin-induced effects. A) Representative dot plots quantifying the ALDH⁺ fraction in MDA-MB-231 cells treated with lovastatin (Lov; 10 μ M) and/or mevalonate (Meva; 100 μ M). B) Quantification of the fraction of ALDH⁺ cells. Graphs show mean \pm SEM from 3 independent experiments. C, D) Mammosphere formation in MDA-MB-231 (C) and Hs578T (D) cells exposed to lovastatin and/or mevalonate for 24 h. Graphs show the mean \pm SEM of a representative experiment performed in octuplicate. Representative pictures are shown; bar = 100 μ m. E) Transactivation of SOX2 promoter in MDA-MB-231 cells, assessed by luciferase reporter assay. Values are mean \pm SEM of 3 independent experiments. Statistical significance was determined by Tukey's multiple comparisons test against the vehicle control; $p < 0.05$ (*), < 0.01 (**), < 0.001 (***), < 0.0001 (****), and against lovastatin; $p < 0.05$ (§), < 0.001 (§§§), < 0.0001 (§§§§). F) Representative western blot evaluating the expression of SOX2 and α -tubulin in MDA-MB-231 and Hs578T cells exposed to lovastatin and/or mevalonate.

Discussion

The CMap platform allows one to select drugs *in silico*, based on their transcriptional effects on multiple cell lines [24]. Thus, CMap analysis generates hypotheses on the drugs that can revert a particular signature, independent of the cellular context [51,52]. Thus, we aimed to pinpoint drugs that could be repurposed as BCSC-targeting drugs using CMap. Our analysis with a BCSC

consensus signature [12] identified 6 candidate drugs with various mechanisms of action. The drugs were structurally dissimilar and induced unrelated global transcriptional profiles, eliminating the possibility that the negative associations with the BCSC signature that were revealed by CMap were elicited through a common mechanism.

Biological evaluation of 5 of the drugs was performed in MDA-MB-231 cells that stably expressed luciferase under control of the

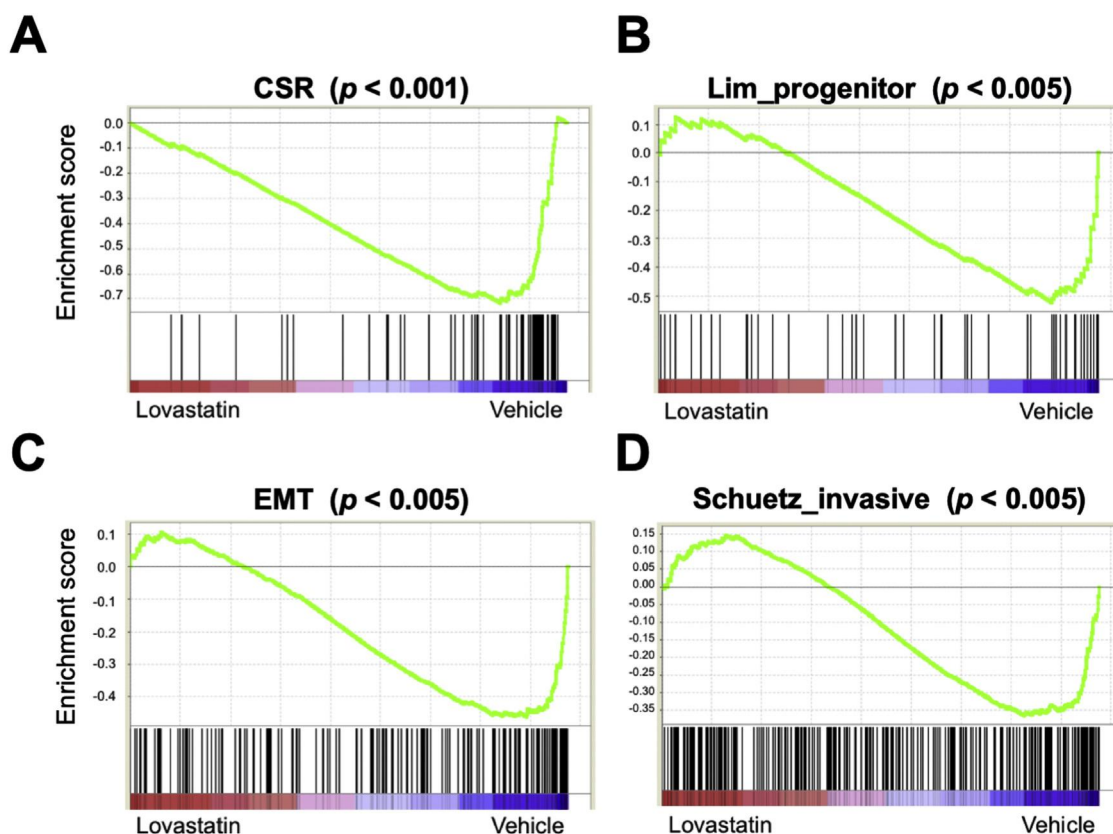


Fig. 6. Enrichment analysis of mammary tumors in mice treated with lovastatin. A–D) Enrichment plots from GSEA. The plots show running enrichment scores (y axis) and positions (black lines) of members of the upregulated gene sets for the CSR (A), luminal progenitors (B), EMT (C), and invasiveness (D).

SOX2 or OCT4 promoter. Lovastatin and fasudil reduced SOX2 promoter transactivation, but none of the drugs affected activation of the OCT4 promoter. SOX2 expression correlates significantly with larger tumors and the presence of lymph node metastases in BC patients [53], and its silencing decreases mammosphere formation *in vitro* and tumorigenicity in animal models [43].

Lovastatin reduced cell viability in adherent cultures of MDA-MB-231 breast cancer cells. Our results are consistent with previous reports that lovastatin induces cell death [54,55] and inhibits the proliferation [56,57] of multiple breast cancer cell lines, including MDA-MB-231.

To validate the CSC-targeting effects of lovastatin, we treated cells for 24 h and analyzed changes in the ALDH⁺ population, SOX2 expression, and mammosphere formation in drug-free cultures. Lovastatin lowered the ALDH⁺ fraction, reduced SOX2 protein levels, and irreversibly decreased the number of mammosphere-initiating cells in 2 triple-negative breast cancer cell lines. High ALDH activity marks the BCSC population and correlates with chemoresistance, self-renewal of tumor CSCs, and a poor prognosis in BC patients [46,58], whereas the efficiency of mammosphere formation is a surrogate measure of CSC content [32,59–61]. These effects of lovastatin support the hypothesis that it reduces the CSC pool. Accordingly, previous studies have shown that statins reduce the CSC pool in models of breast [29,30] and other types of cancer [62–64]. Whether BCSC are more sensitive to lovastatin than other subpopulations of breast cancer cells, remains to be determined.

The computational predictions that were generated by CMap do not provide information on whether the transcriptional changes were caused by on-target or off-target effects. Thus, we examined the function of the canonical target of lovastatin in its BCSC-targeting effects. The addition of mevalonate is sufficient to abolish the effects of the inhibition of HMGCR [65]. For example,

mevalonate reverses the effects of lovastatin on cell viability [54] and G1 arrest [56]. Supplementation of mevalonate to MDA-MB-231 or Hs578T cells reverted the phenotypic (ALDH⁺), functional (mammosphere formation), and transcriptional (SOX2) changes that were induced by lovastatin, indicating that its CSC-targeting effects are, at least in part, attributed to the inhibition of HMGCR. Consistent with these findings, previous studies have shown that the effects of statins on the CSC subpopulation are associated with inhibition of the mevalonate pathway [62], which is particularly active on basal BCSCs [30]. However, we cannot disregard the participation of other mechanisms in these effects. For example, a recent study has demonstrated that lovastatin-induced COX-2 expression and the subsequent COX-2-dependent activation of PPAR γ cause cytotoxicity in lung cancer cells [66].

Although our *in vitro* results demonstrated CSC-targeting effects of lovastatin, our experiments were designed to use similar concentrations of the drug as in the CMap analysis (10 μ M) and in previous reports. Such concentrations are 100- to 1000-fold higher than in plasma of subjects who consume therapeutic doses of lovastatin [67,68], constituting one limitation of the study.

In order to analyze the *in vivo* effects of lovastatin, we studied the transcriptional changes that were induced in mice treated with the drug at a dose (10 mg/kg) that effectively reduces plasma cholesterol [69]. We detected reversions of the gene signatures that define stem/progenitor and invasive cancer cells in mammary tumors of mice that were treated with lovastatin. Lovastatin suppress the expression of a cluster of genes governing EMT, invasion, stemness and apoptosis, including proteins of the Hippo, Notch, Wnt, and HIF pathways [31,55]. Similarly, the administration of atorvastatin to breast cancer patients induces changes in the expression of multiple genes that participate in proliferation

and apoptosis, which may be dependent on changes on the activation of the transcription factors CREB1, ATF, OCT, and SRF [70]. However, the effects of statins on the activation of transcription factors that govern pluripotency are currently unknown. Together, these results validate our *in silico-in vitro* selection, and suggest that lovastatin reduces the stem/progenitor population *in vivo*, warranting further examination.

Conclusion

We have found that lovastatin targets BCSCs by transcriptome-based analysis, combined with *in vitro* evaluations and *in vivo* validation. These effects likely to be caused by the inhibition of HMGR and thus might be elicited by other statins. Determining the precise mechanisms that are involved in the effects of lovastatin on breast cancer cell stemness might encourage its use as an adjuvant therapeutic strategy for breast tumors.

Conflict of interests

There are no conflicts of interest that are associated with this manuscript.

Funding

This work was supported by PAPIIT UNAMIN228616, CONACYT-INFR-2014-01-225313 (M.A.V.-V.), and UDIMEB (S.M.P.-T.). L.X.V.-B. is recipient of a graduate scholarship from CONACYT (294303).

CRedit authorship contribution statement

Luz X. Vázquez-Boehm: Data curation, Formal analysis, Investigation, Visualization, Writing - original draft. **Mireya Velázquez-Paniagua:** Investigation, Formal analysis, Methodology, Visualization. **Sandra S. Castro-Vázquez:** Data curation, Formal analysis, Investigation. **Sandra L. Guerrero-Rodríguez:** Data curation, Formal analysis, Investigation, Visualization. **Abimael Mondragon-Peralta:** Investigation, Visualization, Formal analysis. **Marisol De La Fuente-Granada:** Investigation, Visualization, Formal analysis. **Sonia M. Pérez-Tapia:** Conceptualization, Supervision, Funding acquisition. **Aliesha González-Arenas:** Conceptualization, Supervision, Funding acquisition, Writing - review & editing. **Marco A. Velasco-Velázquez:** Conceptualization, Data curation, Formal analysis, Supervision, Funding acquisition, Writing - review & editing.

Acknowledgments

We thank doctors Diana Casique-Aguirre and Angel J. Ruiz Moreno for technical assistance, Mrs. Josefina Bolado, Head of the Scientific Paper Translation Department from División de Investigación at Facultad de Medicina UNAM, for language editing, and Andi Espinoza, Departamento de Farmacología at Facultad de Medicina UNAM, for graphics enhancing.

Appendix A. Supplementary data

Supplementary material related to this article can be found, in the online version, at doi:<https://doi.org/10.1016/j.pharep.2019.02.011>.

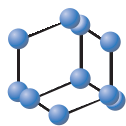
References

- [1] McGuire S. World Cancer Report 2014. Geneva, Switzerland: World Health Organization, International Agency For Research on Cancer. WHO Press; 2015 Adv Nutr. 2016;7(2):418–9.

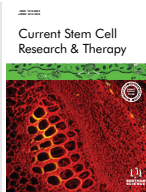
- [2] Tao Z, Shi A, Lu C, Song T, Zhang Z, Zhao J. Breast Cancer: epidemiology and etiology. Cell Biochem Biophys 2015;72(2):333–8.
- [3] Ahmad A. Pathways to breast cancer recurrence. ISRN Oncol 2013;2013:290568.
- [4] Al-Hajj M, Wicha MS, Benito-Hernandez A, Morrison SJ, Clarke MF. Prospective identification of tumorigenic breast cancer cells. Proc Natl Acad Sci U S A 2003;100(7):3983–8.
- [5] Seymour T, Twigger AJ, Kakulas F. Pluripotency genes and their functions in the normal and aberrant breast and brain. Int J Mol Sci 2015;16(11):27288–301.
- [6] Velasco-Velazquez MA, Popov VM, Lisanti MP, Pestell RG. The role of breast cancer stem cells in metastasis and therapeutic implications. Am J Pathol 2011;179(1):2–11.
- [7] Luo M, Clouthier SG, Deol Y, Liu S, Nagrath S, Azizi E, et al. Breast cancer stem cells: current advances and clinical implications. Methods Mol Biol 2015;1293:1–49.
- [8] Li X, Lewis MT, Huang J, Gutierrez C, Osborne CK, Wu MF, et al. Intrinsic resistance of tumorigenic breast cancer cells to chemotherapy. J Natl Cancer Inst 2008;100(9):672–9.
- [9] Balic M, Lin H, Young L, Hawes D, Giuliano A, McNamara G, et al. Most early disseminated cancer cells detected in bone marrow of breast cancer patients have a putative breast cancer stem cell phenotype. Clin Cancer Res 2006;12(19):5615–21.
- [10] Jiao X, Velasco-Velazquez MA, Wang M, Li Z, Rui H, Peck AR, et al. CCR5 governs DNA damage repair and breast Cancer stem cell expansion. Cancer Res 2018;78(7):1657–71.
- [11] Baccelli I, Schneeweiss A, Riethdorf S, Stenzinger A, Schillert A, Vogel V, et al. Identification of a population of blood circulating tumor cells from breast cancer patients that initiates metastasis in a xenograft assay. Nat Biotechnol 2013;31(6):539–44.
- [12] Gupta PB, Onder TT, Jiang G, Tao K, Kuperwasser C, Weinberg RA, et al. Identification of selective inhibitors of cancer stem cells by high-throughput screening. Cell 2009;138(4):645–59.
- [13] Velasco-Velazquez MA, Homsí N, De La Fuente M, Pestell RG. Breast cancer stem cells. Int J Biochem Cell Biol 2012;44(4):573–7.
- [14] Wurth R, Thellung S, Bajetto A, Mazzanti M, Florio T, Barbieri F. Drug-repositioning opportunities for cancer therapy: novel molecular targets for known compounds. Drug Discov Today 2016;21(1):190–9.
- [15] Cavalla D. Therapeutic switching: a new strategic approach to enhance R&D productivity. IDrugs 2005;8(11):914–8.
- [16] Pritchard JE, O'Mara TA, Glubb DM. Enhancing the promise of drug repositioning through genetics. Front Pharmacol 2017;8:896.
- [17] Lussier YA, Chen JL. The emergence of genome-based drug repositioning. Sci Transl Med 2011;3(96)96ps35.
- [18] Sirota M, Dudley JT, Kim J, Chiang AP, Morgan AA, Sweet-Cordero A, et al. Discovery and preclinical validation of drug indications using compendia of public gene expression data. Sci Transl Med 2011;3(96)96ra77.
- [19] Verbist B, Klambauer G, Vervoort L, Talloen W, Consortium Q, Shkedy Z, et al. Using transcriptomics to guide lead optimization in drug discovery projects: lessons learned from the QSTAR project. Drug Discov Today 2015;20(5):505–13.
- [20] Iorio F, Rittman T, Ge H, Menden M, Saez-Rodriguez J. Transcriptional data: a new gateway to drug repositioning? Drug Discov Today 2013;18(7–8):350–7.
- [21] Iorio F, Bosotti R, Scacheri E, Belcastro V, Mithbaakar P, Ferriero R, et al. Discovery of drug mode of action and drug repositioning from transcriptional responses. Proc Natl Acad Sci U S A 2010;107(33):14621–6.
- [22] de Anda-Jauregui G, Guo K, McGregor BA, Hur J. Exploration of the anti-inflammatory drug space through network pharmacology: applications for drug repurposing. Front Physiol 2018;9:151.
- [23] Mirza N, Sills GJ, Pirmohamed M, Marson AG. Identifying new antiepileptic drugs through genomics-based drug repurposing. Hum Mol Genet 2017;26(3):527–37.
- [24] Lamb J, Crawford ED, Peck D, Modell JW, Blat IC, Wrobel MJ, et al. The Connectivity Map: using gene-expression signatures to connect small molecules, genes, and disease. Science 2006;313(5795):1929–35.
- [25] Qu XA, Rajpal DK. Applications of Connectivity Map in drug discovery and development. Drug Discov Today 2012;17(23–24):1289–98.
- [26] Manzotti G, Parenti S, Ferrari-Amorotti G, Soliera AR, Cattelani S, Montanari M, et al. Monocyte-macrophage differentiation of acute myeloid leukemia cell lines by small molecules identified through interrogation of the Connectivity Map database. Cell Cycle 2015;14(16):2578–89.
- [27] Zhan SJ, Liu B, Linghu H. Identifying genes as potential prognostic indicators in patients with serous ovarian cancer resistant to carboplatin using integrated bioinformatics analysis. Oncol Rep 2018;39(6):2653–63.
- [28] Siavelis JC, Bourdakou MM, Athanasiadis EI, Spyrou GM, Nikita KS. Bioinformatics methods in drug repurposing for Alzheimer's disease. Brief Bioinform 2016;17(2):322–35.
- [29] Fiorillo M, Peiris-Pages M, Sanchez-Alvarez R, Bartella L, Di Donna L, Dolce V, et al. Bergamot natural products eradicate cancer stem cells (CSCs) by targeting mevalonate, Rho-GDI-signalling and mitochondrial metabolism. Biochim Biophys Acta 2018;1859(9):984–96.
- [30] Ginestier C, Monville F, Wicinski J, Cabaud O, Cervera N, Josselin E, et al. Mevalonate metabolism regulates Basal breast cancer stem cells and is a potential therapeutic target. Stem Cells 2012;30(7):1327–37.
- [31] Koohestanibarhan S, Salami S, Imeni V, Mohammadi Z, Bayat O. Lipophilic statins antagonistically alter the major epithelial-to-mesenchymal transition

- signaling pathways in breast cancer stem-like cells via inhibition of the mevalonate pathway. *J Cell Biochem* 2018.
- [32] Dontu G, Abdallah WM, Foley JM, Jackson KW, Clarke MF, Kawamura MJ, et al. In vitro propagation and transcriptional profiling of human mammary stem/progenitor cells. *Genes Dev* 2003;17(10):1253–70.
- [33] Shipitsin M, Campbell LL, Argani P, Weremowicz S, Bloushtain-Qimron N, Yao J, et al. Molecular definition of breast tumor heterogeneity. *Cancer Cell* 2007;11(3):259–73.
- [34] Wu K, Jiao X, Li Z, Katiyar S, Casimiro MC, Yang W, et al. Cell fate determination factor Dachshund reprograms breast cancer stem cell function. *J Biol Chem* 2011;286(3):2132–42.
- [35] Schneider CA, Rasband WS, Eliceiri KW. NIH Image to ImageJ: 25 years of image analysis. *Nat Methods* 2012;9(7):671–5.
- [36] Mira E, Carmona-Rodriguez L, Tardaguila M, Azcoitia I, Gonzalez-Martin A, Almonacid L, et al. A lovastatin-elicited genetic program inhibits M2 macrophage polarization and enhances T cell infiltration into spontaneous mouse mammary tumors. *Oncotarget* 2013;4(12):2288–301.
- [37] Subramanian A, Tamayo P, Mootha VK, Mukherjee S, Ebert BL, Gillette MA, et al. Gene set enrichment analysis: a knowledge-based approach for interpreting genome-wide expression profiles. *Proc Natl Acad Sci U S A* 2005;102(43):15545–50.
- [38] Shats I, Gatza ML, Chang JT, Mori S, Wang J, Rich J, et al. Using a stem cell-based signature to guide therapeutic selection in cancer. *Cancer Res* 2011;71(5):1772–80.
- [39] Lim E, Wu D, Pal B, Bouras T, Asselin-Labat ML, Vaillant F, et al. Transcriptome analyses of mouse and human mammary cell subpopulations reveal multiple conserved genes and pathways. *Breast Cancer Res* 2010;12(2):R21.
- [40] Liberzon A, Birger C, Thorvaldsdottir H, Ghandi M, Mesirov JP, Tamayo P. The Molecular Signatures Database (MSigDB) hallmark gene set collection. *Cell Syst* 2015;1(6):417–25.
- [41] Schuetz CS, Bonin M, Clare SE, Nieselt K, Sotlar K, Walter M, et al. Progression-specific genes identified by expression profiling of matched ductal carcinomas in situ and invasive breast tumors, combining laser capture microdissection and oligonucleotide microarray analysis. *Cancer Res* 2006;66(10):5278–86.
- [42] Lachmann A, Xu H, Krishnan J, Berger SI, Mazloom AR, Ma'ayan A. ChEA: transcription factor regulation inferred from integrating genome-wide ChIP-X experiments. *Bioinformatics* 2010;26(19):2438–44.
- [43] Leis O, Eguara A, Lopez-Arribillaga E, Alberdi MJ, Hernandez-Garcia S, Elorriaga K, et al. Sox2 expression in breast tumours and activation in breast cancer stem cells. *Oncogene* 2012;31(11):1354–65.
- [44] Nishi M, Sakai Y, Akutsu H, Nagashima Y, Quinn G, Masui S, et al. Induction of cells with cancer stem cell properties from nontumorigenic human mammary epithelial cells by defined reprogramming factors. *Oncogene* 2014;33(5):643–52.
- [45] Tang B, Raviv A, Esposito D, Flanders KC, Daniel C, Nghiem BT, et al. A flexible reporter system for direct observation and isolation of cancer stem cells. *Stem Cell Reports* 2015;4(1):155–69.
- [46] Ginestier C, Hur MH, Charafe-Jauffret E, Monville F, Dutcher J, Brown M, et al. ALDH1 is a marker of normal and malignant human mammary stem cells and a predictor of poor clinical outcome. *Cell Stem Cell* 2007;1(5):555–67.
- [47] Croker AK, Goodale D, Chu J, Postenka C, Hedley BD, Hess DA, et al. High aldehyde dehydrogenase and expression of cancer stem cell markers selects for breast cancer cells with enhanced malignant and metastatic ability. *J Cell Mol Med* 2009;13(8B):2236–52.
- [48] Croker AK, Allan AL. Inhibition of aldehyde dehydrogenase (ALDH) activity reduces chemotherapy and radiation resistance of stem-like ALDHhiCD44(+) human breast cancer cells. *Breast Cancer Res Treat* 2012;133(1):75–87.
- [49] Goldstein JL, Brown MS. Regulation of the mevalonate pathway. *Nature* 1990;343(6257):425–30.
- [50] Mani SA, Guo W, Liao MJ, Eaton EN, Ayyanan A, Zhou AY, et al. The epithelial-mesenchymal transition generates cells with properties of stem cells. *Cell* 2008;133(4):704–15.
- [51] Gao L, Zhao G, Fang JS, Yuan TY, Liu AL, Du GH. Discovery of the neuroprotective effects of alvespimycin by computational prioritization of potential anti-Parkinson agents. *FEBS J* 2014;281(4):1110–22.
- [52] Beck A, Eberherr C, Hagemann M, Cairo S, Haberle B, Vokuhl C, et al. Connectivity map identifies HDAC inhibition as a treatment option of high-risk hepatoblastoma. *Cancer Biol Ther* 2016;17(11):1168–76.
- [53] Zheng Y, Qin B, Li F, Xu S, Wang S, Li L. Clinicopathological significance of Sox2 expression in patients with breast cancer: a meta-analysis. *Int J Clin Exp Med* 2015;8(12):22382–92.
- [54] Siddiqui RA, Harvey KA, Xu Z, Natarajan SK, Davisson VJ. Characterization of lovastatin-docosahexaenoate anticancer properties against breast cancer cells. *Bioorg Med Chem* 2014;22(6):1899–908.
- [55] Yang T, Yao H, He G, Song L, Liu N, Wang Y, et al. Effects of lovastatin on MDA-MB-231 breast Cancer cells: an antibody microarray analysis. *J Cancer* 2016;7(2):192–9.
- [56] Rao S, Porter DC, Chen X, Herliczek T, Lowe M, Keyomarsi K. Lovastatin-mediated G1 arrest is through inhibition of the proteasome, independent of hydroxymethyl glutaryl-CoA reductase. *Proc Natl Acad Sci U S A* 1999;96(14):7797–802.
- [57] Campbell MJ, Esserman LJ, Zhou Y, Shoemaker M, Lobo M, Borman E, et al. Breast cancer growth prevention by statins. *Cancer Res* 2006;66(17):8707–14.
- [58] Magni M, Shammah S, Schiro R, Mellado W, Dalla-Favera R, Gianni AM. Induction of cyclophosphamide-resistance by aldehyde-dehydrogenase gene transfer. *Blood* 1996;87(3):1097–103.
- [59] Liao MJ, Zhang CC, Zhou B, Zimonjic DB, Mani SA, Kaba M, et al. Enrichment of a population of mammary gland cells that form mammospheres and have in vivo repopulating activity. *Cancer Res* 2007;67(17):8131–8.
- [60] Ponti D, Costa A, Zaffaroni N, Pratesi G, Petrangolini G, Coradini D, et al. Isolation and in vitro propagation of tumorigenic breast cancer cells with stem/progenitor cell properties. *Cancer Res* 2005;65(13):5506–11.
- [61] Lombardo Y, de Giorgio A, Coombes CR, Stebbing J, Castellano L. Mammosphere formation assay from human breast cancer tissues and cell lines. *J Vis Exp* 2015;97.
- [62] Brandi J, Dando I, Pozza ED, Biondani G, Jenkins R, Elliott V, et al. Proteomic analysis of pancreatic cancer stem cells: functional role of fatty acid synthesis and mevalonate pathways. *J Proteomics* 2017;150:310–22.
- [63] Peng Y, He G, Tang D, Xiong L, Wen Y, Miao X, et al. Lovastatin inhibits Cancer stem cells and sensitizes to Chemo- and photodynamic therapy in nasopharyngeal carcinoma. *J Cancer* 2017;8(9):1655–64.
- [64] Kato S, Liberona MF, Cerda-Infante J, Sanchez M, Henriquez J, Bizama C, et al. Simvastatin interferes with cancer 'stem-cell' plasticity reducing metastasis in ovarian cancer. *Endocr Relat Cancer* 2018;25(10):821–36.
- [65] Alonso DF, Farina HG, Skilton G, Gabri MR, De Lorenzo MS, Gomez DE. Reduction of mouse mammary tumor formation and metastasis by lovastatin, an inhibitor of the mevalonate pathway of cholesterol synthesis. *Breast Cancer Res Treat* 1998;50(1):83–93.
- [66] Walther U, Emmrich K, Ramer R, Mittag N, Hinz B. Lovastatin lactone elicits human lung cancer cell apoptosis via a COX-2/PPARgamma-dependent pathway. *Oncotarget* 2016;7(9):10345–62.
- [67] Neuvonen PJ, Jalava KM. Itraconazole drastically increases plasma concentrations of lovastatin and lovastatin acid. *Clin Pharmacol Ther* 1996;60(1):54–61.
- [68] Kyrklund C, Backman JT, Kivisto KT, Neuvonen M, Laitila J, Neuvonen PJ. Plasma concentrations of active lovastatin acid are markedly increased by gemfibrozil but not by bezafibrate. *Clin Pharmacol Ther* 2001;69(5):340–5.
- [69] van de Steeg E, Kleemann R, Jansen HT, van Duyvenvoorde W, Offerman EH, Wortelboer HM, et al. Combined analysis of pharmacokinetic and efficacy data of preclinical studies with statins markedly improves translation of drug efficacy to human trials. *J Pharmacol Exp Ther* 2013;347(3):635–44.
- [70] Bjarnadottir O, Kimbung S, Johansson I, Veerla S, Jonsson M, Bendahl PO, et al. Global transcriptional changes following statin treatment in breast Cancer. *Clin Cancer Res* 2015;21(15):3402–11.

REVIEW ARTICLE


**BENTHAM
SCIENCE**

Targeting Breast Cancer Stem Cells: A Methodological Perspective



Marco A. Velasco-Velázquez^{1,2,*}, Inés Velázquez-Quesada^{1,3}, Luz X. Vásquez-Bochm^{1,4} and Sonia M. Pérez-Tapia³

¹Departamento de Farmacología, Facultad de Medicina, Universidad Nacional Autónoma de México (UNAM), Ciudad de México, México; ²Unidad Periférica de Investigación en Biomedicina Traslacional, Facultad de Medicina, UNAM, Ciudad de México, México; ³Unidad de Desarrollo e Investigación en Bioprocesos, ENCB, Instituto Politécnico Nacional, Ciudad de México, México; ⁴Posgrado en Ciencias Químicas, UNAM, Ciudad de México, México

ARTICLE HISTORY

Received: May 12, 2018
Revised: August 01, 2018
Accepted: August 09, 2018

DOI:
10.2174/1574888X13666180821155701



CrossMark

Abstract: Cancer Stem Cells (CSCs) constitute a subpopulation at the top of the tumor cell hierarchy that contributes to tumor heterogeneity and is uniquely capable of seeding new tumors. Because of their biological properties, CSCs have been pointed out as therapeutic targets for the development of new therapies against breast cancer. The identification of drugs that selectively target breast CSCs requires a clear understanding of their biological functions and the experimental methods to evaluate such hallmarks. Herein, we review the methods to study breast CSCs properties and discuss their value in the preclinical evaluation of CSC-targeting drugs.

Keywords: Cancer stem cells, anticancer drugs, self-renewal, CSC selective toxicity, CSC differentiation, breast tumors.

1. INTRODUCTION

Tumors contain cancer cells with heterogeneous features since they have different morphology, proliferating capacity, and invasiveness. The Cancer Stem Cell (CSC) hypothesis proposes that a subpopulation at the top of the tumor cell hierarchy contributes to tumor heterogeneity and is uniquely capable of seeding new tumors [1, 2]. CSCs proliferate asymmetrically to self-renew and generate a pool of transit amplifying cells that “differentiate” into the non-self-renewing tumor bulk [3, 4] (Fig. 1A). CSCs have the ability of generating and maintaining heterogeneous tumors when implanted into immunocompromised or syngeneic mice. This tumorigenic ability is the functional demonstration of stemness in cancer cells (see [5-7] for extensive reviews on the CSC concept).

At present, it is well accepted that breast CSCs play a key role in therapy resistance and recurrence of mammary tumors [8-11]. For example, breast cancer cells resistant to endocrine or cytotoxic therapy show stem cell characteristics and *vice versa* [12, 13]. Furthermore, therapy increases the self-renewing capability of breast cancer cells [12, 13] and the proportion of breast CSCs [14, 15]. After the selective pressure elicited by cytotoxic therapy, resistance can be inherited from BCSCs to progenitor cells and then to the

non-stem tumor cells [15]. It is thought that this is one of the reasons why cytotoxic therapies are ineffective in the long term.

Furthermore, breast CSCs are essential for metastatic dissemination of tumors [16, 17]. Breast tumors with high metastatic potential contain higher proportions of CSC than poorly metastatic tumors [18, 19] and targeting breast CSCs decrease metastasis [20]. In agreement, there is strong evidence that EMT induction, which is required for metastasis, generates cells with stem cell properties [21, 22].

Because of their biological properties and their role in tumor progression, CSCs have been pointed out as therapeutic targets for the development of new therapies against breast cancer (reviewed in ref. [3, 23-25]). The candidate molecular targets to eradicate breast CSCs have been reviewed previously [3, 26] and more are emerging [27]. Some of the therapeutic agents exploiting those targets have even reached clinical evaluation (see ref. [28] for a recent review). Nevertheless, new agents that target breast CSCs are still required.

Proper development of CSC-targeting drugs requires a clear understanding of the biological functions defining those cells and of the experimental methods to evaluate such hallmarks. Herein, we review the methods to study breast CSC properties and discuss their value during the preclinical evaluation of CSC-targeting drugs. This methodological perspective constitutes the novelty of the review. We also present examples of common errors found when working with

*Address correspondence to this author at the Departamento de Farmacología, Facultad de Medicina, Universidad Nacional Autónoma de México, Circuito interno s/n, Cd. Universitaria 04510 Ciudad de México, México; Tel/Fax: +525556232282; E-mail: marcovelasco@unam.mx

the methods and suggest solutions. This information will help the reader to improve both experimental design and data interpretation.

2. EVALUATING CHANGES IN THE CSC SUBPOPULATION

Three different assays are considered standard during preclinical evaluation of breast CSC-targeting candidates: 1) the quantification of the fraction of cancer cells that express marker(s) associated with the CSC phenotype; 2) the evaluation of the ability of cancer cells to form mammospheres *in vitro*; and 3) the analysis of the tumorigenic capability of cancer cells *in vivo* (Table 1). When properly combined, they provide enough experimental support to demonstrate changes in the size of the CSC subpopulation. On the other hand, since they phenotypically or functionally estimate the CSC fraction, they provide little information about the mechanism involved in such changes.

2.1. Evaluation of CSC-Associated Markers

Human breast CSCs were first described as CD44⁺/CD24^{-low}/lineage- (lack of expression of CD2, CD3, CD10, CD16, CD18, CD31, CD64, and CD140b) [29]. As few as 200 CD44⁺/CD24^{-low} cells were able to form tumors when injected into NOD/SCID mice, while tens of thousands of other cells could not. The generated tumors recapitulated the cellular heterogeneity of the initial sample, containing a minority of CD44⁺/CD24^{-low} cells that could be serially passaged to form new tumors.

This immunophenotype has been extensively used to analyze the fraction of CSCs within breast tumor populations. For example, CD44⁺/CD24⁻ cells isolated from the luminal MCF-7 cell line show increased tumor-forming and metastatic efficiency compared with cells with different immunophenotype [30, 31]. However, in other cellular models, the percentage of CD44⁺/CD24⁻ cells is highly variable and does not correlate with colony-forming efficiency [32] or tumorigenic potential [33]. Furthermore, the presence of cells with a CD44⁺/CD24⁻ phenotype is not a prognosis marker in breast cancer patients [34, 35]. Altogether, this evidence suggests that the CD44⁺/CD24^{-low} subpopulation can be employed to estimate the CSC content in specific models where previous validation exists but cannot be considered a universal marker of breast CSCs.

Aldehyde dehydrogenase (ALDH) is another marker commonly employed to estimate the number of breast CSCs. ALDHs comprise a family of cytosolic NADP(+)-dependent enzymes, which catalyze the oxidation aldehydes into their corresponding carboxylic acids [36]. Increased levels of ALDH have been found in CSCs of different tumor types [37-39]. It has been proposed that one of the roles of ALDH in CSCs is protection from elevated levels of reactive oxygen species (ROS) [40] or chemotherapeutic agents [41]. ALDH1A3 seems to be the principal isoform responsible for the high ALDH activity in breast cancer cells [42, 43]. Accordingly, ALDH1A3 expression in human breast tumors correlates with bad prognosis [43].

Identification of breast CSCs based on ALDH activity uses the substrate BAAA (BODIPY-aminoacetaldehyde),

which is converted by ALDH into the fluorescent product BAA⁻ (BODIPY-aminoacetate) [44] and can be detected by flow cytometry. ALDEFLUOR[®] is a commercial system that includes all the reagents required for such detection and therefore ALDH⁺ cells are commonly referred to as ALDEFLUOR⁺.

Breast tumor cells with high ALDH activity are able to generate tumors in NOD/SCID mice with heterogeneous phenotypes that resemble the parental tumor, suggesting that the ALDH⁺ pool contains the CSC population [37, 45]. However, the fraction of ALDH⁺ breast cancer cells is highly variable. For example, the cell lines SKBR-3 (HER2-positive) and MDA-MB-468 (triple negative) have a high percentage of ALDH⁺ cells (80-100% and 40-60%, respectively). In contrast, the percentage of ALDH⁺ cells is as low 0-1% in the ER-positive T47D and MCF-7 cell lines [43, 45, 46]. Thus, ALDH activity, just as the CD44⁺/CD24⁻ immunophenotype, is not a valid CSC-marker for all breast cancer models.

From an operative point of view, staining with monoclonal antibodies or ALDEFLUOR offers strong advantages since both methods easily determine the number of cells bearing markers associated with breast CSCs. However, the evidence suggests that these techniques may misestimate the number of cells able to perform the functions defining CSCs. Switching to other reported breast CSC markers (see ref. [47] for a recent review) will not overcome this disadvantage. Thus, drug selection based solely on the expression of markers has a minor impact on the field. Accordingly, marker-analysis must be complemented with the functional assays described below in order to demonstrate functional changes in the CSC population.

2.2. Mammosphere Assay

Mammosphere culture was first described as a system allowing the propagation of mammary epithelial cells in an undifferentiated state, based on their ability to proliferate in suspension as non-adherent spheres [48, 49]. It has been shown that such ability is also present in breast cancer progenitor and stem cells, and correlates with both tumorigenic ability and metastatic capacity [29, 50, 51]. In these assay, single-cell suspensions are seeded at a very low density in non-adhering plates under specific culture conditions (see ref. [52] for a detailed protocol). After incubation for several days, the sphere-forming efficiency is calculated by dividing the number of spheres that reached a minimum size by the number of cells seeded.

Since the mammosphere assay allows the *in vitro* estimation of the progenitor and stem fraction within a heterogeneous population of cancer cells, this method has been employed for medium-throughput unbiased drug screening. For example, Yang *et al.* [53] evaluated the activity of 165 compounds and identified that 18 of them inhibited the formation of mammospheres by 50% or more in cell lines of triple-negative breast cancer. Authors corroborated the activity of some of the selected compounds by demonstrating that they significantly inhibited the formation of mammospheres by purified CD44⁺/CD24⁻/ESA⁺ cells. This simple strategy allowed the selection of the compound triptolide, which was further identified as an inducer of MYC proteasomal degra-

dation [53]. Similarly, Lamb *et al.* proposed that mitochondrial-targeted antibiotics and antiparasitic drugs can be repurposed to target breast CSCs based on results from mammosphere assays [54]. Thus, the mammosphere assay can be employed as the main method to identify agents reducing the fraction of breast CSC.

2.2. Tumorigenesis Assay

The gold standard for demonstrating changes in the CSC-pool is the *in vivo* analysis of tumor-initiating ability. In tumorigenic assays, serial dilutions of cancer cells ($\leq 10^5$) are injected to groups of mice [55]. Given the low number of injected cells, tumors will rarely arise, allowing calculation of the frequency of the mice receiving none of the tumor-initiating cells. The frequency of tumor-negative mice follows a Poisson distribution that can be analyzed to estimate the frequency of CSCs within a mixed population of cancer cells [56]. This experimental design is known as Limiting Dilution Transplantation (LDT).

In LDT assays, serial dilutions of breast cancer cells are mixed with Matrigel and introduced into the mammary glands of female mice recipients (see reference [57] for a detailed protocol). Multiple animals (usually 4-10) are injected with each cell number and they are monitored to identify the presence of tumors. Tumor detection can be supported by highly sensitive methods such as bioluminescence imaging [58]. Changes in the fraction of tumor-free animals over time can be analyzed by long-rank test [59]. At a fixed time point, ranging from 8-12 weeks, the ratio of tumorigenic outgrowths per group is calculated and comparisons can be done by extreme limiting dilution analysis (ELDA) [56]. Alternative statistical analyses have been reported when the results do not fit the Single Hit Poisson model [60].

LDT has been employed to study the tumorigenic capability of breast cancer cells with a specific immunophenotype [29, 42, 43], and with forced alterations in the expression of pluripotency factors [53], signaling proteins [61] or miRNAs [62]. However, LDT is time-consuming, expensive, and requires personnel with specialized training. Thus, the assay is not employed for routine screening of CSC targeting drugs but has been extensively used to corroborate the effects of drugs on CSCs. For example, Gupta *et al.* studied the tumorigenic capability of HMLER and 4T1 cancer cells after exposure to CSC-selective drugs. The cells were treated *in vitro* for 7 days, allowed to recover, expanded in the absence of treatment, and then injected into mice. Authors demonstrated that salinomycin pretreatment decreased >100-fold the ability of breast cancer cells to induce tumors, relative to the cytotoxic drug paclitaxel [63]. Similarly, the pretreatment of SUM159 cells with triptolide for 16 h, reduced the frequency of tumor-initiating cells from 0.92% to 0.033% [53].

As a note of caution, we must list two missteps found in the literature reporting tumorigenesis assays. The first one is the injection of a large number of cancer cells. Human breast cancer cell lines can be xenotransplanted into immunocompromised mice [64] if the injected cell number is large enough (usually in the 10^6 range). In such conditions, it is expected that 100% of the animals develop tumors. As stated above, only tumor-negative animals provide evidence that there are no CSCs in the injected population. The second error is not in

the experimental design but in data analysis. Multiple reports use data from LDT experiments (designed to evaluate a quantal response) to compare average tumor size. Tumor growth has a predictive value for the clinical efficacy of anti-cancer compounds [65, 66], but its proper evaluation requires randomization of mice after tumor nodules have been established [67, 68]. In short, the *in vivo* method aiming to evaluate changes in the CSC pool should not be confused with the one extensively used in the last three decades for the *in vivo* testing of anti-cancer compounds.

3. MECHANISTIC ANALYSIS IN CSC TARGETING

CSC eradication can be achieved by one of these three strategies: 1) induction of cytotoxicity on CSCs; 2) promotion of CSC differentiation; or 3) impairment of CSCs self-renewal (Fig. 1B). Any of these actions would lead to a reduction in the CSC pool, but they would do it by different mechanisms. Thus, the working hypothesis should direct what specific methods should be employed during the pre-clinical evaluation of activity (Table 1). In the sections below, we exemplify and discuss the methods used for the evaluation of each biological feature.

3.1. Induction of CSC Death

The evaluation of cancer cell viability *in vitro* is a fast and inexpensive approach to identify cytotoxic compounds [69]. However, the selection of agents inducing selective cytotoxicity on CSCs faces an intrinsic problem of CSC biology: CSCs are a minor fraction of the total cancer cells. Thus, evaluation of CSC death-induction requires purification or enrichment of such cells; otherwise, the response would come predominantly from non-CSCs.

Purification of breast CSCs using validated CSC markers provides a partial solution to this problem. For example, Erol and collaborators purified CD44⁺/CD24^{-low} cells from the MCF-7 cell line by Fluorescence-Activated Cells Sorting (FACS) and studied the antitumor activity of flavopiridol. Authors found that flavopiridol reduces cell viability and proliferation in the isolated population [70]. Similarly, Li *et al.* purified CD44⁺/CD24⁻ MCF-7 cells by FACS and analyzed their response to quercetin. The number of viable cells and the ability to form mammospheres decreases after quercetin exposure, suggesting that the CSC population is reduced. Interestingly, quercetin also induces cell death in the non-CSC fraction [71].

When working with purified breast CSC it is important to consider that the isolated CD44⁺/CD24⁻ cells only transiently retain this phenotype and eventually revert to an equilibrium state in which the expanded population displays the cell surface profile of the population of origin [72, 73]. Additionally, the expression of CSC-associated markers changes depending on the culture conditions, such as cell density, the presence or absence of growth factors, or the frequency of passaging [33]. Thus, researchers should be careful when interpreting results from assays employing adherent cultures of FACS-isolated cells, especially when there is a long time between stimuli addition and the endpoint.

Another reported strategy for CSC enrichment is the propagation of cells in tumorsphere cultures. Growing tu-

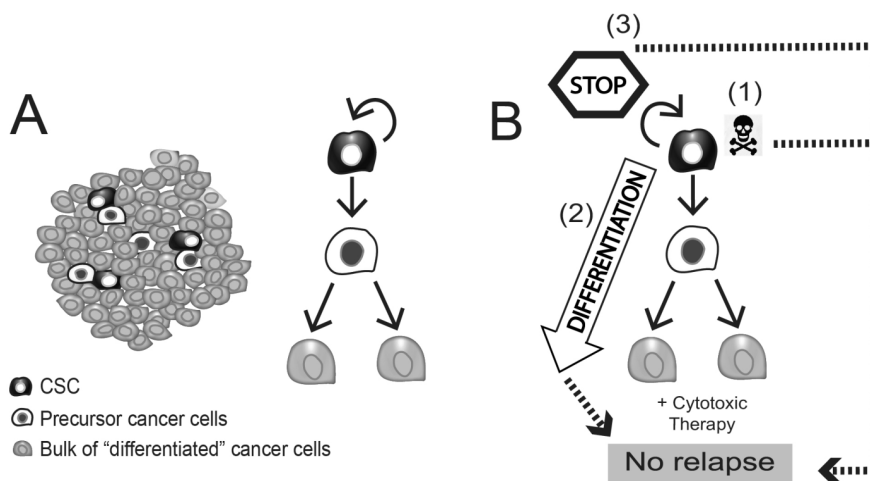


Fig. (1). CSCs in breast tumors. A. Tumors contain heterogeneous cancer cells organized in a hierarchical manner. CSCs self-renew and differentiate to generate bulk cancer cells B. CSC eradication can be achieved by: 1) direct cytotoxicity; 2) promotion of differentiation; or 3) impairment of self-renewal. Any of those strategies, combined with conventional therapy, could prevent relapse in breast cancer patients.

Table 1. Methods employed for screening of CSC-targeting drugs.

-	Reported Experimental Strategy	Observations (⊙) and Cautions (⚡)
Changes in CSC fraction	Analysis of CSC-associated markers by flow cytometry	<ul style="list-style-type: none"> ⊙ Easy and fast to perform ⊙ All reagents commercially available ⚡ Use markers validated for your model ⚡ Must be combined with a functional evaluation
	Mammosphere assay	<ul style="list-style-type: none"> ⊙ Requires specific culture plates and medium ⊙ Needs week-long culture ⚡ Data analysis based in quantification of mammosphere number (not size).
	<i>In vivo</i> tumorigenesis (LDT)	<ul style="list-style-type: none"> ⊙ Gold standard for tumor-initiating capability ⊙ Expensive and time consuming ⊙ Requires multiple animals per cell dose ⚡ Goal is not the evaluation of tumor growth kinetics
Induction of CSC death	Evaluation of cytotoxicity in CSC-enriched cultures	<ul style="list-style-type: none"> ⊙ Requires enrichment of CSC ⊙ FACS allows fast purification of CSC ⊙ Cells can be engineered to maintain a CSC phenotype ⚡ Use validated markers for FACS ⚡ Isolated cells differentiate over time
Impairment of self-renewal	Serial passage in mammosphere assays	<ul style="list-style-type: none"> ⊙ Time consuming
	Serial passage in LDT assays	<ul style="list-style-type: none"> ⊙ Cannot be automatized ⚡ Ideal number of passages is not defined
Induction of CSC differentiation	Quantification of reporter genes responsive to pluripotency pathways	<ul style="list-style-type: none"> ⊙ Needs validation of the reporter system ⊙ Can be combined with analysis of expression of differentiation markers ⚡ Must be combined with evaluation of cell viability

morspheres allows enrichment of glioblastoma [74-76] and ovarian [77, 78] cancer cells with CSC features (*i.e.* express CSC-associated markers and display increased tumorigenicity) without the need to physically separate the CSCs from other cell types. Similarly, breast CSCs can also be expanded in mammosphere culture. MCF-7 cells obtained from mammosphere cultures have larger numbers of CD44⁺/CD24⁻ cells than the parental cell line [79, 80]. Mammosphere-derived MCF-7 cells display increased self-renewal, ALDH expression [81], OCT4 expression, and tumorigenic potential [79]. Using mammosphere culture as CSC enrichment strat-

egy, He and collaborators evaluated the effect of salinomycin on cell viability. To avoid the differentiation of the cells, authors seeded mammosphere-derived cells in non-adherent conditions and evaluated their viability after 48 h of drug exposure. They demonstrated that salinomycin inhibited cell viability in a dose-dependent manner with an IC₅₀ value of 106 nM [79].

However, other groups have reported that in MCF-7 cells isolated from mammosphere cultures the fraction of CD44⁺/CD24⁻ cells is similar than in the parental cell line

[32] or is even undetectable [81], making this method of enrichment controversial. In other breast cancer cell lines, the available information is also inconclusive. For example, in mammospheres derived from MDA-MB-231 cells, some authors report an increase in the CD44⁺/CD24⁻ population [82], whereas others report decreased CD44 expression [32].

Given the methodological and reproducibility problems associated with isolation and enrichment of breast CSC, several groups have developed creative approaches to identify the effect of drugs on this population. A key example is the strategy developed by Gupta and collaborators, who stably knock down the E-cadherin gene in the HMLER tumorigenic mammary cell line to induce EMT and CSC enrichment [63]. The engineered cell line (HMLERshEcad) displays an increased proportion of cells carrying the CD44^{high}/CD24^{low} marker, a ~100-fold increase in mammosphere-forming ability, and can consistently form tumors with only 1,000 cells when xenotransplanted [63]. HMLERshEcad cells have been employed to select drugs that affect breast CSC viability [63, 83]. Using HMLERshEcad and tetrazolium assays to evaluate their viability, salinomycin and abamectin were selected from a high-throughput screening as agents that selectively induce breast CSC death. The same model allowed the demonstration that the copper (II) phenanthroline metalloproteinase is a potent inducer of cytotoxicity in breast CSCs [83].

3.2. Impairing CSC Self-Renewal

Self-renewal is the ability to divide generating at least one cell with similar multipotency and proliferative capacity than the original one [84, 85]. Self-renewal is a fundamental function of stem cells and thus it has been described as the Achilles heel of CSC [24, 86]. Impairing self-renewal would reduce the long-term self-sustainability of tumors, improving therapy responses and reducing recurrence and metastasis.

Experimentally, self-renewal of cancer cells is hard to evaluate. Studying mammosphere formation efficiency, asymmetric division, or proliferation does not provide evidence of changes in self-renewal. Correct assessment of self-renewal in breast CSC can be done by: i) serial passaging of mammosphere-derived cells; or ii) serial passaging cancer cells in LDT assays. These functional strategies determine if a cell population preserves its clonogenic (mammospheres) or tumorigenic (LDT) capacities during several proliferation cycles. There is not a consensus regarding how many passages are required to study self-renewal, but it is clear that one single passage is not enough. On normal tissues, stem cells are still able to form new spheres after 10 passages [87], whereas prostate CSCs can regenerate tumors up to four generations [88]. In multiple breast cancer cell lines, the mammosphere-forming efficiency is constant at least during five passages [89]. Serial mammosphere passing demonstrated that single exposure to the flavonoid genistein impairs self-renewal of CD44⁺/CD24⁻/ESA⁺ cells [90].

Since self-renewal cannot be assessed in a single-step protocol, it is practically impossible to analyze it during medium-throughput drug screening. Alternatively, some groups have used as endpoint the expression or activity of molecules from signaling pathways relevant in self-renewal, such as Hedgehog, Polycomb, Notch and Wnt, in diverse tumor types [91-93]. In breast cancer cells, Xu and collaborators

demonstrated that the anthelmintic drug pyriminopyrrolidone (PP) reduces the expression of several genes of Wnt signaling pathway [94]. Additional assays showed that PP decreases mammosphere formation ability, the expression of SOX2, OCT4 and NANOG, and decreases the CD44^{high}/CD24^{low} and ALDEFLUOR⁺ populations. All these data support the conclusion that PP reduces the CSC population. Nevertheless, self-renewal capacity of cells was never tested, and thus the authors' conclusion that PP impairs self-renewal [94] overestimates the methods employed.

Please note that relevant self-renewal genes are not exclusively expressed on CSC but can be present in non-stem cancer cells and in normal tissues [84, 95, 96]. Additionally, since self-renewal requires cell proliferation, any compound that blocks CSC-proliferation will indirectly impact self-renewal.

3.3. Induction of CSC Differentiation

CSCs generate daughter cancer cells with different phenotype and biological features. Those "differentiated" cancer cells, commonly referred to as tumor bulk cells, possess high proliferative capacity but low/negative tumorigenic capacity. When compared with CSC, bulk cells from breast tumors have dissimilar immunophenotype [29], display different transcriptomic profile [45, 97, 98], and show increased drug sensitivity [40, 99]. Thus, stimulation of the differentiation of breast CSC will convert them into non-tumorigenic cancer cells, which could be eradicated with conventional cytotoxic therapies. A main disadvantage of this strategy is that tumor bulk cells could dedifferentiate back to CSCs given their increased plasticity (see ref. [1] for a review).

Identification of compounds promoting differentiation in CSCs has been limited by our knowledge of the relevant differences to be searched. As aforementioned, the use of markers to define the breast CSC and non-CSC populations has drawbacks, and therefore should be employed carefully. In order to overcome these methodological limitations, Sachlos *et al.* developed a straightforward approach to identify compounds that induce CSC differentiation [100]. As a proof of concept, they worked in the previously characterized neoplastic human pluripotent stem cell (hPSC) line V1H9 [101], which reproduces *in vitro* and *in vivo* cancer stem cell features [102]. In V1H9 cells, differentiation is characterized by a reduction of the expression of the pluripotency factors OCT4 and SOX2. Thus, V1H9 cells were engineered to express GFP under the control of a promoter with OCT4 or SOX2 binding motifs to follow cell differentiation [100]. In the engineered cells, CSC can be identified as GFP⁺, whereas differentiated cells as GFP⁻. Using such a surrogate model, the group validated a screening platform with the simultaneous evaluation of cell number by Hoechst staining.

After evaluation of 590 compounds from the NIH or the Canadian Compound Collection, authors identified compounds that induced the highest loss of GFP with less than 70% Hoechst-reduction, including thioridazine, azathioprine and mefloquine. Furthermore, they compared Acute Myeloid Leukemia cells *vs.* Hematopoietic Stem Cells, finding that thioridazine selectively induces the expression of the differentiation marker CD11b and reduces *in vivo* engraftment in neoplastic cells [100].

Apparently, the effect of thioridazine is due to higher expression levels of dopamine receptors -the canonical targets of thioridazine- in cancer than in normal stem cells. In primary samples of breast cancer tumors, a subfraction of cells within the CD44⁺/CD24^{-low} population express dopamine receptors, suggesting that dopamine-induced signaling may be also be controlling differentiation in breast CSCs [100]. Accordingly, it has been reported that thioridazine could be useful for treating resistant breast tumors [103, 104].

Other reporter constructions containing the promoters of Nanog [105] and Sox2 [106] or response elements to NOTCH [107] or OCT4/SOX2 [108] have been proven to be useful in the identification of breast CSC, and thus they may be employed for the screening of compounds inducing differentiation. In such evaluations, a simultaneous analysis of cell viability must be included in order to distinguish non-cytotoxic agents inducing differentiation *vs.* those causing CSC death.

CONCLUSIONS AND PERSPECTIVES

Development of agents targeting CSC is one of the priorities in cancer research. Because of the urgency of identifying active compounds, it is common to find reports in which the methods employed do not fully match the pursued goals. Consequently, those studies misinterpret the results and/or inappropriately magnified their conclusions. Only proper combination of the strategies developed to evaluate CSC hallmarks can provide evidence strong enough to propose the clinical translation of the results.

Expression analyses are fast and simple to perform, and therefore they are commonly used during drug screening. However, heterogeneity on breast CSCs and ubiquitous expression of some stem cell markers should be considered. *In vitro* functional assays, such as mammosphere formation or cell viability assessment, have been successfully employed in medium-throughput screening, proving that these assays provide relevant information about anti-CSC activity. Still, CSCs are functionally defined by their ability to generate tumors in animal models; hence, we suggest performing *in vivo* LDT as a final test for efficacy of CSC-targeting drug, even when this assay is time and money consuming.

These methods can also be employed for analysis of selectivity on cancer *vs.* normal stem cells and may be useful in the evaluation of the clinical effects of CSC-targeting drugs. For example, Schott *et al.* have quantified the CD44⁺/CD24⁻ and ALDH⁺ populations as well as the mammosphere-forming efficiency during the clinical evaluation of the effects of gamma-secretase inhibitors plus docetaxel in breast cancer patients [109]. Similarly, Smith *et al.* evaluated the clinical efficacy of the antibody demcizumab against CSCs through analysis of the regulation of the Notch and Wnt pathway genes [110].

In the near future, the methods described here will be strengthened by information obtained by integrative genomic, transcriptomic and proteomic analyses at single cell level. For example, single cell transcriptomic analysis has allowed the identification of relevant pathways on normal [111, 112] and cancer stem cells [113]. However, the cost

and the availability of these strategies may limit their use in high throughput analyses for drug development.

CONSENT FOR PUBLICATION

Not applicable.

FUNDING

This work was supported by PAPIIT-UNAM IN228616 and CONACYT 221103 to M.A. Velasco-Velázquez. L.X. Vásquez-Boehm received graduate scholarship from CONACYT (294303). Founding sources had no role in the collection, analysis and interpretation of data, the writing of the report, or the decision to submit the article for publication.

CONFLICT OF INTEREST

The authors declare no conflict of interest, financial or otherwise.

ACKNOWLEDGEMENTS

Authors thank students from the Mexican Society for Stem Cell Research (SOMICET) for bringing to our attention the topic of this review. We also thank Mrs. Josefina Bolado, Head of the Scientific Paper Translation Department, from División de Investigación at Facultad de Medicina, UNAM, for language editing.

REFERENCES

- [1] Velasco-Velazquez MA, Homsí N, De La Fuente M, Pestell RG. Breast cancer stem cells. *Int J Biochem Cell Biol* 2012; 44(4): 573-7.
- [2] Shibue T, Weinberg RA. EMT, CSCs, and drug resistance: The mechanistic link and clinical implications. *Nat Rev Clin Oncol* 2017; 14(10): 611-29.
- [3] McDermott SP, Wicha MS. Targeting breast cancer stem cells. *Mol Oncol* 2010; 4(5): 404-19.
- [4] Pattabiraman DR, Weinberg RA. Tackling the cancer stem cells - what challenges do they pose? *Nat Rev Drug Discov* 2014; 13(7): 497-512.
- [5] Baumann M, Krause M, Hill R. Exploring the role of cancer stem cells in radioresistance. *Nat Rev Cancer* 2008; 8(7): 545-54.
- [6] Loeffler M, Roeder I. Tissue stem cells: definition, plasticity, heterogeneity, self-organization and models--a conceptual approach. *Cells Tissues Organs* 2002; 171(1): 8-26.
- [7] Valent P, Bonnet D, Maria R, *et al.* Cancer stem cell definitions and terminology: The devil is in the details. *Nat Rev Cancer* 2012; 12(11): 767-75.
- [8] Dean M, Fojo T, Bates S. Tumour stem cells and drug resistance. *Nat Rev Cancer* 2005; 5(4): 275-84.
- [9] Lou H, Dean M. Targeted therapy for cancer stem cells: The patched pathway and ABC transporters. *Oncogene* 2007; 26(9): 1357-60.
- [10] Yu Y. The role of cancer stem cells in relapse of solid tumors. *Front Biosci* 2012; E4(1): 1528.
- [11] Flemming A. Cancer stem cells: Targeting the root of cancer relapse. *Nat Rev Drug Discov* 2015; 14(3): 165.
- [12] Creighton CJ, Li X, Landis M, *et al.* Residual breast cancers after conventional therapy display mesenchymal as well as tumorigenic features. *Proc Natl Acad Sci U S A* 2009; 106(33): 13820-5.
- [13] Chu JE, Allan AL. The role of cancer stem cells in the organotropism of breast cancer metastasis: A mechanistic balance between the "seed" and the "soil"? *Int J Breast Cancer* 2012; 2012: 1-12.
- [14] Yu F, Yao H, Zhu P, *et al.* let-7 regulates self renewal and tumorigenicity of breast cancer cells. *Cell* 2007; 131(6): 1109-23.

- [15] Shafee N, Smith CR, Wei S, *et al.* Cancer stem cells contribute to cisplatin resistance in Brca1/p53-mediated mouse mammary tumors. *Cancer Res* 2008; 68(9): 3243-50.
- [16] Velasco-Velazquez MA, Popov VM, Lisanti MP, Pestell RG. The role of breast cancer stem cells in metastasis and therapeutic implications. *Am J Pathol* 2011; 179(1): 2-11.
- [17] Shiozawa Y, Nie B, Pienta KJ, Morgan TM, Taichman RS. Cancer stem cells and their role in metastasis. *Pharmacol Ther* 2013; 138(2): 285-93.
- [18] Brabletz T. To differentiate or not - routes towards metastasis. *Nat Rev Cancer* 2012; 12(6): 425-36.
- [19] Liu H, Patel MR, Prescher JA, *et al.* Cancer stem cells from human breast tumors are involved in spontaneous metastases in orthotopic mouse models. *Proc Natl Acad Sci U S A* 2010; 107(42): 18115-20.
- [20] Klingbeil P, Marhaba R, Jung T, Kirmse R, Ludwig T, Zöller M. CD44 variant isoforms promote metastasis formation by a tumor cell-matrix cross-talk that supports adhesion and apoptosis resistance. *Mol Cancer Res* 2009; 7(2): 168-79.
- [21] Morel A-P, Lièvre M, Thomas C, Hinkal G, Ansieau S, Puisieux A. Generation of breast cancer stem cells through epithelial-mesenchymal transition. *PLoS One* 2008; 3(8): e2888.
- [22] Taube JH, Herschkowitz JI, Komurov K, *et al.* Core epithelial-to-mesenchymal transition interactome gene-expression signature is associated with claudin-low and metaplastic breast cancer subtypes. *Proc Natl Acad Sci U S A* 2010; 107(35): 15449-54.
- [23] Lv J, Shim J. Existing drugs and their application in drug discovery targeting cancer stem cells. *Arch Pharm Res* 2015; 38(9): 1617-26.
- [24] Wicha MS. Targeting self-renewal, an Achilles' heel of cancer stem cells. *Nat Med* 2014; 20(1): 14-5.
- [25] Chen K, Huang Y-h, Chen J-l. Understanding and targeting cancer stem cells: Therapeutic implications and challenges. *Acta Pharmacol Sinica* 2013; 34(6): 732-40.
- [26] Velasco-Velázquez MA, Jiao X, Pestell RG. Breast Cancer Stem Cells. *Cancer Stem Cells Theories and Practice*: InTech; 2011.
- [27] Zucchi I, Sanzone S, Astigiano S, Pelucchi P, Scotti M, Valsecchi V, *et al.* The properties of a mammary gland cancer stem cell. *Proc Natl Acad Sci U S A* 2007; 104(25): 10476-81.
- [28] Lin CY, Barry-Holson KQ, Allison KH. Breast cancer stem cells: are we ready to go from bench to bedside? *Histopathology* 2016; 68(1): 119-37.
- [29] Al-Hajj M, Wicha MS, Benito-Hernandez A, Morrison SJ, Clarke MF. Prospective identification of tumorigenic breast cancer cells. *Proc Natl Acad Sci U S A* 2003; 100(7): 3983-8.
- [30] Wang L, Duan W, Kang L, *et al.* Smoothed actin activates breast cancer stem-like cell and promotes tumorigenesis and metastasis of breast cancer. *Biomed Pharmacother* 2014; 68(8): 1099-104.
- [31] Yan W, Chen Y, Yao Y, Zhang H, Wang T. Increased invasion and tumorigenicity capacity of CD44+/CD24- breast cancer MCF7 cells *in vitro* and in nude mice. *Cancer Cell Int* 2013; 13(1): 62.
- [32] Liu S, Cong Y, Wang D, *et al.* Breast cancer stem cells transition between epithelial and mesenchymal states reflective of their normal counterparts. *Stem Cell Reports* 2014; 2(1): 78-91.
- [33] Fillmore CM, Kuperwasser C. Human breast cancer cell lines contain stem-like cells that self-renew, give rise to phenotypically diverse progeny and survive chemotherapy. *Breast Cancer Res* 2008; 10(2): R25.
- [34] Ryspayeva DE, Smolanka, II, Dudnichenko AS, *et al.* Are CD44(+)/CD24(-) cells the assumed cancer stem cells in breast cancer? *Exp Oncol* 2017; 39(3): 224-8.
- [35] Ahmed MA, Aleskandarany MA, Rakha EA, *et al.* A CD44(-)/CD24(+) phenotype is a poor prognostic marker in early invasive breast cancer. *Breast Cancer Res Treat* 2012; 133(3): 979-95.
- [36] Marchitti SA, Bocker C, Stagos D, Vasiliou V. Non-P450 aldehyde oxidizing enzymes: the aldehyde dehydrogenase superfamily. *Expert Opin Drug Metab Toxicol* 2008; 4(6): 697-720.
- [37] Ginestier C, Hur MH, Charafe-Jauffret E, Monville F, Dutcher J, Brown M, *et al.* ALDH1 is a marker of normal and malignant human mammary stem cells and a predictor of poor clinical outcome. *Cell Stem Cell* 2007; 1(5): 555-67.
- [38] Moreb JS. Aldehyde dehydrogenase as a marker for stem cells. *Curr Stem Cell Res Ther* 2008; 3(4): 237-46.
- [39] Boonyaratanakornkit JB, Yue L, Strachan LR, *et al.* Selection of tumorigenic melanoma cells using ALDH. *J Invest Dermatol* 2010; 130(12): 2799-808.
- [40] Raha D, Wilson TR, Peng J, *et al.* The cancer stem cell marker aldehyde dehydrogenase is required to maintain a drug-tolerant tumor cell subpopulation. *Cancer Res* 2014; 74(13): 3579-90.
- [41] Sladek NE, Kollander R, Sreerama L, Kiang DT. Cellular levels of aldehyde dehydrogenases (ALDH1A1 and ALDH3A1) as predictors of therapeutic responses to cyclophosphamide-based chemotherapy of breast cancer: a retrospective study. Rational individualization of oxazaphosphorine-based cancer chemotherapeutic regimens. *Cancer Chemother Pharmacol* 2002; 49(4): 309-21.
- [42] Croker AK, Rodriguez-Torres M, Xia Y, *et al.* Differential functional roles of ALDH1A1 and ALDH1A3 in mediating metastatic behavior and therapy resistance of human breast cancer cells. *Int J Mol Sci* 2017; 18(10): pii: E2039.
- [43] Marcatò P, Dean CA, Pan D, *et al.* Aldehyde dehydrogenase activity of breast cancer stem cells is primarily due to isoform ALDH1A3 and its expression is predictive of metastasis. *Stem Cells* 2011; 29(1): 32-45.
- [44] Christ O, Lucke K, Imren S, *et al.* Improved purification of hematopoietic stem cells based on their elevated aldehyde dehydrogenase activity. *Haematologica* 2007; 92(9): 1165-72.
- [45] Charafe-Jauffret E, Ginestier C, Iovino F, *et al.* Breast cancer cell lines contain functional cancer stem cells with metastatic capacity and a distinct molecular signature. *Cancer Res* 2009; 69(4): 1302-13.
- [46] Croker AK, Goodale D, Chu J, *et al.* High aldehyde dehydrogenase and expression of cancer stem cell markers selects for breast cancer cells with enhanced malignant and metastatic ability. *J Cell Mol Med* 2009; 13(8B): 2236-52.
- [47] Schwarz-Cruz YCA, Espinosa M, Maldonado V, Melendez-Zajgla J. Advances in the knowledge of breast cancer stem cells. A review. *Histol Histopathol*. 2016; 31(6): 601-12.
- [48] Dontu G, Abdallah WM, Foley JM, *et al.* *In vitro* propagation and transcriptional profiling of human mammary stem/progenitor cells. *Genes Dev*. 2003; 17(10): 1253-70.
- [49] Dontu G, Jackson KW, McNicholas E, Kawamura MJ, Abdallah WM, Wicha MS. Role of Notch signaling in cell-fate determination of human mammary stem/progenitor cells. *Breast Cancer Res* 2004; 6(6): R605-15.
- [50] Ponti D, Costa A, Zaffaroni N, *et al.* Isolation and *in vitro* propagation of tumorigenic breast cancer cells with stem/progenitor cell properties. *Cancer Res* 2005; 65(13): 5506-11.
- [51] Dontu G, Wicha MS. Survival of mammary stem cells in suspension culture: implications for stem cell biology and neoplasia. *J Mammary Gland Biol Neoplasia* 2005; 10(1): 75-86.
- [52] Lombardo Y, de Giorgio A, Coombes CR, Stebbing J, Castellano L. Mammosphere formation assay from human breast cancer tissues and cell lines. *J Vis Exp*. 2015; (97): e52671.
- [53] Yang A, Qin S, Schulte BA, Ethier SP, Tew KD, Wang GY. MYC inhibition depletes cancer stem-like cells in triple-negative breast cancer. *Cancer Res* 2017; 77(23): 6641-50.
- [54] Lamb R, Ozsvari B, Lisanti CL, *et al.* Antibiotics that target mitochondria effectively eradicate cancer stem cells, across multiple tumor types: treating cancer like an infectious disease. *Oncotarget* 2015; 6(7): 4569-84.
- [55] Deshpande AJ, Ahmed F, Buske C. Identification of murine and human acute myeloid leukemia stem cells. *Methods Mol Biol* 2009; 568: 21-35.
- [56] Hu Y, Smyth GK. ELDA: Extreme limiting dilution analysis for comparing depleted and enriched populations in stem cell and other assays. *J Immunol Methods* 2009; 347(1-2): 70-8.
- [57] Jiao X, Rizvanov AA, Cristofanilli M, Miftakhova RR, Pestell RG. Breast Cancer Stem Cell Isolation. *Methods Mol Biol* 2016; 1406: 121-35.
- [58] Jiao X, Velasco-Velazquez MA, Wang M, *et al.* CCR5 governs DNA damage and breast cancer stem cell expansion. *Cancer Res* 2018; 78(7): 1657-71.
- [59] Shi P, Liu W, Tala, Wang H, Li F, Zhang H, *et al.* Metformin suppresses triple-negative breast cancer stem cells by targeting KLF5 for degradation. *Cell Discov* 2017; 3: 17010.
- [60] Wei W, Tweardy DJ, Zhang M, *et al.* STAT3 signaling is activated preferentially in tumor-initiating cells in claudin-low models of human breast cancer. *Stem Cells* 2014; 32(10): 2571-82.
- [61] Vazquez-Santillan K, Melendez-Zajgla J, Jimenez-Hernandez LE, *et al.* NF-kappaB-inducing kinase regulates stem cell phenotype in breast cancer. *Sci Rep* 2016; 6: 37340.

- [62] El Helou R, Pinna G, Cabaud O, *et al.* miR-600 Acts as a Bimodal Switch that Regulates Breast Cancer Stem Cell Fate through WNT Signaling. *Cell Rep* 2017; 18(9): 2256-68.
- [63] Gupta PB, Onder TT, Jiang G, *et al.* Identification of selective inhibitors of cancer stem cells by high-throughput screening. *Cell* 2009; 138(4): 645-59.
- [64] Holliday DL, Speirs V. Choosing the right cell line for breast cancer research. *Breast Cancer Res* 2011; 13(4): 215.
- [65] Johnson JI, Decker S, Zaharevitz D, *et al.* Relationships between drug activity in NCI preclinical *in vitro* and *in vivo* models and early clinical trials. *Br J Cancer* 2001; 84(10): 1424-31.
- [66] Voskoglou-Nomikos T, Pater JL, Seymour L. Clinical predictive value of the *in vitro* cell line, human xenograft, and mouse allograft preclinical cancer models. *Clin Cancer Res* 2003; 9(11): 4227-39.
- [67] Teicher BA. Tumor models for efficacy determination. *Mol Cancer Ther* 2006; 5(10): 2435-43.
- [68] Hollingshead MG. Antitumor efficacy testing in rodents. *J Natl Cancer Inst* 2008; 100(21): 1500-10.
- [69] Yakisich JS. System models, assays and endpoint parameters to evaluate anticancer compounds during preclinical screening. *Curr Med Chem* 2014; 21(35): 3985-98.
- [70] Erol A, Acikgoz E, Guven U, *et al.* Ribosome biogenesis mediates antitumor activity of flavopiridol in CD44(+)/CD24(-) breast cancer stem cells. *Oncol Lett* 2017; 14(6): 6433-40.
- [71] Li X, Zhou N, Wang J, *et al.* Quercetin suppresses breast cancer stem cells (CD44(+)/CD24(-)) by inhibiting the PI3K/Akt/mTOR-signaling pathway. *Life Sci* 2018; 196: 56-62.
- [72] Meyer MJ, Fleming JM, Ali MA, Pesesky MW, Ginsburg E, Vonderhaar BK. Dynamic regulation of CD24 and the invasive, CD44posCD24neg phenotype in breast cancer cell lines. *Breast Cancer Res* 2009; 11(6): R82.
- [73] Sajithlal GB, Rothermund K, Zhang F, *et al.* Permanently blocked stem cells derived from breast cancer cell lines. *Stem Cells* 2010; 28(6): 1008-18.
- [74] Yu SC, Ping YF, Yi L, *et al.* Isolation and characterization of cancer stem cells from a human glioblastoma cell line U87. *Cancer Lett* 2008; 265(1): 124-34.
- [75] Lathia JD, Mack SC, Mulkearns-Hubert EE, Valentim CL, Rich JN. Cancer stem cells in glioblastoma. *Genes Dev.* 2015; 29(12): 1203-17.
- [76] Qiang L, Yang Y, Ma YJ, *et al.* Isolation and characterization of cancer stem like cells in human glioblastoma cell lines. *Cancer Lett* 2009; 279(1): 13-21.
- [77] House CD, Hernandez L, Annunziata CM. *In vitro* enrichment of ovarian cancer tumor-initiating cells. *J Vis Exp* 2015; (96): e52446.
- [78] Martinez-Serrano MJ, Caballero-Banos M, Vilella R, Vidal L, Pahisa J, Martinez-Roman S. Is sphere assay useful for the identification of cancer initiating cells of the ovary? *Int J Gynecol Cancer* 2015; 25(1): 12-7.
- [79] He M, Fu Y, Yan Y, *et al.* The Hedgehog signalling pathway mediates drug response of MCF-7 mammosphere cells in breast cancer patients. *Clin Sci* 2015; 129(9): 809-22.
- [80] Xie G, Zhan J, Tian Y, *et al.* Mammosphere cells from high-passage MCF7 cell line show variable loss of tumorigenicity and radioresistance. *Cancer Lett* 2012; 316(1): 53-61.
- [81] Laranjo M, Carvalho MJ, Costa T, *et al.* Mammospheres of hormonal receptor positive breast cancer diverge to triple-negative phenotype. *Breast* 2017; 38: 22-9.
- [82] Liu Y, Nenutil R, Appleyard MV, *et al.* Lack of correlation of stem cell markers in breast cancer stem cells. *Br J Cancer* 2014; 110(8): 2063-71.
- [83] Jafari SM, Joshaghani HR, Panjehpour M, Aghaei M, Zargar Balajam N. Apoptosis and cell cycle regulatory effects of adenosine by modulation of GLI-1 and ERK1/2 pathways in CD44(+) and CD24(-) breast cancer stem cells. *Cell Prolif* 2017; 50(4): e12345, doi: 10.1111/cpr.12345.
- [84] Flamme M, Cressey PB, Lu C, *et al.* Induction of Necroptosis in Cancer Stem Cells using a Nickel(II)-Dithiocarbamate Phenanthroline Complex. *Eur J Chem.* 2017; 23(40): 9674-82.
- [85] Fuchs E, Chen T. A matter of life and death: Self-renewal in stem cells. *EMBO Rep* 2013; 14(1): 39-48.
- [86] Al-Hajj M, Clarke MF. Self-renewal and solid tumor stem cells. *Oncogene* 2004; 23(43): 7274-82.
- [87] Borah A, Raveendran S, Rochani A, Maekawa T, Kumar DS. Targeting self-renewal pathways in cancer stem cells: clinical implications for cancer therapy. *Oncogenesis* 2015; 4(11): e177.
- [88] Reynolds BA, Weiss S. Clonal and population analyses demonstrate that an EGF-responsive mammalian embryonic CNS precursor is a stem cell. *Dev Biol* 1996; 175(1): 1-13.
- [89] Qin J, Liu X, Laffin B, Chen X, *et al.* The PSA(-/lo) prostate cancer cell population harbors self-renewing long-term tumor-propagating cells that resist castration. *Cell Stem Cell* 2012; 10(5): 556-69.
- [90] Smart CE, Morrison BJ, Saunus JM, *et al.* *In vitro* analysis of breast cancer cell line tumourspheres and primary human breast epithelia mammospheres demonstrates inter- and intrasphere heterogeneity. *PLoS One* 2013; 8(6): e64388.
- [91] Montales MT, Rahal OM, Kang J, *et al.* Repression of mammosphere formation of human breast cancer cells by soy isoflavone genistein and blueberry polyphenolic acids suggests diet-mediated targeting of cancer stem-like/progenitor cells. *Carcinogenesis* 2012; 33(3): 652-60.
- [92] Clement V, Sanchez P, de Tribolet N, Radovanovic I, Ruiz i Altaba A. HEDGEHOG-GLI1 Signaling Regulates Human Glioma Growth, Cancer Stem Cell Self-Renewal, and Tumorigenicity. *Curr Biol* 2007; 17(2): 165-72.
- [93] Kreso A, van Galen P, Pedley NM, *et al.* Self-renewal as a therapeutic target in human colorectal cancer. *Nat Med* 2014; 20(1): 29-36.
- [94] Zhu L, Ni C, Dong B, *et al.* A novel hedgehog inhibitor iG2 suppresses tumorigenesis by impairing self-renewal in human bladder cancer. *Cancer Med* 2016; 5(9): 2579-86.
- [95] Xu L, Zhang L, Hu C, *et al.* WNT pathway inhibitor pyrvinium pamoate inhibits the self-renewal and metastasis of breast cancer stem cells. *Int J Oncol* 2016; 48(3): 1175-86.
- [96] Gattinoni L. Memory T Cells Officially Join the Stem Cell Club. *Immunity* 2014; 41(1): 7-9.
- [97] Graef P, Buchholz VR, Stemberger C, *et al.* Serial Transfer of Single-Cell-Derived Immunocompetence Reveals Stemness of CD8+ Central Memory T Cells. *Immunity* 2014; 41(1): 116-26.
- [98] Hardt O, Wild S, Oerlecke I, Hofmann K, Luo S, Wiencek Y, *et al.* Highly sensitive profiling of CD44+/CD24- breast cancer stem cells by combining global mRNA amplification and next generation sequencing: evidence for a hyperactive PI3K pathway. *Cancer Lett* 2012; 325(2): 165-74.
- [99] Gomez-Miragaya J, Palafox M, Pare L, *et al.* Resistance to Taxanes in Triple-Negative Breast Cancer Associates with the Dynamics of a CD49f+ Tumor-Initiating Population. *Stem Cell Reports* 2017; 8(5): 1392-407.
- [100] Sachlos E, Risueño RM, Laronde S, Shapovalova Z, Lee J-HH, Russell J, *et al.* Identification of drugs including a dopamine receptor antagonist that selectively target cancer stem cells. *Cell* 2012; 149(6): 1284-97.
- [101] Chadwick K, Wang L, Li L, Menendez P, Murdoch B, Rouleau A, *et al.* Cytokines and BMP-4 promote hematopoietic differentiation of human embryonic stem cells. *Blood* 2003; 102(3): 906-15.
- [102] Werbowetski-Ogilvie TE, Bossé M, Stewart M, Schnerch A, Ramos-Mejia V, Rouleau A, *et al.* Characterization of human embryonic stem cells with features of neoplastic progression. *Nat Biotechnol* 2009; 27(1): 91-7.
- [103] Ke X-YY, Lin Ng VW, Gao S-JJ, Tong YW, Hedrick JL, Yang YY. Co-delivery of thioridazine and doxorubicin using polymeric micelles for targeting both cancer cells and cancer stem cells. *Biomaterials* 2014; 35(3): 1096-108.
- [104] Liu H, Lv L, Yang K, Yang K. Chemotherapy targeting cancer stem cells. *Am J Cancer Res* 2015; 5(3): 880-93.
- [105] Thiagarajan PS, Hitomi M, Hale JS, *et al.* Development of a Fluorescent Reporter System to Delineate Cancer Stem Cells in Triple-Negative Breast Cancer. *Stem Cells* 2015; 33(7): 2114-25.
- [106] Liang S, Furuhashi M, Nakane R, *et al.* Isolation and characterization of human breast cancer cells with SOX2 promoter activity. *Biochem Biophys Res Commun* 2013; 437(2): 205-11.
- [107] D'Angelo RC, Ouzounova M, Davis A, *et al.* Notch reporter activity in breast cancer cell lines identifies a subset of cells with stem cell activity. *Mol Cancer Ther* 2015; 14(3): 779-87.
- [108] Tang B, Raviv A, Esposito D, *et al.* A flexible reporter system for direct observation and isolation of cancer stem cells. *Stem Cell Reports* 2015; 4(1): 155-69.
- [109] Schott AF, Landis MD, Dontu G, *et al.* Preclinical and clinical studies of gamma secretase inhibitors with docetaxel on human breast tumors. *Clin Cancer Res* 2013; 19(6): 1512-24.

- [110] Smith DC, Eisenberg PD, Manikhas G, *et al.* A phase I dose escalation and expansion study of the anticancer stem cell agent demcizumab (anti-DLL4) in patients with previously treated solid tumors. *Clin Cancer Res* 2014; 20(24): 6295-303.
- [111] Wilson NK, Kent DG, Buettner F, *et al.* Combined Single-Cell Functional and Gene Expression Analysis Resolves Heterogeneity within Stem Cell Populations. *Cell Stem Cell* 2015; 16(6): 712-24.
- [112] Treutlein B, Brownfield DG, Wu AR, *et al.* Reconstructing lineage hierarchies of the distal lung epithelium using single-cell RNA-seq. *Nature* 2014; 509(7500): 371-5.
- [113] Patel AP, Tirosh I, Trombetta JJ, *et al.* Single-cell RNA-seq highlights intratumoral heterogeneity in primary glioblastoma. *Science* 2014; 344(6190): 1396-401.

Video Article

In Vitro Methods for Comparing Target Binding and CDC Induction Between Therapeutic Antibodies: Applications in Biosimilarity Analysis

Nohemi Salinas-Jazmín^{1,2}, Edith González-González¹, Luz X. Vásquez-Bochm³, Sonia M. Pérez-Tapia^{4,5}, Marco A. Velasco-Velázquez⁶¹Unit for Development and Research in Bioprocesses Unit (UDIBI), National School of Biological Sciences, National Polytechnic Institute (IPN), University of Mexico (UNAM)²School of Chemistry, National Autonomous University of Mexico (UNAM)³Graduate Program in Chemical Sciences, National Autonomous University of Mexico (UNAM)⁴Unit for Development Research and Medical Innovation in Biotechnology (UDIMEB), National School of Biological Sciences, National Polytechnic Institute (IPN)⁵Department of Immunology, National School of Biological Sciences, National Polytechnic Institute (IPN)⁶Department of Pharmacology and Unit of Translational Biomedicine (CMN 20 de noviembre), School of Medicine, National Autonomous University of Mexico (UNAM)Correspondence to: Marco A. Velasco-Velázquez at marcovelasco@unam.mxURL: <https://www.jove.com/video/55542>DOI: [doi:10.3791/55542](https://doi.org/10.3791/55542)

Keywords: Immunology, Issue 123, Rituximab, biosimilar, anti-CD20, therapeutic mAb, CDC, flow cytometry, Daudi cells

Date Published: 5/4/2017

Citation: Salinas-Jazmín, N., González-González, E., Vásquez-Bochm, L.X., Pérez-Tapia, S.M., Velasco-Velázquez, M.A. *In Vitro* Methods for Comparing Target Binding and CDC Induction Between Therapeutic Antibodies: Applications in Biosimilarity Analysis. *J. Vis. Exp.* (123), e55542, doi:10.3791/55542 (2017).

Abstract

Therapeutic monoclonal antibodies (mAbs) are relevant to the treatment of different pathologies, including cancers. The development of biosimilar mAbs by pharmaceutical companies is a market opportunity, but it is also a strategy to increase drug accessibility and reduce therapy-associated costs. The protocols detailed here describe the evaluation of target binding and CDC induction by rituximab in Daudi cells. These two functions require different structural regions of the antibody and are relevant to the clinical effect induced by rituximab. The protocols allow the side-to-side comparison of a reference rituximab and a marketed rituximab biosimilar. The evaluated products showed differences both in target binding and CDC induction, suggesting that there are underlying physicochemical differences and highlighting the need to analyze the impact of those differences in the clinical setting. The methods reported here constitute simple and inexpensive *in vitro* models for the evaluation of the activity of rituximab biosimilars. Thus, they can be useful during biosimilar development, as well as for quality control in biosimilar production. Furthermore, the presented methods can be extrapolated to other therapeutic mAbs.

Video Link

The video component of this article can be found at <https://www.jove.com/video/55542/>

Introduction

Therapeutic antibodies are recombinant monoclonal antibodies (mAbs) developed for the treatment of different pathologies, including cancers, autoimmune and chronic diseases, neurologic disorders, and others¹. Currently, the FDA has granted approval to more than 40 therapeutic mAbs, and more are expected to reach the market in the following years.

Rituximab is a high-affinity chimeric monoclonal IgG1 antibody approved for the treatment of CD20⁺ B-cell non-Hodgkin's lymphoma (NHL), CD20⁺ follicular NHL, chronic lymphocytic leukemia, and rheumatoid arthritis^{2,3}. The recognition of CD20, which is overexpressed in B cells, by rituximab induces apoptosis; complement activation; and antibody-dependent cell mediated cytotoxicity (ADCC)³. The patents of this drug expired in Europe and in the U.S. in 2013 and 2016, respectively. Thus, pharmaceutical companies worldwide are developing rituximab biosimilars. As in any other drug for human consumption, biosimilars require approval from regulatory agencies. International guidelines indicate that for mAbs, biosimilarity should be demonstrated by comparing the physicochemical characteristics, pharmacokinetics, efficacy, and safety of the new and reference products⁴.

Accordingly, the methodologies used in such comparisons must assess the structural and functional characteristics of the mAbs, especially those with clinical relevance. To that end, *in vitro* assays show several advantages over *in vivo* experiments (reviewed in Chapman *et al.*)⁵: i) *in vitro* studies are more sensitive to differences between the proposed biosimilar and the reference product; ii) *in vivo* studies must be performed in relevant species, which for many mAbs are non-human primates; and iii) since the mechanism of action, the preclinical toxicology, and the clinical effects of the reference product are well known, *in vivo* studies with biosimilars may not provide additional useful information. Accordingly, the European Union's Guidance for biosimilars allows candidates to enter clinical trials based on robust *in vitro* data alone⁶.

Here, we present two fast, economic, and simple assays that evaluate the biological activity of rituximab using CD20⁺ cultured cells. These assays can be included as part of the comparability exercise for rituximab biosimilar candidates.

Protocol

1. Evaluation of Target Binding by Flow Cytometry

1. Preparation of biological materials and reagents

1. Make 500 mL of RPMI culture medium supplemented with 10% heat-inactivated fetal bovine serum (H-IFBS).
2. Culture Daudi Burkitt's Lymphoma (Daudi) cells and Daudi GFP⁺ cells using RPMI and 75-cm² culture flasks. Maintain the cultures at 37 °C in a 5% CO₂ humidified atmosphere until they reach 6 - 9 x 10⁵ cells/mL.
3. Make 50 mL of staining buffer by diluting 1/100 H-IFBS in PBS; this buffer is stable at 2 - 8 °C for at least one month.
4. Prepare the test solutions for the reference and biosimilar mAbs. Make ten 1:2 serial dilutions (500 µL each) in staining buffer, starting from 5 µg/mL.
5. Use staining buffer to dilute human IgG (isotype control) to 5 µg/mL and PE-Cy5 mouse anti-human IgG (secondary antibody) to the concentration suggested by the manufacturer.
6. Prepare 4% paraformaldehyde in PBS (fixation buffer).

2. Target binding

1. Collect the Daudi and Daudi GFP⁺ cell suspensions from the 75-cm² culture flasks and transfer them to a 15-mL centrifuge tube. Centrifuge at 400 x g for 5 min.
2. Wash the cells by adding 5 mL of PBS and centrifuging the cell suspension at 400 x g for 5 min.
3. Resuspend the cells in PBS and perform a cell count and viability analysis with trypan blue. Use cultures with cell viability levels ≥ 95% for the analysis.
4. Dilute the cell suspension to 4 x 10⁶ cells/mL with cold staining buffer.
5. In 1.5-mL microcentrifuge tubes, add 50 µL of the cell suspension to 100 µL of the different test concentrations of the reference or biosimilar mAbs. Include replicates for each experimental condition.
6. Prepare additional tubes for the isotype control (human IgG1 instead of rituximab) and negative control (secondary antibody without primary antibody).
7. Incubate at 4 °C for 20 - 30 min.
8. Wash the cells by adding 1 mL of PBS and centrifuging the cell suspension at 400 x g for 5 min at 10 °C. Discard the supernatant.
9. Suspend the cells in 100 µL of the secondary antibody and incubate for 20 - 30 min at 4 °C, protected from light.
10. Wash the cells twice with PBS and suspend them in 200 µL of fixation buffer.
11. Analyze the cells on a flow cytometer.

NOTE: The signal remains stable for several days if the samples are stored at 4 °C and protected from light.

3. Data acquisition

1. Open two dot-plots on a worksheet of the flow cytometer operating software. Set the FSC-A versus FSC-H in the first and the FSC-A versus SSA-A in the second. Open a histogram for the PE-Cy5 channel.
2. In the FSC-A versus FSC-H plot, make a gate (R1) selecting singlet events (**Figure 1A**).
3. Set the R1 population in the FSC-A versus SSA-A dot-plot and then make a new gate (R2) selecting target cells (**Figure 1B**). Set the R2 population in the PE-Cy5 intensity histogram to view the frequency distribution of the cells.
4. Adjust the lower fluorescence intensity (FI) limit for the PE-Cy5 channel using the negative and isotype control (**Figure 1C**).
5. Acquire 10,000 events within R2 from the sample with the higher concentration of the reference product. FI of this sample should be the highest expected (**Figure 1C**).
6. Acquire the rest of the samples.
7. For each sample, get the median fluorescence intensity (MFI) in the PE-Cy5 channel.
8. For samples with the reference or biosimilar mAb, calculate the difference between sample MFI and that of the isotype control (ΔMFI).

2. Assessment of CDC

1. Preparation of biological materials and reagents

1. Prepare cell culture medium and culture Daudi and Daudi GFP⁺ cells as described above (steps 1.1.1 - 1.1.2).
NOTE: Additionally, the CDC assay requires serum-free RPMI.
2. Dilute normal human serum complement (NHSC) 1:2 with serum-free RPMI. Prepare 2.5 mL.
3. Prepare 1 mL of heat-inactivated (30 min/56 °C) NHSC diluted 1:2 with RPMI.
4. Prepare sets of test solutions for the reference and biosimilar mAbs in serum-free RPMI. Make ten dilutions (200 µL each) from 1 to 0.025 µg/mL.

2. CDC assay

1. Collect the Daudi and Daudi GFP⁺ cells from the cultures and quantify the cell viability (see steps 1.2.1 - 1.2.3).
2. Prepare a cell suspension with 4 x 10⁵ cells/mL in serum-free RPMI.
3. Add 50 µL of cell suspension to 50 µL of each reference or biosimilar mAb test concentration in 96-well conical (V)-bottom microplates. Include replicates for each experimental condition.
4. Prepare additional wells for the negative control (*i.e.*, without mAb), basal death control (*i.e.*, heat-inactivated NHSC in the presence of mAb), and staining positive control (*i.e.*, cells exposed to 50 µL of 70% EtOH).
5. Incubate the cells for 20 - 30 min at 37 °C in a 5% CO₂ humidified atmosphere.
6. Add 50 µL of NHSC (diluted 1:2) to each well and incubate the opsonized cells for 2.5 h at 37 °C in a 5% CO₂ humidified atmosphere. Use heat-inactivated NHSC in the basal death control wells.

7. Centrifuge at 400 x g for 5 min at 10 °C. Discard the supernatant.
8. Wash the cells by adding 150 µL of PBS and centrifuging the cell suspension for 5 min at 400 x g and 10 °C. Discard the supernatant.
9. Stain the samples with 7-aminoactinomycin (7-AAD), as previously described^{7,8}.
10. Analyze the cells on a flow cytometer on the same day.

3. Data acquisition

1. Open two dot-plots on a worksheet of the flow cytometer operating software. Set those plots as in steps 1.3.1 - 1.3.3 (**Figure 2A-B**). Create a third plot that is a dot-plot for GFP versus 7-AAD on the R2 population.
2. Define the adequate FI limits using the Daudi cells, Daudi GFP⁺ cells, and death positive control (**Figure 2C**).
3. For each sample, measure the percentage of 7-AAD⁺ target cells. Acquire at least 5,000 events from R2.
4. Calculate the specific mAb-induced cytotoxicity by subtracting the percentage of 7-AAD⁺ in the basal death control from the percentage found in samples with different concentrations of mAbs (**Figure 2D**).

3. Biosimilarity Analysis

1. Enter the concentration and response values into a graphing software.
2. Generate graphs and calculate non-linear regressions with the following considerations: i) use the log-transformation of the mAb concentration as "X"; ii) use the variable slope mathematical model ($Y = \text{minimum response} + (\text{maximal response} - \text{minimum response}) / (1 + 10^{-(\text{LogEC}_{50} - X) * \text{Hill slope}})$); and iii) constrain the bottom values to zero, since the basal response has been subtracted.
NOTE: Curves with a symmetrical sigmoidal shape are expected.
3. Compare both non-linear fits with a global fit using an F-test (many graphing software programs include this feature).
NOTE: Such tests establish as the null hypothesis that the maximal response, logEC₅₀, and the Hill slope are the same for the two datasets, which matches the biological question intended to be addressed.

Representative Results

Using the protocols described above, target binding and the CDC induction of reference rituximab were compared in parallel with those of a biosimilar rituximab produced and commercially available in Asia.

In Daudi cells, both mAbs bound CD20 in a concentration-dependent manner (**Figure 1D**). Non-linear regressions of binding data displayed an r^2 of 0.978 and 0.848 for reference and biosimilar rituximab, respectively (**Figure 1E**). Statistical analysis of the concentration-response curves showed that they, and therefore the pharmacodynamic parameters calculated from them, are significantly different between mAbs ($P < 0.0001$). The maximal response for the biosimilar was 2.16-fold lower than that of the reference product. These results suggest that the two evaluated mAbs have different capacities to bind CD20 expressed on the membrane of leukemic cells.

CDC induction was also compared to the two mAbs. Reference and biosimilar products stimulated CDC in Daudi cells in a concentration-dependent manner (**Figure 2E**). Importantly, the concentrations at which the mAbs induced CDC were different than those required for target binding. Non-linear regressions of the CDC data showed $r^2 > 0.980$ for both products. The statistical comparison of the concentration-response curves indicated that they are significantly different ($P < 0.01$), making the biosimilar less potent. These data indicate that the capacity to induce CDC is different for the analyzed mAbs.

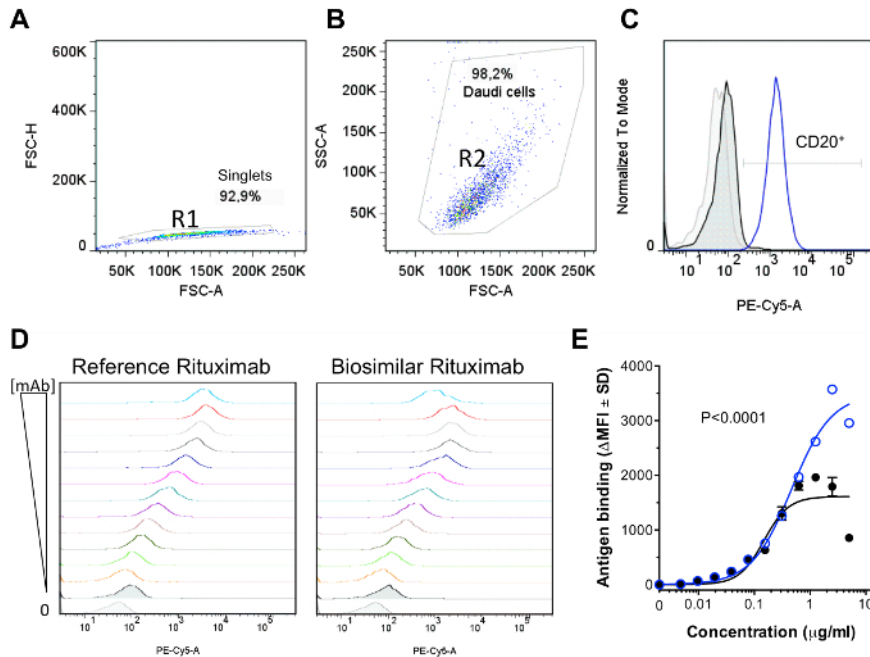


Figure 1. *In Vitro* Target-binding of Anti-CD20 Therapeutic mAbs. Daudi GFP⁺ cells were exposed to different concentrations of the mAbs (4.8 ng/mL to 5 μg/mL) and then stained with PE-Cy5-conjugated anti-human secondary antibody. Fluorescence intensity (FI) was measured by flow cytometry on single events (A), with size and granularity corresponding to those of the Daudi cells (B). Unstained cells (light grey), isotype controls (dark grey), and 5 μg/mL of the reference rituximab (blue) were employed to set the FI limits (C). Both evaluated mAbs bound Daudi cells in a concentration-dependent manner (D). Responses (ΔMFI; see text) were used to generate concentration-response curves for reference (blue) or biosimilar (black) rituximab (E). Statistical comparison of the non-linear regressions showed differences between the mAbs (P < 0.0001; Fisher exact test). [Please click here to view a larger version of this figure.](#)

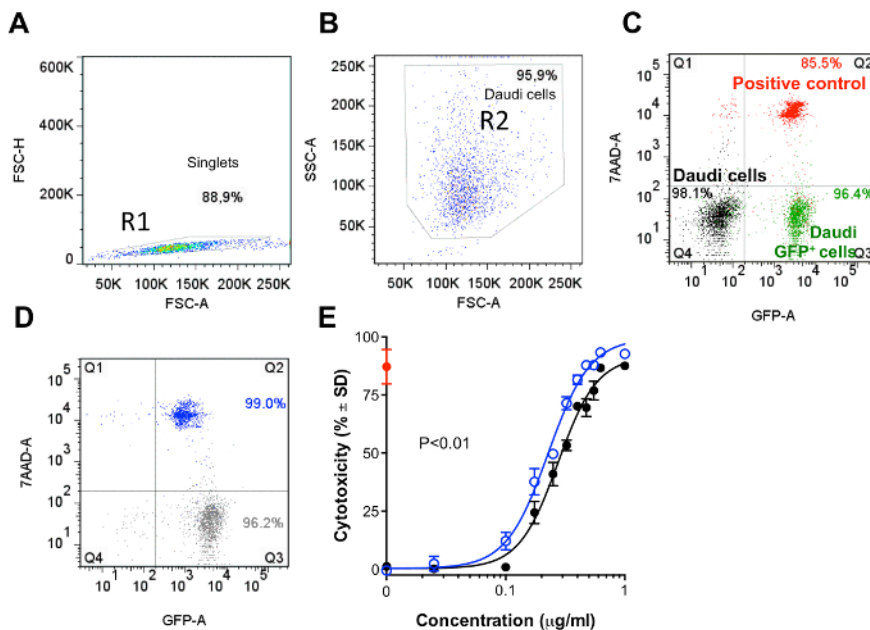


Figure 2. CDC Induction by anti-CD20 Therapeutic mAbs. Daudi GFP⁺ cells opsonized with different concentrations of mAbs were exposed to the human complement. Cell death was evaluated by 7-AAD staining and the flow cytometric analysis of fluorescence intensity (FI) on single events (A), with size and granularity corresponding to the Daudi cells (B). Unstained GFP- (black) and GFP⁺ (green) cells and ethanol-killed cells (red) were included as controls (C). Quantification of the 7-AAD⁺ cells in the basal-death control (grey) and rituximab samples (blue) allowed for the calculation of the mAb-induced cytotoxicity (D). Concentration-response curves obtained for reference (blue) or biosimilar (black) rituximab (E). Statistical comparison of the non-linear regressions showed differences between the responses induced by the two mAbs (P < 0.01; Fisher exact test). [Please click here to view a larger version of this figure.](#)

ANTIBODY (TRADE NAME)	TYPE	TARGET	LICENSED INDICATION	TARGET CELLS	REFERENCES
Rituximab (Rituxan)	Chimeric IgG1	CD20	non-Hodgkin's lymphoma (NHL), chronic lymphocytic leukemia (CLL) and rheumatoid arthritis	Daudi, TK, KML-1, Z-138	[17], [18], [19]
Trastuzumab (Herceptin)	Humanized IgG1	HER-2	HER-2 positive breast cancer	Raji	[20]
Infliximab (Remicade)	Chimeric IgG1	TNF- α	Crohn's disease, ulcerative colitis, psoriasis, psoriatic arthritis, ankylosing spondylitis, and rheumatoid arthritis	Jurkat T, Sp2/0-11AS-1 cells transfected with mTNF, SKOV3	[21], [22]
Etanercept (Enbrel)	Fusion protein IgG1	TNF- α	Rheumatoid arthritis, juvenile rheumatoid arthritis, psoriatic arthritis, plaque psoriasis and ankylosing spondylitis	Jurkat T, mononuclear cell-enriched PMC	[21], [22]
Alemtuzumab (Campath)	Humanized IgG1	CD52	B- cell chronic lymphocytic leukemia	Raji, CLL cells	[20], [23]
Adalimumab (Humira)	Human IgG1	TNF- α	Rheumatoid arthritis, psoriatic arthritis, ankylosing spondylitis, Crohn's disease, ulcerative colitis, psoriasis and juvenile idiopathic arthritis	Jurkat T, peripheral blood mononuclear cells (PBMC)	[21], [22]
Cetuximab (Erbixub)	Chimeric IgG1	EGFR	Colorectal cancer and squamous cell carcinoma of the head and neck	A549, H358, Calu-3, H460	[24]
Panitumumab (Vectibix)	Human IgG2	EGFR	Metastatic colorectal carcinoma	A431, MCF7	[25]
Certolizumab Pegol (Cimzia)	Humanized IgG Fab fragment	TNF- α	Crohn's disease, rheumatoid arthritis, psoriatic arthritis	Jurkat T, TNF6.5	[26], [27]
Oritumumab (Arzerra)	Human IgG1	CD20	CLL	SU-DHL-4, Daudi, Raji	[28]
Golimumab (Simponi)	Human IgG1k	TNF- α	Rheumatoid arthritis, psoriatic arthritis and ankylosing spondylitis	Jurkat T	[26]

Table 1. Monoclonal Antibodies Approved for Therapeutic Use, with Target Cells for the CDC Assay. Please click here to view a larger version of this figure.

Discussion

The patent expiration of a therapeutic mAb is promoting the development of biosimilars. Thus, there is a need for simple methods that can identify differences in clinically relevant activities of these products. CD20⁺ cultured cells were employed for the evaluation of two key functional characteristics of rituximab: target binding and CDC induction. The former activity requires the recognition of CD20 by the Fab region of the mAb, while the latter depends mainly on the interaction of the Fc region with its complement⁹. Therefore, these assays provide a way to link the structural and functional characteristics of mAbs.

The target binding of therapeutic mAbs is usually evaluated by isothermal titration calorimetry (ITC), surface plasmon resonance (SPR), or biolayer interferometry^{10,11,12}. These assays allow affinity calculation, but they require specialized equipment and training. The protocol described here evaluates target binding in a side-to-side comparison to identify differences between products, even without affinity data. The method is simple and employs a relevant cellular context for activity assessment. On the other hand, CDC induction by rituximab can be evaluated by ATP measurement¹³, the quantification of released lactate dehydrogenase (LDH)¹⁴ or alamarBlue¹⁵, and MTT assays¹⁶. The method reported here, using 7-AAD staining, has a low background and can be combined with other stains for multiparametric flow cytometric analysis.

In the representative experiments presented, dose-response curves fitted the four-parameter logistical model, allowing for the calculation of the EC₅₀, Hill slope, and maximal response. Notably, the ranges of concentrations employed to generate such curves were different for each assay, highlighting the importance of analyzing and defining adequate ranges in preliminary experiments. Changes in key reagents, such as fluorochromes and complements, or the use of a cell line with a different target level, may displace the effective range of concentrations.

Statistical analysis identified differences between one batch of a biosimilar rituximab commercially available in Asia and the reference product, both in target binding and in CDC induction. It is important to consider that, even when the manufacturing process of the mAbs is tightly controlled, each attribute of the reference product displays a range. Accordingly, the minimum number of batches that should be tested during the evaluation of a similar biotherapeutic depends on the extent of variability of the reference product and on the assay variability⁴. Thus, these protocols must be applied to different batches during the evaluation of comparability.

The presented methods can be extrapolated to other pairs of therapeutic mAbs-targets, as long as the cells expressing the antigen are accessible. **Table 1** lists therapeutic mAbs other than rituximab for which CDC induction is relevant to the clinical efficacy and compiles information on the previously reported cellular models for each mAb.

In conclusion, the two assays described here are simple, fast, and inexpensive, allowing for their execution in most labs. The methods can be used during early steps of biosimilar development or after regulatory approval for batch-to-batch comparison during production.

Disclosures

N. Salinas-Jazmín, E. González-González, and S. M. Pérez-Tapia are employees of UDIBI, which performs biosimilarity studies for several pharmaceutical companies.

Acknowledgements

The authors have no acknowledgements.

References

- Schimizzi, G.F., Biosimilars from a practicing rheumatologist perspective: An overview. *Autoimmun Rev.* **15** (9), 911-6 (2016).
- Cuello, H.A., *et al.*, Comparability of Antibody-Mediated Cell Killing Activity Between a Proposed Biosimilar RTX83 and the Originator Rituximab. *Bio Drugs.* **30** (3), 225-31 (2016).
- Iwamoto, N., *et al.*, Validated LC/MS Bioanalysis of Rituximab CDR Peptides Using Nano-surface and Molecular-Orientation Limited (nSMOL) Proteolysis. *Biol Pharm Bull.* **39** (7), 1187-94 (2016).
- World Health Organization. *Guidelines on evaluation of monoclonal antibodies as similar biotherapeutic products (SBPs)*. Available at: www.who.int/biologicals/expert_committee/mAb_SBP_GL-ECBS_review_adoption-2016.10.26-11.7post_ECBS-Clean_Version.pdf?ua=1 (2016).
- Chapman, K., *et al.*, Waiving in vivo studies for monoclonal antibody biosimilar development: National and global challenges. *MAbs.* **8** (3), 427-35 (2016).
- EMA. EMEA/CHMP/BMWP/42832/2005 Rev1. *Guideline on similar biological medicinal products containing biotechnology-derived proteins as active substance: non-clinical and clinical issues*. Available at: www.ema.europa.eu/docs/en_GB/document_library/Scientific_guideline/2015/01/WC500180219.pdf (2014).
- Zembruski, N.C., *et al.*, 7-Aminoactinomycin D for apoptosis staining in flow cytometry. *Anal Biochem.* **429** (1), 79-81 (2012).
- Salinas-Jazmin, N., E. Hisaki-Itaya, and M.A. Velasco-Velazquez, A flow cytometry-based assay for the evaluation of antibody-dependent cell-mediated cytotoxicity (ADCC) in cancer cells. *Methods Mol Biol.* **1165**, 241-52 (2014).
- Teeling, J.L., *et al.*, The Biological Activity of Human CD20 Monoclonal Antibodies Is Linked to Unique Epitopes on CD20. *J Immunol.* **177** (1), 362-371 (2006).
- Miranda-Hernandez, M.P., *et al.*, Assessment of physicochemical properties of rituximab related to its immunomodulatory activity. *J Immunol Res.* **2015**, 910763 (2015).
- Visser, J., *et al.*, Physicochemical and functional comparability between the proposed biosimilar rituximab GP2013 and originator rituximab. *BioDrugs.* **27** (5), 495-507 (2013).
- Ylera, F., *et al.*, Off-rate screening for selection of high-affinity anti-drug antibodies. *Anal Biochem.* **441** (2), 208-13 (2013).
- Broyer, L., L. Goetsch, and M. Broussas, Evaluation of complement-dependent cytotoxicity using ATP measurement and C1q/C4b binding. *Methods Mol Biol.* **988**, 319-29 (2013).
- Herbst, R., *et al.*, B-cell depletion in vitro and in vivo with an afucosylated anti-CD19 antibody. *J Pharm Exp Ther.* **335** (1), 213-22 (2010).
- Lazar, G.A., *et al.*, Engineered antibody Fc variants with enhanced effector function. *Proc Natl Acad Sci U S A.* **103** (11), 4005-10 (2006).
- Winiarska, M., *et al.*, Statins impair antitumor effects of rituximab by inducing conformational changes of CD20. *PLoS medicine.* **5** (3), e64 (2008).
- Zhou, X., W. Hu, and X. Qin, The role of complement in the mechanism of action of rituximab for B-cell lymphoma: implications for therapy. *Oncologist.* **13** (9), 954-66 (2008).
- Hayashi, K., *et al.*, Gemcitabine enhances rituximab-mediated complement-dependent cytotoxicity to B cell lymphoma by CD20 upregulation. *Cancer Sci.* **107** (5), 682-9 (2016).
- Mossner, E., *et al.*, Increasing the efficacy of CD20 antibody therapy through the engineering of a new type II anti-CD20 antibody with enhanced direct and immune effector cell-mediated B-cell cytotoxicity. *Blood.* **115** (22), 4393-402 (2010).
- Lapalombella, R., *et al.*, A novel Raji-Burkitt's lymphoma model for preclinical and mechanistic evaluation of CD52-targeted immunotherapeutic agents. *Clin Cancer Res.* **14** (2), 569-78 (2008).
- Mitoma, H., *et al.*, Mechanisms for cytotoxic effects of anti-tumor necrosis factor agents on transmembrane tumor necrosis factor alpha-expressing cells: comparison among infliximab, etanercept, and adalimumab. *Arthritis Rheum.* **58** (5), 1248-57 (2008).
- Kaymakalan, Z., *et al.*, Comparisons of affinities, avidities, and complement activation of adalimumab, infliximab, and etanercept in binding to soluble and membrane tumor necrosis factor. *Clin Immunol.* **131** (2), 308-16 (2009).
- Zent, C.S., *et al.*, Direct and complement dependent cytotoxicity in CLL cells from patients with high-risk early-intermediate stage chronic lymphocytic leukemia (CLL) treated with alemtuzumab and rituximab. *Leuk Res.* **32** (12), 1849-56 (2008).
- Goswami, M.T., *et al.*, Regulation of complement-dependent cytotoxicity by TGF-beta-induced epithelial-mesenchymal transition. *Oncogene.* **35** (15), 1888-98 (2016).
- Wang, A., *et al.*, Induction of anti-EGFR immune response with mimotopes identified from a phage display peptide library by panitumumab. *Oncotarget.* (2016).
- Ueda, N., *et al.*, The cytotoxic effects of certolizumab pegol and golimumab mediated by transmembrane tumor necrosis factor alpha. *Inflamm Bowel Dis.* **19** (6), 1224-31 (2013).
- Nesbitt, A., *et al.*, Mechanism of action of certolizumab pegol (CDP870): in vitro comparison with other anti-tumor necrosis factor alpha agents. *Inflamm Bowel Dis.* **13** (11), 1323-32 (2007).
- Teeling, J.L., *et al.*, Characterization of new human CD20 monoclonal antibodies with potent cytolytic activity against non-Hodgkin lymphomas. *Blood.* **104** (6), 1793-800 (2004).